



UNIVERSITÀ
DEGLI STUDI
FIRENZE

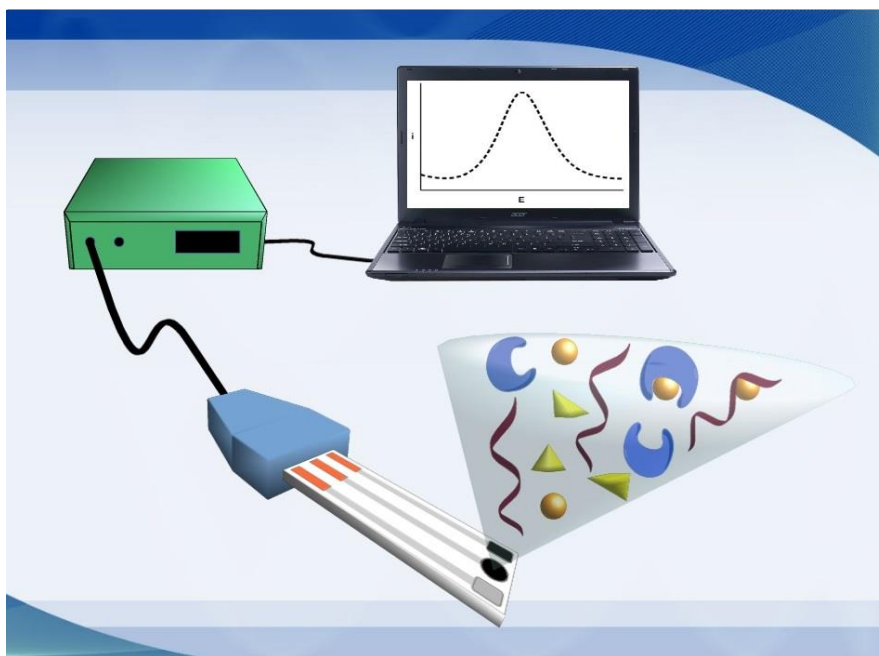
DOTTORATO DI RICERCA IN SCIENZE CHIMICHE

CURRICULUM DI CHIMICA

CICLO XXIX

Coordinatore Prof. Piero Baglioni

IMPROVEMENTS OF SENSING USING SYNTHETIC BIO- MIMETIC RECEPTORS



Dottorando

Dott. Riccardo Rapini

Tutore

Prof. Giovanna Marrazza



UNIVERSITÀ
DEGLI STUDI
FIRENZE

DOTTORATO DI RICERCA IN SCIENZE CHIMICHE

CURRICULUM DI CHIMICA

CICLO XXIX

Coordinatore Prof. Piero Baglioni

IMPROVEMENTS OF SENSING USING SYNTHETIC BIO-MIMETIC
RECEPTORS

Settore Scientifico Disciplinare CHIM/01

Dottorando

Dott. Riccardo Rapini

Tutore

Prof. Giovanna Marrazza

Coordinatore

Prof. Piero Baglioni

Anni 2013/2016

Abstract

This thesis describes the development of new kind of biosensors based on bio-mimetic probe molecules. Biosensor development can be classified as an interdisciplinary field that is one of the most active research areas in analytical chemistry. As well as others analytical methods, biosensors' performances are evaluated considering their detection limit (LOD), their sensitivity, selectivity and reproducibility, the obtained linear and dynamic range and their response to interfering substance. Probably most used receptors in biosensing applications are Antibodies (ABs). They are able to bind the target providing high selectivity and sensitivity but their use is characterised by some limitations. Recent progresses in bio-analytical applications led to the synthesis and characterisation of new classes of bio-mimetic receptors. These kinds of probes are composed by biological “bricks” assembled in vitro or by synthetic molecules assembled in order to mimic ABs recognition capability. This thesis work will provide examples of applications of DNA aptamers and molecularly imprinted polymers (MIPs).

In detail this dissertation is divided in chapters:

In CHAPTER 1 an introduction to the thesis is provided, defining the concept of biosensor and highlighting classification and advantages of electrochemical ones. Moreover, bio-mimetic receptors used in the experimental part are also introduced, including a short description of aptamers and molecularly imprinted polymers.

In CHAPTER 2 the role of biosensors in pesticide monitoring for food analysis is described. The review contains a characterisation of pesticides, divided by their chemical classes and a description of available types of

biosensors for their analysis, food sample pretreatments are also reported, as well as an analysis of recently published papers in this field.

In CHAPTER 3 recent innovations in electrochemical based aptasensors for pollutants and crops and food contaminants are reported. The review analyses advantages of electrochemical transduction coupled to aptamer-based sensors, comparing classical devices and screen-printed cells. Recently published papers on these topics are then reported and summarised.

In CHAPTER 4 electrochemical techniques applied in the project reported in this dissertation are introduced, describing their basic principles.

In CHAPTER 5 the first proposed aptasensor for acetamiprid detection is reported. The aptasensor is based on a dual signal amplified strategy by employing a gold-polyaniline modified screen-printed electrode as sensor platform and an enzyme-linked label for sensitive detection. The polyaniline-gold nanocomposite modified electrodes were firstly modified with a mixed monolayer of a thiol-tethered DNA aptamer and 6-mercapto-1-hexanol. The acetamiprid solution was then incubated with the aptasensor. An enzyme-amplified detection scheme, based on the coupling of a streptavidin-alkaline phosphatase conjugate and a secondary biotinylated aptamer was then applied. The enzyme catalysed the hydrolysis of the electro-inactive 1-naphthyl-phosphate to 1-naphthol. This electroactive product was then detected by means of differential pulse voltammetry. A calibration curve between 0-200 nM acetamiprid concentration range was obtained.

In CHAPTER 6 a successive development of approach described in CHAPTER 5 is presented. In this work, a simple and sensitive aptasensor based on sandwich approach for acetamiprid detection is presented. The aptamer, immobilised on polyaniline and gold nanoparticles modified graphite screen-printed electrodes, is used to capture the analyte from sample solution. The sandwich assay is then performed by adding a secondary biotinylated aptamer. An enzyme-amplified detection scheme, based on the coupling of a streptavidin-alkaline phosphatase conjugate and biotinylated aptamer has been then applied. The enzyme catalysed the hydrolysis of the electro-inactive 1-naphthyl phosphate to 1-naphthol. The enzymatic product is instead electro-active and was detected by differential pulse voltammetry. The experimental parameters were investigated and optimised. The analytical performances of aptasensor in terms of sensitivity, reproducibility and selectivity were studied.

In CHAPTER 7 a competitive aptasensor for sensitive multidetection of acetamiprid based on a competitive format and disposable screen-printed arrays is described. To improve the sensitivity of the aptasensor, polyaniline film and gold nanoparticles were progressively electrodeposited on the graphite screen-printed electrode surface by cyclic voltammetry. Gold nanoparticles were then employed as platform for thiol-tethered DNA aptamer immobilisation. Different acetamiprid solutions containing a fixed amount of biotinylated complementary oligonucleotide sequence by DNA aptasensor arrays were analysed. Streptavidin-alkaline phosphatase conjugate was then added to trace the affinity reaction. The enzyme catalysed the hydrolysis of 1-naphthyl phosphate to 1-naphthol. The enzymatic product was then detected by differential pulse voltammetry. A decrease of the signal was obtained when the pesticide concentration was increased, making the sensor work

as signal-off sensor. Under optimised conditions by testing key experimental parameters, a dose-response curve was constructed between 0.25-2.0 μM acetamiprid concentration range and a limit of detection of 0.086 μM was calculated. The selectivity of the aptasensor was also confirmed by the analysis of atrazine pesticide. Finally, preliminary experiments in fruit juice samples spiked with acetamiprid were also performed.

In CHAPTER 8 an innovative electrochemical sensor with reduced interference signal based on molecularly imprinted polymeric nanoparticles (nanoMIPs) is described. NanoMIPs were synthesized using a solid-phase approach, using ascorbic acid as template. NanoMIPs were prepared in aqueous environment and their size and shape were characterized via dynamic light scattering (DLS) measurements and transmission electron microscopy (TEM). A multi-pulsed amperometric detection for ascorbic acid was applied, using graphite screen printed electrodes (GSPEs) and measuring its oxidation current. Measurements were carried out also in presence of synthesized nanoMIPs, evaluating their ability to subtract electroactive analyte from sample solution, suppressing its oxidation signal. Measurements of dopamine in presence of selected concentration of ascorbic acid as interfering species were carried out. By means of synthesized nanoMIPs it was possible to measure dopamine in the range 100 – 500 nM in presence of 50 nM of ascorbic acid eliminating its interfering signal without any sample pretreatment. Finally, experiments in real samples (spiked human serum) were also carried out.

In CHAPTER 9 general conclusions are reported.

Table of Contents

CHAPTER 1	1
1.1 Introducing biosensors	1
1.1.1 Definitions	1
1.1.2 Electrochemical biosensors	3
1.2 Bio-mimetic receptors	5
1.2.1 Aptamers	6
1.2.2 MIPs – molecularly imprinted polymers	8
1.3 References	10
CHAPTER 2	13
2.1 Biosensors potential in pesticide monitoring	13
2.1.1 Abstract	13
2.1.2 Introduction	14
2.1.3 Foods: sampling and pre-treatment	23
2.1.4 Sensing of pesticides for food safety	25
2.1.5 Conclusions and future perspectives	51
2.2 References	54
CHAPTER 3	67

3.1	Electrochemical aptasensors for contaminants detection in crops and food and environment: recent advances	67
3.1.1	Abstract	67
3.1.2	Introduction	67
3.1.3	Aptasensors Format.....	70
3.1.4	Pesticides.....	71
3.1.5	Pollutants.....	72
3.1.6	Drugs	78
3.1.7	Toxins.....	87
3.1.8	New approaches for electrochemical aptasensors based on screen printed transducers	94
3.1.9	Conclusions	102
3.1.10	Summary tables	104
3.2	References	107
CHAPTER 4.....		121
4.1	Electrochemical techniques.....	121
4.1.1	Cyclic voltammetry	121
4.1.2	Electrochemical impedance spectroscopy	123
4.1.3	Differential pulse voltammetry	126

4.1.4	Multi-pulsed amperometry	128
4.2	References	131
CHAPTER 5		133
5.1	DNA technology for small molecules sensing: a new approach for acetamiprid detection	133
5.1.1	Abstract	133
5.1.2	Introduction	134
5.1.3	Materials and methods.....	136
5.1.4	Experimental procedure	137
5.1.5	Results and discussion.....	139
5.1.6	Conclusions	140
5.2	References	141
CHAPTER 6		143
6.1	Recent progress in biosensors for acetamiprid pesticide detection.....	143
6.1.1	Abstract	143
6.1.2	Introduction	143
6.1.3	Experimental	145
6.1.4	Results and discussion.....	149
6.1.5	Conclusion.....	152

6.1.6	Aknowledgement	152
6.2	References	154
CHAPTER 7.....		155
7.1	Acetamiprid multidetection by disposable electrochemical DNA aptasensor	155
7.1.1	Abstract	155
7.1.2	Introduction	156
7.1.3	Materials and methods	158
7.1.4	Results and discussion	166
7.1.5	Conclusions	176
7.2	References	178
CHAPTER 8.....		181
8.1	MIP-based electrochemical sensor with reduced interference signal.....	181
8.1.1	Abstract	181
8.1.2	Introduction	182
8.1.3	Experimental	184
8.1.4	Results and discussion	190
8.1.5	Conclusions	201

8.2	References	203
CHAPTER 9		205
9.1	General conclusions	205

Figures

Figure 1.1: Schematic representation of a biosensor..... 2

Figure 1.2: Schematic representation of SELEX process. Reprinted with permission of Elsevier [14]. 7

Figure 1.3: Schematic representation of nanoMIPs synthesis..... 9

Figure 2.1: The environmental diffusion ways of pesticides. 16

Figure 2.2: Schematic illustration of the stepwise AChE biosensor fabrication process and immobilised AChE inhibition in pesticide solution. Reprinted from Biosensors and Bioelectronics, 42, Chen Zhai, Xia Sun, Wenping Zhao, Zhili Gong, Xiangyou Wang, Acetylcholinesterase biosensor based on chitosan/prussian blue/multiwall carbon nanotubes/hollow gold nanospheres nanocomposite film by one-step electrodeposition, 124-130, 2013, with permission from Elsevier [73]. 37

Figure 2.3: Schematic illustration of the conductimetric immunosensor. An amount of the secondary antibody (Ab_2) is bound to the specific antibody (Ab_1). Previously, the amount of Ab_1 bound to the pesticide was evacuated. The amount of gold nanoparticles is indirectly related to the pesticide residue concentration. Reprinted from Food Chemistry, 122, Enrique Valera, Javier Ramón-Azcón, Alejandro Barranco, Begoña Alfaro, Francisco Sánchez-Baeza, M.-P. Marco, Ángel Rodríguez, Determination of atrazine residues in red wine samples. A conductimetric solution, 888-894, 2010, with permission from Elsevier [103]. 43

Figure 2.4: Schematic illustration of the aptasensor: sensitive detection of iprobenfos (IBF) and edifenphos (EDI) has been successfully conducted X

by using a colorimetric method. Reprinted from *Analytica Chimica Acta*, 868, Young Seop Kwon, Van-Thuan Nguyen, Je Gun Park, Man Bock Gu, Detection of Iprobenfos and Edifenphos using a new Multi-aptasensor, 60-66, 2015, with permission from Elsevier [124].47

Figure 2.5: Schematic representation of the hexazinone (HXZ) sensor response. In the first step, an accumulation potential (-0.5 V) is used to pre-concentrate HXZ within the MIP cavities of the paste, after which the applied potential resulted in quantitative reduction of HXZ (in an acidic medium) and its return to the solution. Reprinted from *Sensors and Actuators B: Chemical*, 208, Maricely Janette Uria Toro, Luiz Diego Marestoni, Maria Del Pilar, Taboada Sotomayor, A new biomimetic sensor based on molecularly imprinted polymers for highly sensitive and selective determination of hexazinone herbicide, 299-306, 2015, with permission from Elsevier [146].51

Figure 3.1: Scheme of the proposed aptasensor for bisphenol-A detection. Highly dispersed Pt nanoparticles/acid-oxidised carbon nanotubes, functionalised with polyethyleneimine were deposited on a glassy carbon electrode. An ammine-capped DNA oligonucleotide, complementary to the specific aptamer, was bound to the nanostructured surface, in order to bind the aptamer forming a double strand structure. DPV measurements, using $[\text{Fe}(\text{CN})_6]^{3-/4-}$ as electrochemical mediator were carried out, observing a decrease of the signal in presence of the analyte. Reprinted with permission of Elsevier [45].77

Figure 3.2: Scheme of the proposed aptasensor for Hg^{2+} detection based on a self-assembly of thiolated β -cyclodextrins on a gold electrode. Orderly arranged molecularly layer showed interspaces among β -cyclodextrins that let electrochemical probe $[\text{Fe}(\text{CN})_6]^{3-/4-}$ to reach

electrode surface. Thionine labelled aptamer was then linked to β -cyclodextrins and hybridised with a DNA oligonucleotide, letting interspaces free. Interaction with the target brought to the formation of a secondary structure that closed interspaces, lowering the DPV signal. Reprinted with permission of Elsevier [57]. 78

Figure 3.3: Scheme of the proposed aptasensor for ricin toxin. The competitive assay is based on a kinetic competition between a specific ricin toxin A-chain aptamer, a short DNA sequence used as blocker and a molecular beacon labelled with a fluorophore and a quencher. The more was the target, the more blocker bound the beacon increasing fluorescence. The work describes also an electrochemical approach based on the same sequences. The kinetic competition was carried out between a DNA oligonucleotide with the same sequence as the molecular beacon, immobilised on a gold electrode, the same blocker labelled with methylene blue and the aptamer. Even in this case, the assay worked as a signal on sensor. Reprinted with permission from: Y. Du, S.J. Zhen, B. Li, M. Byrom, Y.S. Jiang, A.D. Ellington, *Anal. Chem.*, 88: 2250-2257, 2016. Copyright 2016 American Chemical Society [135]. 93

Figure 3.4: Per cent relevance of electrochemical aptasensors, with particular focus on screen printed electrodes utilisation and environmental and food contaminants analysis. Source: Scifinder 2016. 95

Figure 3.5: Scheme of the proposed label-free aptasensor for chloramphenicol detection. A graphite SPE was modified with a dendritic nanostructure based on mesoporous silica (SBA-15) functionalised with 1,4-diazabicyclo[2,2,2]octane (DABCO) in order to increase Au

nanoparticles immobilisation, enhancing surface conductivity. The specific aptamer was bound via Au-S interaction, and analyte capturing was monitored via DPV, using hemin as electrochemical. Reprinted with Springer permission [169].99

Figure 3.6: Scheme of the label-free impedimetric aptasensor for ochratoxin-A detection. A graphite SPE was modified with a thin film of electrodeposited polythionine and IrO₂ nanoparticles, on which the probe aptamer was electrostatically immobilised. The sensor was able to detect the target in buffered samples by means of EIS, using [Fe(CN)₆]^{3-/4-} as redox probe. Reprinted with permission from: L. Rivas, C.C. Mayorga-Martinez, D. Quesada-González, A. Zamora-Gálvez, A. de la Escosura-Muñiz, A. Merkoçi, *Anal. Chem.*, 87: 5167-5172, 2015. Copyright 2015 American Chemical Society [179].102

Figure 4.1: Potential vs. time scan applied in CV.121

Figure 4.2: Example of voltammogram for a reversible redox process. .122

Figure 4.3: Typical EIS alternate applied potential (E_a) and relative current response (I_r), separated by the phase-shift Φ [5].124

Figure 4.4: Example of Nyquist plot.125

Figure 4.5: Equivalent Randles circuit.126

Figure 4.6: Typical potential-time waveform of a DPV measurement. ..127

Figure 4.7: Typical DPV voltammogram.128

Figure 4.8: Typical potential-time waveform of a multi-pulsed amperometry measurement (single pulsed potential).129

Figure 4.9: Typical MPA chronoamperogram.	130
Figure 5.1: Acetamidrid structural formula.....	135
Figure 5.2: Enzyme-amplified detection scheme of the aptasensor.....	139
Figure 5.3: Typical Nyquist plots from bare graphite, polyaniline and gold-polyaniline modified screen–printed electrodes, obtained in 5 mM $K_3Fe(CN)_6/K_4Fe(CN)_6$, 0.1 M KCl.	140
Figure 5.4: Calibration curve obtained of acetamidrid buffered solutions. Each point was repeated at least 3 times.	140
Figure 6.1: Scheme of aptamer-based sandwich assay for acetamidrid detection.	148
Figure 6.2: Curve calibration of the aptasensor.	152
Figure 7.1: Scheme of the aptasensor assay for acetamidrid detection: A) electropolymerisation of aniline; B) electrodeposition of gold nanoparticles (AuNPs); C) oligo1 immobilization; D) mixed SAM formation with 6-mercapto-1-hexanol; E) competitive reaction between acetamidrid and complementary sequence (oligo2); F) coupling with streptavidin-alkaline phosphatase enzyme conjugate; G) incubation with 1-naphtylphosphate and electrochemical detection of enzymatic product by DPV.....	164
Figure 7.2: Predicted secondary structures of oligo1 (A) and oligo2 (B) sequences obtained by MFold software at 25°C in solution with NaCl 0.1M, $MgCl_2$ 5mM.....	167

Figure 7.3: Recorded melting curves of oligo1, oligo2 and hybrid formed from 1.0 μM oligo1 and 1.0 μM oligo2 solution is 61.3 $^{\circ}\text{C}$. The temperature was increased at a constant rate of 1.0 $^{\circ}\text{C}/\text{min}$ from 25 $^{\circ}\text{C}$ to 95 $^{\circ}\text{C}$. Further details are described in the 7.1.3.3 paragraph. 168

Figure 7.4: R_{ct} values obtained by EIS spectra for bare graphite screen-printed electrodes (GSPEs), AuNPs and PANI/AuNPs modified graphite screen-printed electrodes in 0.01 M $[\text{Fe}(\text{CN})_6]^{4-/3-}$ equimolecular mixture with 0.1 M KCl solution. PANI was electropolymerised with 10 cycles and AuNPs were electrodeposited with 15 cycles as described in section 2.5.1. Inset: Nyquist plots for GSPE/PANI/AuNPs and bare GSPE. The measurements were repeated at least 8 times using different GSPEs. 170

Figure 7.5: DNA aptasensor response for different target concentrations (oligo2) using 20 min hybridisation times. Further details are described in the 7.1.4.2.2 paragraph. Each point was repeated at least 8 times using different DNA aptamer biosensors. 171

Figure 7.6: The dose-response curve of acetamiprid (●). The points correspond to $\%S_x/S_o \pm \text{R.S.D.}$. The line that joins the points is referred to the theoretical curve calculated by sigmoidal data interpolation. Control experiments were carried out using several concentrations of an atrazine solution (◀). Each point was repeated at least 8 times using different aptasensors. 174

Figure 8.1: Scheme of the solid-phase synthesis process. A: OH activated glass beads are grafted with GOPTS (3-glycidyloxypopyl trimethoxysilane); B: silanised glass beads are incubated with ascorbic acid (AA), which is then bound for their functionalisation; C: functionalised glass beads are immersed in a solution containing the

polymerisation mixture and purged with N₂ flow: initiators are then added in order to carry out the synthesis; D: a first elution step using RT (room temperature) DI water is used to remove unreacted monomers, free template and low affinity nanoMIPs; E: a second elution step using T = 65°C DI water is used to remove and collect synthesised nanoMIPs. 188

Figure 8.2: Collected TEM images for synthesised nanoMIPs. Particles size and shape appear homogeneous, with diameter dimensions within the range 11 – 36 nM. 191

Figure 8.3: Recorded UV spectrum of synthesised nanoMIPs solution compared to those obtained from monomers mixture with and without the template. 193

Figure 8.4: Obtained voltammograms for solutions containing ascorbic acid (AA) 1mM and dopamine (DA) 1mM. Reported potentials are related to the Ag/AgCl pseudo-reference electrode of the GSP cell..... 194

Figure 8.5: Examples of recorded chrono-amperograms. Current values are collected continuously and plotted vs. time. Highlighted in blue are AA concentrations in sample solution after every addition. 195

Figure 8.6: Recorded current values after successive additions of ascorbic acid (AA) in different sample solutions. Δi values refer to the difference $i_x - i_{\text{blank}}$ where x is the concentration of AA in sample solution after each addition and i_{blank} refers to the current value recorded before the first addition..... 195

Figure 8.7: Recorded current values after successive additions of ascorbic acid (AA) in different sample solutions. Δi values refer to the difference i_x

- i_{blank} where x is the concentration of AA in sample solution after each addition and i_{blank} refers to the current value recorded before the first addition.196

Figure 8.8: Recorded current values after successive additions of ascorbic acid (AA) in different sample solutions. Δi values refer to the difference $i_x - i_{\text{blank}}$ where x is the concentration of AA in sample solution after each addition and i_{blank} refers to the current value recorded before the first addition.198

Figure 8.9: Recorded current values after successive additions of ascorbic acid (AA) in different sample solutions. Δi values refer to the difference $i_x - i_{\text{blank}}$ where x is the concentration of AA in sample solution after each addition and i_{blank} refers to the current value recorded before the first addition.200

Figure 8.10: Recorded current values after successive additions of ascorbic acid (AA) in different sample solutions. Δi values refer to the difference $i_x - i_{\text{blank}}$ where x is the concentration of AA in sample solution after each addition and i_{blank} refers to the current value recorded before the first addition.201

Tables

Table 2.1: Classification of pesticides including main commercially available molecules and their toxic effects	18
Table 3.1: Summary of reported works about pesticides and pollutants	104
Table 3.2: Summary of reported works about drugs	105
Table 3.3: Summary of reported works about toxins	106
Table 6.1: Affinity reaction studies of Apt1 and Apt2 aptasensors performed by EIS measurements.	150
Table 6.2: Optimisation of the incubation time of the affinity reaction with acetamiprid.	150
Table 6.3: Concentration and incubation time optimisation of secondary aptamer	151
Table 7.1: Optimisation of the incubation time. The signals are expressed in $\%S_x/S_0$. S_x is the signal of a solution containing 0.500 μM acetamiprid and 0.010 μM oligo2. S_0 is the signal obtained with 0 μM acetamiprid and 0.010 μM oligo2. The measurements were repeated at least 8 times using different aptasensors. The relative standard deviation (%RSD) is calculated as measure of inter-assay reproducibility.....	172
Table 7.2: Recoveries, biases of fruit juice samples spiked with acetamiprid using different dilution ratio. Each concentration was repeated at least 8 times using different aptasensors and 3 times with subsequently injections in HPLC analysis.	176

Table 8.1: Obtained per cent ratios of recorded currents between buffered water solution measurements and nanoMIPs solution measurements for the tested AA concentrations.....196

Table 8.2: Obtained per cent ratios of recorded currents between buffered water solution measurements and nanoMIPs solution measurements for the tested AA concentrations.....199

CHAPTER 1

1.1 Introducing biosensors

1.1.1 Definitions

According to IUPAC (International Union of Pure and Applied Chemistry) definition, “*a chemical sensor is a device that transforms chemical information, ranging from the concentration of a specific sample component to total composition analysis, into an analytically useful signal. Chemical sensors usually contain two basic components connected in series: a chemical (molecular) recognition system (receptor) and a physico-chemical transducer. Biosensors are chemical sensors in which the recognition system utilises a biochemical mechanism*” [1].

The bio-recognition element is able to convert information about the target analyte, usually its concentration, into a chemical output signal that can be detected by a transducer. The bio-recognition element should provide a high selectivity towards the chosen target (specific bio-recognition) or the chosen chemical class of molecules (non-specific bio-recognition). The other main component of the biosensor device is the transducer that, connected to the detector, is in charge to produce a detectable signal. The signal is then processed by a signal processor that collects, amplifies and displays it (Figure 1.1) [2].

Biosensor development can be classified as an interdisciplinary field and it is also one of the most active research areas in analytical chemistry. The use of biosensor devices has the aim to eliminate, or to strongly reduce, sample pretreatment. As well as others analytical methods, biosensors' performances are evaluated considering their detection limit (LOD), their sensitivity, selectivity and reproducibility, the obtained linear and dynamic

CHAPTER 1

range and their response to interfering substance (concerning this final issue an interesting and innovative approach will be discussed in CHAPTER 8). Other characteristics that can classify sensor's performances include response time (i.e. the time needed to reach 95% of its final sensor's response after analyte addition), its stability (operational one and, mainly, storage one), easiness of use and portability. Ideally, the sensing surface should be regenerable in order to be used for several consecutive measurements [3].

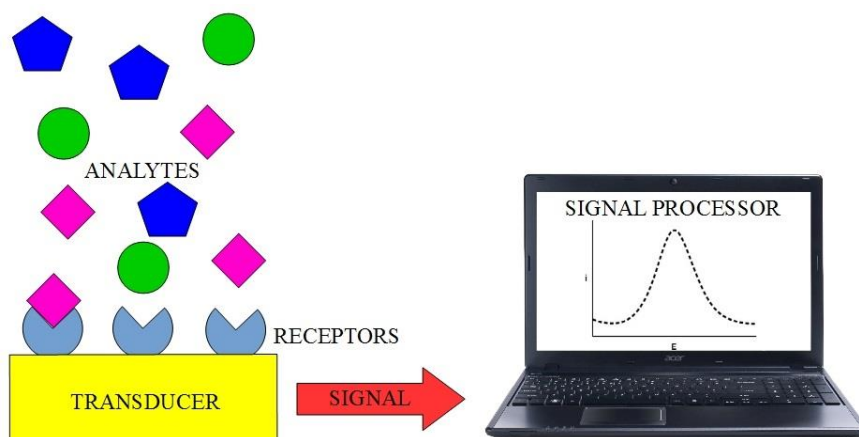


Figure 1.1: Schematic representation of a biosensor.

For many food and environmental applications, the used analytical method should be capable of continuously monitoring the analyte on field (especially concerning screening analysis); nevertheless, disposable, single-use biosensors are satisfactory alternatives that allow to lower costs and skilled technician requirements and, if coupled with portable devices, represent a valid way for in situ monitoring in these important applications.

Biosensors can be classified, considering the transduction method, in:

- electrochemical biosensors: based on the determination of electroactive species that can be produced and consumed at electrode surface or bound to receptor molecule, working as electrochemical mediator (to let current flow from bulk solution to electrode surface) [2]
- optical biosensors: based in changes of receptor's optical properties as a result of target interaction by itself or mediated by appropriate labels or probes [4]
- piezoelectric biosensors: based on a signal produced by application of mechanical stress to a piezoelectric crystal onto the surface of which the receptor is immobilised (monitoring changes produced by target interaction) [5]
- thermometric biosensors: based on heat absorbed or generated by a biochemical reaction measurements [6]
- magnetic biosensors: based on monitoring variations of system magnetic properties after interaction with the analyte [7].

1.1.2 Electrochemical biosensors

This work will be focused on electrochemical biosensors. Electrochemical transduction system is particularly interesting due to its low costs, high detection speed, high sensitivity, portability and, above all, high compatibility with miniaturised technology (a deepened explanation of electrochemical techniques used in this thesis work will be provided in CHAPTER 4).

Electrochemical detection techniques can be classified into six main ensembles, depending of the employed transduction system:

CHAPTER 1

amperometric, voltammetric, impedimetric, conductometric, potentiometric and field effect (or ion charge) [1, 8].

Amperometric biosensors are based on continuous measurements of the resulting current from oxidation or reduction of an electroactive species after application of a constant (or stepped) DC potential to the working electrode. Measured current, that is directly proportional to the electron transfer rate of the reaction (therefore, also to analyte concentration) is plotted against time, obtaining characteristic plots called amperograms [3, 8].

Voltammetric biosensors are based on current and voltage measurement after application of a potential sweep, within a selected range, to the working electrode. The technique is probably the most versatile [9] (it can be applied in many ways, e.g. cyclic voltammetry, linear sweep voltammetry, differential pulse voltammetry, stripping voltammetry etc.) and, being recorded peaks positions characteristic of every electroactive analyte, it is able to detect multiple compounds in a single potential sweep. Moreover voltammetry is characterised by a low signal noise, which can endow the biosensor with higher sensitivity [3, 8].

Impedimetric biosensors are based on electrochemical impedance spectroscopy (EIS), divided in faradic impedance methods (in presence of a redox probe) and non-faradic capacitance methods. This approach is based on the change in the impedance values at solution-electrode surface interface caused by the analyte-probe bio-recognition. Even if EIS can provide label-free detection, LODs are higher, compared to the traditional electrochemical methods [8, 10].

Conductometric biosensors are based on ionic concentration changes induced by the bio-recognition event, that are measured applying an AC potential to two electrodes separated by a certain distance inside the electrochemical cell: change in conductance is taken as analytical signal. Despite several technical advantages (reference electrode unnecessary, low costs, ease of miniaturisation), this transduction method is less sensitive compared to the others and strongly buffer sensitive [3, 8].

Potentiometric biosensors are based on the changes in potential recorded at the working electrode (measured vs. a proper reference electrode) when no current (or a square wave current for chronopotentiometry) flows into the cell. Signal response is high even for small concentrations changes, making this technique useful for low concentration measurements [3, 8].

Field effect biosensors are based on field effect-transistor semiconductors (formed by three elements called source, drain and gate), used to measure conductivity of a channel (a current path formed between the source and the drain, that have no physical contact between them). The bio-recognition event causes a change in accumulated charge carrier generating a signal (called drain current), that is proportional to analyte concentration [3, 8].

1.2 Bio-mimetic receptors

Probably most used receptors in biosensing applications are Antibodies (ABs). They provide high selectivity and sensitivity but their use is characterised by some limitations. First of all, ABs (both monoclonal and polyclonal) are selected and produced inducing immune-reactions in cavy animals. Clearly, this production method is difficult when selected

CHAPTER 1

target molecule belongs to a toxic class of analytes as well as chemical compounds not well tolerated by the cavy animal. Furthermore, the use of host animals presents non-neglectable ethical issues.

As bio-recognition probes, ABs are temperature-sensitive and often present reactivity that changes from batch to batch. Recent progresses in bio-analytical applications led to the synthesis and characterisation of new classes of bio-mimetic receptors. This kind of probes is composed by biological “bricks” assembled *in vitro* or synthetic molecules assembled in order to mimic ABs bio-recognition capability. This work will provide examples of applications of DNA aptamers and molecularly imprinted polymers (MIPs).

1.2.1 Aptamers

Aptamers are short and single-stranded nucleic acid chains (DNA or RNA), isolated *in vitro* from a synthetic oligonucleotides library (composed approximately by 10^{15} - 10^{16} individual molecules, flanked by constant 5' and 3' ends primer sequences) using an automated technique named SELEX (selection evolution of ligands by exponential enrichment), first described in 1990 [11, 12]. Oligonucleotides from the library are selected according to their affinity toward a target molecule (e.g. disease biomarkers, metal ions, small synthetic molecules) looking for the best selectivity and specificity (Figure 1.2) [13].

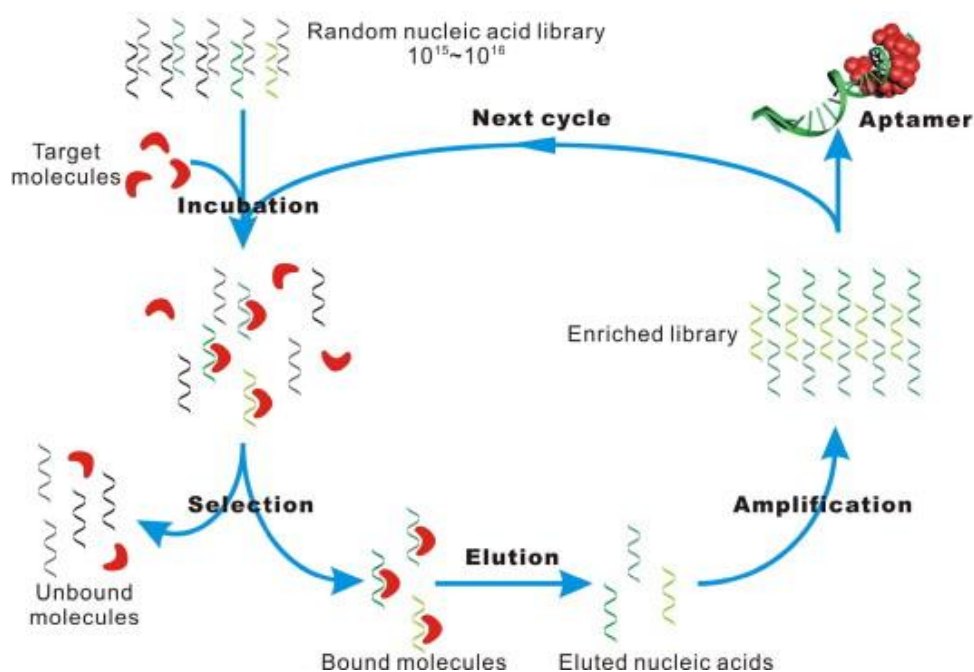


Figure 1.2: Schematic representation of SELEX process. Reprinted with permission of Elsevier [14].

During this procedure, the small fraction of the starting sequences able to interact with the target is immobilised on a solid support, while unbound sequences are separated from the rest of the library via a washing step. Bound sequences are then eluted, amplified via polymerase chain reaction (PCR) and prepared for the following selection cycle. After a certain number of selection and amplification rounds (usually from 8 to 15) the enriched library is cloned and sequenced to obtain the sequence information of each member. Selected sequences are then truncated, in order to remove the primers and characterised respect to their affinity to the selected target [15].

Selected aptamers show low values of dissociation constants (K_d), often within nanomolar and picomolar range. Aptamers offer interesting properties compared to other probe biomolecules such as chemical

synthesis obtaining method (reducing production costs), high purity degree (that reduces batch to batch variations), high temperature stability, the possibility of reversible denaturation and the possibility to easily modify them using several functional groups [15, 16].

1.2.2 MIPs – molecularly imprinted polymers

Another promising alternative to classical immunosensors is given by molecularly imprinted polymers (MIPs), due to their reliability in non-biological conditions (especially in organic solvents and at extremes pH values and temperatures), in which ABs exhibit poor stability, and their lower realisation costs. [17]. MIPs are realised by a process of molecular imprinting, in which monomers and cross-linkers are polymerised in an appropriate solvent in presence of template molecules, that can be free or immobilised on a solid support [18]. Removing the template, the polymeric matrix maintain pre-organised recognition cavities that are complementary to the template, in terms of size, shape and functionality and are able to bind it or a chemical analogue molecule (lock and key mechanism) (Figure 1.3). MIPs are characterised by high stability and the possibility of being employed both in aqueous and organic solvents [19, 20]. One of their peculiar characteristic is the possibility to synthesise them using lots of many imprinting “subjects”, from low-molecular-weight compounds to biopolymers and even pre-cell species (e.g. phages, viruses) and cells [21]. Anyway, a critical step of MIPs synthesis still remains template removal. It can be a difficult procedure and, most of all, it may not be complete, bringing to analyte loss during the analysis (altering analyte concentration) [22]. Despite this operative critical issue, their specific recognition ability can be applied in many chemical methods

for the separation or detection of (bio)molecules, from affinity chromatography to biosensing application [21, 23].

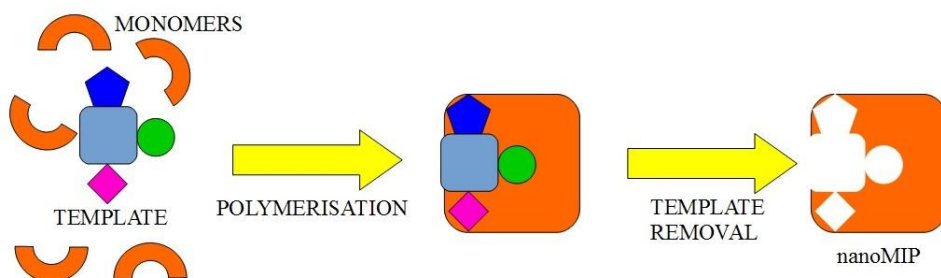


Figure 1.3: Schematic representation of nanoMIPs synthesis.

Molecular imprinted polymers can be realised and applied both as a bulk polymeric matrix as well as realising MIP nanoparticles (nanoMIPs). Respect to bulk MIPs, nanoMIPs show several advantages: nanometric dimensions provide a much higher surface-to-volume ratio and greater total surface area per weight unit of polymer. Moreover, binding sites are more in number and easily accessible by the target, increasing template removal during synthesis phase and binding kinetic during analysis. This results in high recognition capabilities [24, 25].

For these reasons, even if classical bio-molecular probe still remain more diffused in biosensors development, MIPs and, in particular, nanoMIPs are continuously gaining more interest by scientists due to improvements in their synthesis and target recognition ability.

This work will provide an innovative application of nanoMIPs in electrochemical measurements (see CHAPTER 8).

1.3 References

- [1] D.R. Thévenot, K. Toth, R.A. Durst, G.S. Wilson, *Biosensors Bioelectron.*, 16: 121-131, 2001.
- [2] N.J. Ronkainen, H.B. Halsall, W.R. Heineman, *Chem. Soc. Rev.*, 39: 1747-1763, 2010.
- [3] *Chemical sensors and biosensors*, John Wiley & Sons 2008.
- [4] S.M. Borisov, O.S. Wolfbeis, *Chem. Rev.*, 108: 423-461, 2008.
- [5] F. Lucarelli, S. Tombelli, M. Minunni, G. Marrazza, M. Mascini, *Anal. Chim. Acta*, 609: 139-159, 2008.
- [6] K. Ramanathan, B. Danielsson, *Biosensors Bioelectron.*, 16: 417-423, 2001.
- [7] J. Llandro, J. Palfreyman, A. Ionescu, C. Barnes, *Med Biol Eng Comput*, 48: 977-998, 2010.
- [8] *Biosensors and Bioelectronics*, Elsevier 2015.
- [9] P. Protti, *Introduction to modern voltammetric and polarographic analysis techniques*, Amel Electrochemistry, 2001.
- [10] J.S. Daniels, N. Pourmand, *Electroanal.*, 19: 1239-1257, 2007.
- [11] C. Tuerk, L. Gold, *Science*, 249: 505-510, 1990.
- [12] A.D. Ellington, J.W. Szostak, *Nature*, 346: 818-822, 1990.
- [13] J.H. Lee, M.V. Yigit, D. Mazumdar, Y. Lu, *Adv Drug Deliv Rev*, 62: 592-605, 2010.
- [14] S. Song, L. Wang, J. Li, C. Fan, J. Zhao, *TrAC Trends in Analytical Chemistry*, 27: 108-117, 2008.
- [15] M. Mascini (Ed.) *Aptamers: ligands for all reasons*, in: *Aptamers in Bioanalysis* Wiley 2009.
- [16] T. Mairal, V.C. Özalp, P.L. Sánchez, M. Mir, I. Katakis, C.K. O'Sullivan, *Anal. Bioanal. Chem.*, 390: 989-1007, 2008.

- [17] F. Canfarotta, M.J. Whitcombe, S.A. Piletsky, *Biotechnol. Adv.*, 31: 1585-1599, 2013.
- [18] F. Canfarotta, A. Poma, A. Guerreiro, S. Piletsky, *Nat. Protocols*, 11: 443-455, 2016.
- [19] E.V. Piletska, A.R. Guerreiro, M.J. Whitcombe, S.A. Piletsky, *Macromolecules*, 42: 4921-4928, 2009.
- [20] A. Poma, A.P. Turner, S.A. Piletsky, *Trends Biotechnol.*, 28: 629-637, 2010.
- [21] E.V. Dmitrienko, I.A. Pyshnaya, O.N. Martyanov, D.V. Pyshnyi, *Russian Chemical Reviews*, 85: 513, 2016.
- [22] R.A. Lorenzo, A.M. Carro, C. Alvarez-Lorenzo, A. Concheiro, *Int. J. Mol. Sci.*, 12: 4327-4347, 2011.
- [23] T.S. Bedwell, M.J. Whitcombe, *Anal. Bioanal. Chem.*, 408: 1735-1751, 2016.
- [24] D. Gao, Z. Zhang, M. Wu, C. Xie, G. Guan, D. Wang, *J. Am. Chem. Soc.*, 129: 7859-7866, 2007.
- [25] S. Tokonami, H. Shiigi, T. Nagaoka, *Anal. Chim. Acta*, 641: 7-13, 2009.

CHAPTER 2

2.1 Biosensors potential in pesticide monitoring

Published in: *Rapini R, Marrazza G (2016) Biosensor potential in pesticide monitoring. In: Scognamiglio V, Rea G, Arduini F, Palleschi G (eds) Biosensors for Sustainable Food - New Opportunities and Technical Challenges, 1st Edition. Elsevier, p 500.*

2.1.1 Abstract

The use of pesticides is an essential necessity in modern agriculture and their detection remains one of the most important targets for environmental analytical chemistry. Most diffused methods for pesticide detection are based on chromatographic analysis (liquid or gas chromatography). These techniques are very sensitive and standardised. Nevertheless, they often are too laborious and time-consuming. Furthermore, they need complex and expensive instrumentation, often available only in very well equipped and centralised laboratories and their use require high-trained technicians. Over the last years, biosensor use has usually been reported as a promising alternative to traditional methods for pesticide detection. They are fast, economic, and at least as sensitive as usual chromatographic techniques. We summarised the legislative framework and current design strategies in biosensor development. In this review, biosensors have been classified according to the immobilised molecular receptor: enzyme, antibody, aptamer and molecular imprinted polymer. Recent advances in the field of nanomaterials merit special mention. The incorporation of nanomaterials provides highly sensitive sensing devices allowing the efficient detection of pesticides.

CHAPTER 2

Keywords: pesticides, food, sensors, biosensors, nanomaterials

2.1.2 *Introduction*

The pesticide is any substance or mixture of substances used to control the growth of infesting species that can compromise the agricultural production. Infesting species includes insect, weeds, little mammals, fungi and others. The official definition of the Food and Agriculture Organisation (FAO) says that they are defined as substances intended for preventing, destroying, attracting, repelling or controlling any pest, included unwanted species of plants or animals, during the production, storage, transport, distribution and processing of food, agricultural commodities, or animal feeds, for use as a plant growth regulator, defoliant, desiccant, fruit thinning agent or sprouting inhibitor and substances applied to crops either before or after transport. The active molecules, defined as “the components of a formulation responsible for the direct or indirect biological activity against pests and diseases, or in regulating metabolism/growth, etc.”, of a commercial pesticide, are the main ingredient of a formulation that can be available as emulsion concentrate or solid mixture (i.e. soluble or wet powders, granules) and usually need to be diluted prior to use. Moreover, a single active ingredient may be comprised of one or more chemical or biological entities, which may differ in relative activity. A formulation may contain one or more active ingredients [1]. The recent history of agricultural production has been characterised from the use of different kinds of chemical substances to control pests, starting with inorganic compounds e.g. sulphur, arsenic, mercury and lead and observing a great change after

the discovery of dichlorodiphenyltrichloroethane (DDT) as insecticide in 1939 by Paul Müller, that became soon widely used all over the world [2].

Nowadays, worldwide consumption of pesticide can be estimated as 2 million tonnes per year, about 45% of which used in Europe, 25% in the USA and 25% in the remaining countries, and has been estimated that around one third of the agricultural production would be lost without their use [3, 4]. Despite the intense usage pesticides are some of the most toxic, stable and mobile substances released in the environment and we know that they can have toxic effects also against non-target organisms, including humans: for this reason, their presence in food is particularly dangerous [5]. Mainly diffused health problems, derived from the exposure to those substances and eventual bioaccumulation can range from asthma, skin rashes, chronic disorders and neurological diseases [6-9]. Nevertheless, due to the well-studied real and perceived impact of those substances on environment and human health, a strict regulation of their application and residue levels in drinkable water and especially in food supplies has been compiled. Maximum residue limits admitted in food products and drinkable water are regulated in European Union (UE) by EFSA (European Food Safety Authority) or by international bodies such as the Codex Alimentarius [10]. Moreover, despite the strict regulations, due to prevent environmental contaminations and risks for human health that can be caused also from food frauds, intense researches have been developed over the years to obtain sensitive and selective approaches for the detection of pesticides.

Considering pollution caused by pesticides, is known that their intense use bring to a diffused contamination in soil, groundwater and even in air. Nevertheless, the main problem is related to the fact that some toxic

CHAPTER 2

compounds, that can be both active molecules from the pesticide formulation or degradation products, can accumulate in crops, reaching then directly human alimentation products or passing by farm animals and their derivative products. The environmental fate of pesticides is showed in Figure 2.1.

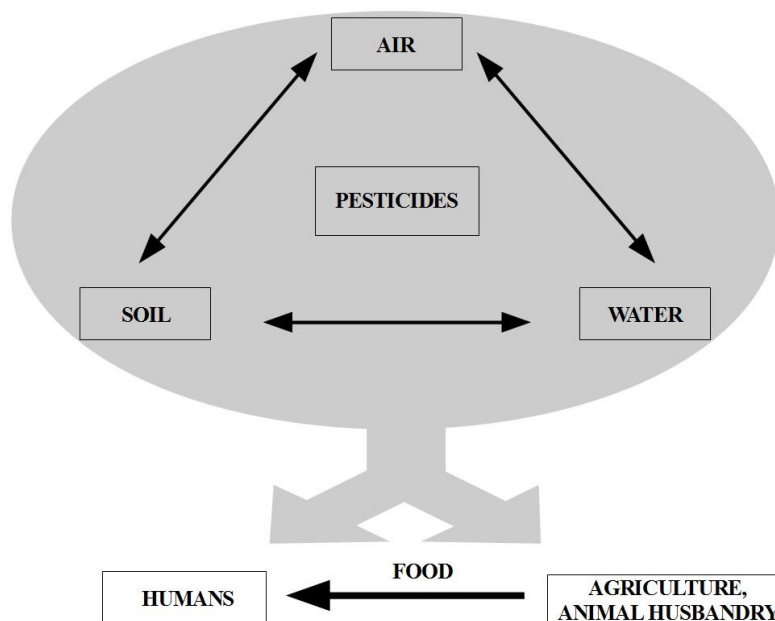


Figure 2.1: The environmental diffusion ways of pesticides.

At present, the detection and the quantification of the pesticides are generally based on chromatographic methods coupled with mass spectroscopy [11, 12]. Although highly sensitive and selective, conventional analytical methods are time-consuming and laborious when a large number of samples must be screened. Besides, they require expensive equipment, skilled operators and complicated pre-treatment. Thus, researchers have been investigating alternative methods of detection and screening that are cheaper and more user-friendly. Recently, there has been an increasing interest in biosensor technology for fast pesticide

detection using easy and rapid procedures. Biosensors have the potential to complement or replace the classical analytical methods by simplifying or eliminating sample preparation and making field-testing easier and faster with significant decrease in cost per analysis.

Focusing on the recent activity of worldwide researchers, without pretending to being exhaustive, the aim of this chapter is to give the readers an overview of recent innovation in the field of pesticide biosensors, after an introduction of the main chemical classes of pesticides, their sampling and extraction from food samples.

2.1.2.1 Pesticides: properties, persistence and regulatory

Pesticides are characterised by a great diversity of chemical structures, action mechanisms and usages, things that make it very difficult to create a classification. Currently, over 800 active ingredients, belonging to more than one hundred substances classes are present in a wide range of commercially available products [13]. They can be listed according to many criteria: e.g. their toxicity, their purpose of application, their environmental stability, the ways by which they penetrate target and non-target organisms, and, of course, their chemical structures. Considering the aim of this work, we are going to focus on a short description of the main classes of pesticides, dividing them in three major groups: 1) herbicides, substances used to control unwanted plants growth or to kill weeds; 2) insecticides, used to kill infesting insects; 3) fungicides, used to control the proliferation of fungi. It should be considered that some chemical classes might fall into more than one major group. In Table 2.1, a classification of the most important pesticides and their toxic effects is showed.

CHAPTER 2

Table 2.1: Classification of pesticides including main commercially available molecules and their toxic effects

Groups	Chemical class	Representative examples	Examples of toxic effects
Herbicides	phenoxy acids	2,4-D, 2,4-DB, dichloprop, MCPA, MCPB, mecoprop, 2,4,5-T	carcinogenicity [14, 15]
	ureas (phenylurea, sulfonylurea)	chlorotoluron, diuron, fenuron, isoproturon, linuron, metoxuron, monolinuron, neburon, chlorimuron-ethyl, chlorsulfuron, metsulfuron-methyl, sulfometuron-methyl, triasulfuron	embryonic development diseases [16]
	triazines	atrazine, ametryn, cyanazine, prometryn, propazine, simazine, terbutryn	carcinogenicity [17]
Insecticides	carbamates	aldicarb, carbaryl, carbofuran, fenoxycarb, methiocarb, methomyl, oxamyl, pronicarb	reversible inhibition of red blood cell AChE and plasma BChE [18], nervous system diseases [19]
	organochlorines	DDT, chlordane, dicofol, endosulfan, endrin, heptachlor, lindane, methoxychlor	oxidative stress [18], carcinogenicity, endocrine disturbance [20]
	organophosphorus	malathion, parathion, acephate, azinphos-methyl, chlorpyrifos, diazinon, dimethoate, phosmet	irreversible inhibition of red blood cell AChE and plasma BChE [18], oxidative stress [21], neurotoxicity [22]
	neonicotinoids	acetamiprid, imidacloprid, thiamethoxam, clothianidin, dinotefuran, nitenpyram	nicotinic ACh receptors activation (low effects on mammals) [23], genotoxicity [24, 25], carcinogenicity [26]
	pyrethroids	allethrin, bifenthrin, cyfluthrin, cyhalothrin, cypermethrin, deltamethrin, fenvalerate	neurotoxic effects [27]
Fungicides	dithiocarbamates	mancozeb, ferbam, maneb, metiram, propineb, thiram, zineb, ziram	neurotoxic chronic effects [28]
	dicarboximides	chlzolinate, iprodione, procymidone, vinclozolin	antiandrogenic effects [29]
	organomercurials	methyl-mercury, phenyl-mercuric-acetate	neurotoxic effects [30]

Referring to the chemical classes division, the most diffused groups are organochlorine, organophosphorus, and organonitrogen (including carbamates, triazines and other derivatives).

Organochlorine pesticides are reported as probably the most toxic class [31, 32], to which belong some of the oldest types of compounds used in this way, characterised by active molecules that can persist in environment for more than 30 years. For this reason, over the last years, compounds like organochlorines are begun to be replaced by compounds and formulations characterised by a faster biodegradation, like the above-mentioned organophosphorus (OP) pesticides [13].

2.1.2.1.1 Herbicides

Implementation in agriculture mechanisation and increase of crops production require a control of weeds growth and herbicides has played a very important role.

Phenoxy acids are many compounds formed by a phenoxy radical linked to a low carbon number alcanoic acid. They can be both soil and foliar applied and they generally have a short persistence in soil [33].

Urea-derivates are one of the most important agricultural herbicide groups. They are usually applied as aqueous emulsions to the surface of soil. Almost all of the urea compounds with good herbicidal action are tri-substituted urea, containing a free imino-hydrogen. The urea bridge is substituted by triazine, benzothiazole, sulfonyl, phenyl, alkyl or other moieties [34].

Triazine compounds are characterised by heterocyclic chemical structures, containing one or more than one nitrogen heteroatoms, with a wide range of uses. They act as inhibitors of electron transport in photosynthesis.

CHAPTER 2

Triazines are some of the oldest herbicides, with research initiated on their weed control properties during the early 1950s. Atrazine, one of the most representative compounds of this group and probably the most diffused, has been banned in the European Union in 2003 because of its ubiquity in drinking water, its demonstrated harmful effects on wildlife, and its potential health hazards for humans [35].

2.1.2.1.2 *Insecticides*

The importance of eliminating insects and other plants parasites is a crucial aspect, in order to maintain a high productivity in agriculture.

Carbamate insecticides is a broad group composed by esters and thioesters of the carbamic acid ($R_1-O-CO-NR_2R_3$, $R_1-S-CO-NR_2R_3$), having a great variety of chemical, physical and biological properties. They are generally soluble in water and in polar organic solvents and commercially available as wet powders, dusts granules and emulsion concentrates. Used also as herbicides they are usually soil applied and absorbed by root and shoot. These compounds are usually decomposed by soil microorganisms in 3-5 weeks [33].

Three chemically different sub-groups compose organochlorine group: DDT analogues, benzene hexachloride isomers and cyclodiene compounds. DDT has a wide spectrum activity on different families of insects and related organisms and it is one of the most persistent contact insecticides because of its low water solubility and low vapour pressure. Cyclodiene compounds are also characterised by a high environmental persistence. Due to these characteristics and their high toxicity, the

majority of these compounds have been banned or their use has been strongly restricted [33].

Hydrocarbon compounds compose organophosphorus group, containing at least one phosphorus atom in their structure. The great structural variety of these compounds makes them the most versatile insecticides, being also characterised by a generally low persistence in biological systems. The group include both molecules with non-residual action and prolonged residual action, broad spectrum pesticides and ones with very specific action, all soluble in water and easily hydrolysed, making them dissipated from soil in a few weeks after application. For these reasons, they are widely used as systemic insecticides. Compounds that have a broad spectrum and non-selective herbicide activity also form organophosphorus group. They are extensively used for foliar application, both in agricultural and non-agricultural areas. Their main degradation product is aminomethylphosphonic acid (AMPA), which can be found in plants, soil and water [33].

Neonicotinoids are neuro-active substances derived from nicotine. Acting as nicotinic acetylcholine receptor agonist, these compounds cause to the contaminated organisms paralysis followed by death and they are active against many sucking and biting insects. Depending on the application form (seeds or foliar treatment) of neonicotinoid insecticides there are different routes of exposure of non-target organisms to these pesticides [36].

Pyretroid insecticides are composed by synthetic derivative of pyrethrum, a substance extracted from some species of chrysanthemum flowers. They generally show low toxicity for non-target organisms (birds, mammals) and they are used as contact poisons, affecting insects' nervous system and

CHAPTER 2

depolarising neuronal membranes. These molecules are degraded in soil and can be used in domestic ambiances to control flies and mosquitoes [33].

2.1.2.1.3 *Fungicides*

Fungicides are used in agriculture to control fungal disease on plant crops and can be applied pre- or post-harvest on many kinds of cultivations.

Dithiocarbamates are applied worldwide on a great number of crops, due to their high efficiency in controlling plant fungal diseases, and are characterised by a relatively low mammalian acute toxicity. Their toxicity is given by the degradation (metabolic or not) product ethylenethiourea, known for its carcinogenic and teratogenic action in laboratory animals [37].

Dicarboximides fungicides are rapidly converted to 3, 5-dichloroaniline in soil. Their repeated use over several years reduces their effectiveness. It is known that some kind of resistance against their action has developed in many plant species and protected crops. For this reason, dicarboximides are recommended to be used in conjunction with other fungicides [38].

Organomercurials are composed by some of the oldest kind of fungicides and the most diffused of its compounds are the methyl-, ethyl-, methoxyethyl- and phenyl- substitute molecules. Applied on seeds, aerobic microorganisms can convert organomercurial compounds to aliphatic or aromatic hydrocarbons and mercury (oxide or sulphide), that is accumulated in soil and can be absorbed by plants. In this way, it can be assimilated and accumulated in mammals tissues. For this reason, the use of organomercurials compounds is strongly decreasing [39].

2.1.3 *Foods: sampling and pre-treatment*

Continuous development of analytical methods has brought to many different approaches for the detection of pesticides, either using classical instrumental analytical tools or using biosensors. Despite of this, the necessity to measure very low concentrations of active molecules or degradation products in complex and variable matrices like fruit, vegetables and biological samples, still make the necessity of developing effective sampling and pre-treatment procedures one of the most important targets for analytical chemists. We are going to focus this short description on the several stages commonly necessary to perform food analysis.

It is possible to make a list of subsequent actions that are required to prepare a sample for the analysis, using as more as possible validated procedures [5]:

- Sampling
- Fixing, transport, homogenisation and storage
- Extraction from the sample and eventual enrichment
- Extract clean-up and preparation for the analysis
- Analysis

The realisation of the whole procedure is strictly connected to analyte and sample characteristics: considering food matrices, a primary division should be made evaluating the amount of fat content. The threshold value is usually set at 2%, where the majority of matrices for pesticide analysis is composed by non-fatty foods like fruits and vegetable, usually consumed raw or with very light postharvest treatment, giving the highest risks for consumers in case of contamination. Detection of lipophilic

CHAPTER 2

pesticides, like organochlorines, is then the main reason of fatty matrices sampling and in this case health risks come from the possible accumulation of toxic substances in lipid tissues [40]. The sampling and subsequent pre-treatment of matrices, should conserve their representativeness, considering their origin and amount [41]. In this way, sampling is crucial for food analysis because of peculiarities of samples: a rapid preparation helps to prevent composition changes given by degradation and it is useful to carry it out at low temperature, as well as prepare a frozen storage if the samples cannot be analysed immediately. It is important to consider that the analytical sample could be just one part of the whole material collected, so a size reduction has to be carried out using appropriate procedures, with different approaches for dry solid (granules, powders), wet solid (fruits, vegetables) and liquid samples [41].

After homogenising the sample, all the moist materials such meats, tissues, fruits, vegetables (leaves, roots or tubers) are fine-sliced using mechanical devices like e.g. mortars or mixers. If necessary (especially for moisture rich samples or fatty samples) a pre-drying or de-fatting procedure can be performed.

Target analytes have then to be extracted from the homogenised samples and eventually enriched, because their concentration (this is true especially considering pesticides) can be relatively low in all various environmental matrices. The extraction and the eventual pre-concentration involve the transfer of the target pesticide from the primary matrix to a secondary one, eliminating the majority of interfering compounds [42-44]. For analysis of solid samples such as fruit and vegetables, the pesticide would be extracted by using different solvent extraction techniques (e.g. accelerated

solvent extraction, microwave solvent extraction, ultrasound assisted solvent extraction, or supercritical fluid solvent extraction) [45, 46].

Unfortunately, food sample extract contains a large amount of components that can create difficulties in the determinative step. A clean-up procedure is often necessary to remove co-extracted interfering species without decreasing target pesticide recovery. The degree of clean-up procedure depends from the technique that is going to be used for the analysis and many different approaches are available [5], but the most used remains solid phase extraction [47, 48].

The last step of the analytical procedure involves the detection of the analyte, recent and various approaches of pesticides detection using biosensors-based devices will be dealt in following paragraphs.

2.1.4 Sensing of pesticides for food safety

Food safety can be defined as the inverse of food risk, i.e. the probability of not suffering some hazard from consuming a specific food [49]. Potential hazardous residues in foods include a great amount of substances, natural and environmental contaminants (e.g. mycotoxins, dioxins, etc.), human and veterinary drugs, growth promoters, packaging components, and, especially, agro-chemicals pollutants like pesticides [50]. For this reason, the development of fast and sensitive analytical techniques for their detection remains one of the most interesting targets for chemists. The use of (bio)sensors offers the possibility to develop a large amount of simple to use devices with low costs, fast and sensitive response and high selectivity. For these reasons, they are particularly suitable for on field screening analysis, being easily coupled with portable devices.

CHAPTER 2

A biosensor is a device composed of two intimately associated elements: a molecular receptor, that is an immobilised sensitive biological or biomimetic element recognising the analyte, and a transducer, that is used to convert the (bio)chemical signal resulting from the interaction of the analyte with the molecular receptor into an electronic one. The intensity of generated signal is directly or inversely proportional to the analyte concentration. In literature, a great variety of biosensors for pesticide detection based on different transducers (e.g. electrochemical, optical, thermal, calorimetric, or piezoelectric) are reported. However, the recognition elements are the most important part of biosensors since they are responsible for the recognition of target analyte. Thus, we specifically provide an overview on some recent pesticide sensing classified as for the molecular receptors used in assay format. Application of novel nano and hybrid advanced functional material (e.g. quantum dots, carbon nanotubes, graphene, and metal organic frameworks) is another key to develop next-generation sensor systems. Consequently, in this chapter, particular emphasis is given to new (bio)sensing based on nanomaterials.

2.1.4.1 Enzyme biosensors

The enzyme biosensors are based on enzymes in intimate contact with the transducers. The enzyme reacts selectively with its substrate (target analyte). Many works have been already published and detection of pesticides is included in the group of analyte that can be detected using enzymes [51-55]. Enzyme biosensors can measure the catalysis or the inhibition of enzymes by the target analyte. In this way, the biosensor detects produced or consumed species, respectively. Commonly, only one enzyme is used in enzymatic biosensors but progress in this field involves

combining enzymes to obtain multi-enzyme systems where several enzymes are incorporated into the same assay.

Biosensors based on a catalytic reaction are superior to the inhibition mode since they can be potentially reused and are suitable for continuous monitoring. Here, electrochemical enzyme biosensors have been reviewed.

A growing class of bacterial enzymes known as phosphotriesterases has recently been characterised. These enzymes catalyse the hydrolysis of organophosphorus pesticides (OPs) with a high turnover rate. The typical one is organophosphorus hydrolase (OPH), an enzyme that can hydrolyse large number organophosphorus pesticides, and this approach can be useful to perform a continuous monitoring of the analyte concentration [56]. OPH acts on the p-nitrophenyl group on the target molecule (many OP pesticides have a p-nitrophenyl substituent, e.g. paraoxon, parathion) hydrolysing it to p-nitrophenol, that can be detected with electrochemical or optical devices [57, 58]. Recently, several types of OPH-based electrochemical biosensors based on nanomaterials have been introduced.

Choi et al. developed an amperometric biosensor coupling a conductive reduced graphene oxide/Nafion hybrid films with OPH enzyme. The biosensor exhibited a sensitivity of 10.7 nA/ μM and a detection limit of $1.37 \cdot 10^{-7}$ M [59]. A novel biosensor based on organophosphorus hydrolase and mesoporous carbon and carbon black as an anodic layer has been developed from Lee et al. [60]. The well-ordered nanopores and high surface area of the mesoporous carbon resulted in increased sensitivity, and allowed for nanomolar-range detection of the analyte paraoxon. The biosensor had a detection limit of 0.12 μM for paraoxon.

CHAPTER 2

Methyl parathion degrading enzyme (MPDE) is one kind of OPH. It can detect methyl parathion (MP), which is an extensively used OP pesticide, with high selectivity since MPDE hydrolyses the P–S bond-containing agent. MPDE catalyses the hydrolysis of MP to generate an equimolar amount of p-nitrophenol, which, in turn, is electrochemically oxidised at the working electrode poised at a fixed potential to generate a current that is proportional to the pesticide concentration. An amperometric biosensor for highly selective and sensitive determination of methyl parathion (MP) has been developed from Du et al. [61]. The biosensor is based on dual-signal amplification: a large amount of introduced enzyme on the electrode surface and synergistic effects of nanoparticles towards enzymatic catalysis. The detection limit of the biosensor is found 1.0 ng/mL.

The same research group has then developed an OPH biosensor for detection of methyl parathion, based on self-assembly of methyl parathion hydrolase (MPH) on $\text{Fe}_3\text{O}_4/\text{Au}$ nanocomposite. The magnetic nanocomposite provides an easy way to construct the enzyme biosensor by simply exerting an external magnetic field, and it provides a simple way to renew the electrode surface by removing the magnet. Under optimal conditions, the biosensor shows rapid response and high selectivity for the detection of methyl parathion, with a detection limit of 0.1 ng/mL [62].

The enzyme inhibition-based biosensors have been applied for organophosphorus and organochlorine pesticides, derivatives of insecticides, heavy metals and glycoalkaloids. The choice of enzyme/analyte system is because these toxic analytes inhibit normal enzyme function.

Inhibition-based biosensors have been the subject of several recent reviews [63-66]. The use of this approach requires a quantitative measurement of the enzyme activity before and after exposure to a target analyte and the experimental procedure can be summarised in three main steps: initial measurement of the enzymatic activity, incubation of a sample containing a certain concentration of the target pesticide and measurement of the inhibited enzymatic activity.

The mainly used enzymes as biological receptors in the enzyme inhibition-based biosensors are acetylcholinesterase (AChE), butyrylcholinesterase (BChE) and urease [67]. The acetylcholinesterase enzyme is the most used because is characterised by high turnover and its substrate is soluble in aqueous solution and is not so expensive. Further, several compounds such as organophosphorus pesticides and nerve agents inhibit AChE and a fast and in situ detection for these analytes is very useful. AChE active site is composed by three amino acids, histidine, serine and aspartic acid: the hydroxyl group of the serine can hydrolyse acetylcholine (ACh) by deprotonation when its quaternary ammonium group (positively charged) electrostatically interacts with the aspartic acid residue. In presence of an organophosphorus pesticide, its phosphorus group covalently binds the nucleophilic serine, inactivating the enzyme [68, 69].

While many studies have looked at the effect of single pesticides on AChE, the effect of mixtures of pesticides still requires extensive investigation. This is important to evaluate the cumulative risk in the case of simultaneous exposure to multiple pesticides. Mwila et al. studied the effect of five different pesticides (carbaryl, carbofuran, parathion, demeton-S-methyl, and aldicarb) on AChE activity to determine whether combinations had an additive, synergistic, or antagonistic inhibitory effect.

CHAPTER 2

The data from the assays of the mixtures have been used to develop and train an artificial neural network. The obtained results indicated that the mixtures had an additive inhibitory effect on AChE activity [19].

In recent years, AChE has been immobilised onto various nanomaterial-modified surfaces, such as carbon nanotubes (CNT), graphene, gold nanoparticles (AuNPs) and quantum dots (QDs) and nanohybrid materials in order to improve the response and the stability in trace-pesticide detection.

CNTs are of special interest due to their ability both to form 3D-nets with high adsorptive activity toward enzymes and to establish electric contact with the electrode [70, 71].

The CNTs have been often combined with other materials in order to modify the sensor with novel nanocomposites such as 7,7,8,8-tetracyanoquinodimethane [72]. The biosensor developed by immobilisation of acetylcholinesterase in sol–gel allowed the detection of two reference AChE inhibitors, paraoxon-methyl and chlorpyrifos with detection limits of 30 pM and 0.4 nM, respectively.

Wang's group reported an AChE biosensor based on chitosan/prussian blue/multiwall carbon nanotubes/hollow gold nanospheres nanocomposite film formed by one-step electrodeposition. Based on the inhibition by pesticides of the AChE activity, using malathion, chlorpyrifos, monocrotophos and carbofuran as model compounds, this biosensor showed a wide range, low detection limit, good reproducibility and high stability. A schematic representation is reported in Figure 2.2 [73]. A simple and reliable technique has been developed for the construction of

an amperometric acetylcholinesterase biosensor based on screen-printed carbon electrodes modified single-walled carbon nanotubes and Co phthalocyanine. This procedure has been proposed to decrease the working potential and to increase the signal of thiocholine oxidation. The reliability of the inhibition measurements has been confirmed by testing spiked samples of sparkling and tap waters.

The immobilisation of acetylcholinesterase on multi-walled carbon nanotubes- β -cyclodextrin (β -CD) composite modified glassy carbon electrode has been proposed from Du et al. [74]. Due to the good dispersion of porous structures of MWCNTs- β -CD composite, the resulting surface provided a favourable microenvironment for acetylcholinesterase biosensor fabrication and maintained the bioactivity of AChE for screening of OPs exposure. The same research group later proposed AChE biosensor based on nanocomposites using multiwalled carbon nanotube coating gold nanoparticles (MWCNTs-Au). The formed MWCNTs-Au nanocomposites offered an extremely hydrophilic surface for biomolecule adhesion, leading to a stable acetylcholinesterase biosensor [75].

Since conducting polymers show some numerous features for sensing and biosensing, they have recently attracted a lot of attention in this field. Incorporation of CNT, metals and metal oxides in the conductive polymers can enhance electron transfer through a direct or mediated mechanism with improved conductivity and enhanced stability [76-78]. The polymer is used to provide a high surface, protection against the fouling of the metal catalyst, and a scaffold for high dispersion and anchoring of the metal particles.

CHAPTER 2

A simple method to immobilise acetylcholinesterase on polypyrrole (PPy) and polyaniline (Pan) copolymer doped with multi-walled carbon nanotubes (MWCNTs) has been proposed. The synthesized PAn-PPy-MWCNTs copolymer presented a porous and homogeneous morphology, which provided an ideal size to entrap enzyme molecules [79].

A macromolecular polymer and carboxyl multi-walled carbon nanotubes (MWNTs-COOH) coated with acetylcholinesterases on the Ag-coated crystal surfaces has been presented from Shang et al. The authors determined pesticide residue in freshly picked radishes 4 and 8 days post application of phoxim and chlorpyrifos. The sensitivity of the method has been compared with gas chromatography. The results showed that there was no significant difference between the two methods [80]. The use of nanocomposites allows for detecting the inhibitors at very low detection limit, but very often requires high potential, even higher than the sensor modified with only carbon nanotubes.

Some electrochemical biosensors based on enzyme inhibition have been assembled using graphene. Graphene, as a new two-dimensional carbon nanomaterial, has attracted increasing attention during recent years by virtue of its outstanding physical, chemical properties and excellent electrocatalytic ability. The special properties of graphene may provide insight into the fabrication of novel biosensors for virtual applications: the high surface area is helpful in increasing the surface loading of the target enzyme molecules, the excellent conductivity and small band gap are favourable for conducting electrons from the biomolecules.

Li et al. [81] reported the sensitive amperometric biosensing of OPs using AChE modifying glassy carbon/reduced graphene oxide electrode. This electrochemical biosensor displayed a detection limit of 0.5 ng mL^{-1} with good reproducibility and stability.

Xue et al. also reported a graphene–nafion matrix modified glassy carbon electrode for the determination of OPs. Methyl parathion is detected over a concentration range of $0.02\text{--}20 \text{ }\mu\text{g/mL}$ in vegetable samples [82].

Graphene-based composite materials possessing three-dimensional (3D) porous architectures are preferred owing to their very large surface areas and low mass transport resistance. Graphene can enhance direct electron transfer between enzymes and electrodes. It has been also reported that the use of graphene associated with metal nanoparticles can form exceptionally stable and cost-effective biosensors.

A sensitive amperometric acetylcholinesterase biosensor based on NiO nanoparticles, carboxylic graphene and nafion modified glassy carbon electrode has been developed from Yang et al. [83]. The nanocomposite material showed excellent conductivity, catalysis and biocompatibility, and offered an extremely hydrophilic surface for AChE adhesion. Under optimum conditions, the biosensor detected methyl parathion and chlorpyrifos in the linear range from 1.0×10^{-13} to $1.0 \times 10^{-10} \text{ M}$ and from 1.0×10^{-10} to $1.0 \times 10^{-8} \text{ M}$, with the detection limit of $5.0 \times 10^{-14} \text{ M}$. The biosensor detected carbofuran in the linear range from 1.0×10^{-12} to $1.0 \times 10^{-10} \text{ M}$ and from 1.0×10^{-10} to $1.0 \times 10^{-8} \text{ M}$, with the detection limit of $5.0 \times 10^{-13} \text{ M}$.

A green synthesis procedure for preparing zinc oxide nanoparticle decorated multiwalled carbon nanotube-graphene hybrid composite by using solar energy and its application as a transducer candidate for

CHAPTER 2

organophosphorus biosensor has been proposed from Nayak [84]. The fabricated biosensor using this composite as a transducer candidate shows a high affinity to acetyl cholinesterase. It exhibits a linear response for Paraoxon detection from 1 to 26 10^{-6} M with a detection limit of 1 10^{-9} M.

Gold nanoparticles are characterised by relevant electrochemical properties such as high superficial area, conductivity and electron transfer rate [85]. Graphene and the gold nanoparticles have been often coupled for designing biosensors.

Wang et al. synthesised a nanohybrid of AuNPs and chemically reduced graphene-oxide nanosheets (cr-Gs). Then, an electrochemical sensor based on AChE/AuNPs/cr-Gs, which has been prepared by self-assembling AChE on an AuNPs/cr-Gs nanohybrid, has been developed for ultrasensitive detection of paraoxon. The nanosize effect of AuNPs scattered on cr-Gs sheets leads to greatly improved electrochemical detection of the enzymatically-generated thiocholine product, including a potential negative shift in operation, great electrochemical-signal amplification, and higher sensitivity and stability [86].

A stable AChE biosensor based on self-assembling AChE to graphene nanosheet (GN)-gold nanoparticles nanocomposite electrode for investigation of inhibition, reactivation and aging processes of different pesticides has been proposed from Zhang et al. [87].

A nanohybrid of gold nanoparticles, polypyrrole, and reduced graphene oxide sheets has been achieved by electrochemical deposition of reduced graphene oxide with pyrrole and the introduction of gold nanoparticles. Acetylcholinesterase has been further encapsulated in a silica matrix and

immobilised on the Au-PPy-rGO nanocomposite by co-deposition. The presence of PPy helped to avoid the aggregation of rGO caused by van der Waals interactions between individual sheets and significantly increased the surface area of the modified electrode. Since AChE molecules have been protected by the circumambient silica matrix, which provided a biocompatible environment and facilitated mass transport, the fabricated AChE biosensor displayed high stability and excellent activity together with a fast response to organophosphorus pesticides [88].

An amperometric biosensor based on immobilising acetylcholinesterase on 3-carboxyphenylboronic/reduced graphene oxide–gold nanocomposites modified electrode has been developed for the detection of organophosphorus and carbamate pesticides from Liu et al. [89]. The biosensor showed good sensitivity owing to the excellent properties of gold nanoparticles and reduced graphene oxide, which promoted electron transfer reaction and enhanced the electrochemical response.

A new method based on specific binding between glycoprotein acetylcholinesterase and boronic acid functionalised Fe@Au magnetic nanoparticles has been presented for the development of acetylcholinesterase biosensor [90]. Based on enzyme inhibition, carbamate pesticide has been detected using Furadan as a model compound. Two linear ranges of 0.05-15 and 15-400 ppb have been obtained with a detection limit of 0.01 ppb. The biosensor also showed acceptable reproducibility and relatively good storage stability. Moreover, satisfactory results have been obtained in real samples analysis.

Pesticides can be detected not only by single enzyme systems, but also by bi-enzyme systems. Recently, a biosensor composed of bi-enzymes acetylcholinesterase and choline oxidase and CdTe QDs has been

CHAPTER 2

developed to determine dichlorvos, with a linear range of 4.49–6780 10^{-6} M and an LOD of 4.49 10^{-6} M [91]. This biosensor has good performance in detecting residues of dichlorvos in real samples, such as apples.

A. Hatefi-Mehriajrdi described another bienzymatic sensor. AChE and COx were covalently immobilised on the mercaptopropionic acid self-assembled monolayer on gold electrode to detect carbaryl at nanomolar level [92].

A bi-enzymatic biosensor (Laccase and tyrosinase) for carbamates has been prepared in a single step by electrodeposition of a hybrid film onto a graphene doped carbon paste electrode. The biosensor proposed was able to determine carbaryl, formetanate hydrochloride, propoxur and ziram in citrus fruits based on their inhibitory capacity on the polyphenol oxidases activity [93].

Recently, the realisation and characterisation of a tyrosinase based biosensor for the determination of atrazine has been reported. The developed biosensor is based on the inhibition effect of atrazine towards the catalytic activity of the blue copper protein tyrosinase. Tyrosinase has been immobilised on the electrode surface by either polyvinyl alcohol with styrylpyridinium groups. The developed inhibition biosensor displays a linearity range towards atrazine within 0.5–20 ppm, a limit of detection of 0.3 ppm and acceptable repeatability and stability. This analysis method has been applied to spiked drinking water samples [94].

Inhibition-based methods have unfortunately some disadvantages and can give to false positives as handling and storage could cause loss of enzyme activity. As a result, baseline testing prior to sample application must be

carried out which lengthens testing time. Further, various compounds can interfere with the OP pesticides interaction with AChE, like heavy metals, fluoride, nicotine, etc. and for this reason in some cases is useful to use a different approach.

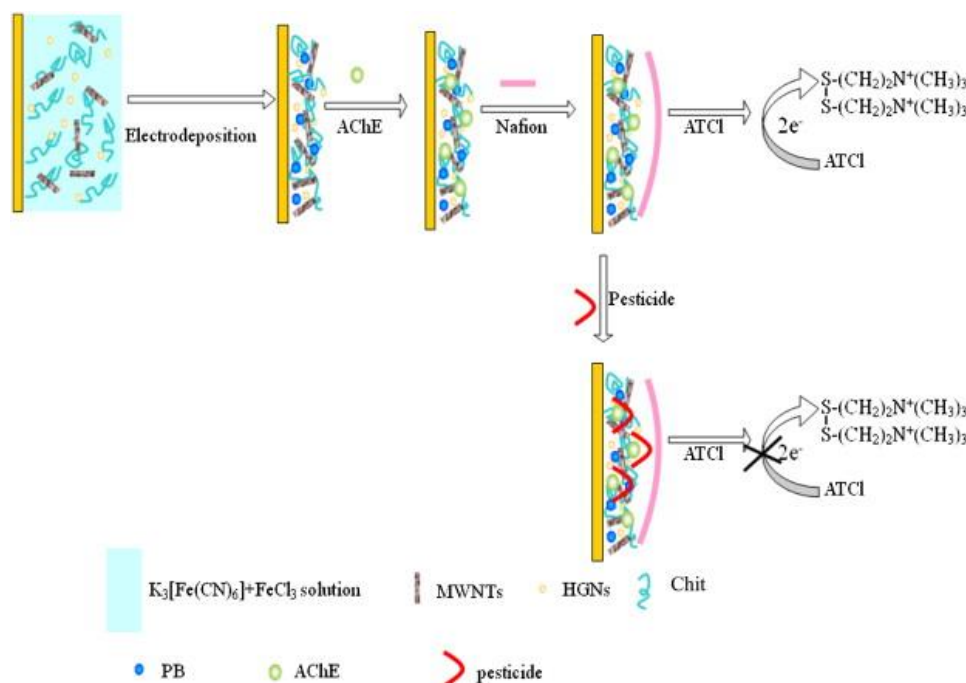


Figure 2.2: Schematic illustration of the stepwise AChE biosensor fabrication process and immobilised AChE inhibition in pesticide solution. Reprinted from *Biosensors and Bioelectronics*, 42, Chen Zhai, Xia Sun, Wenping Zhao, Zhili Gong, Xiangyou Wang, Acetylcholinesterase biosensor based on chitosan/prussian blue/multiwall carbon nanotubes/hollow gold nanospheres nanocomposite film by one-step electrodeposition, 124-130, 2013, with permission from Elsevier [73].

2.1.4.2 Immunosensors

As mentioned above, especially for complex matrices, the use of enzyme inhibition based biosensors for pesticide detection can be affected from the presence of interfering substances and in this case, the response of the biosensor is given from a sum of effects that contribute to the inhibition of the enzymatic activity, losing the quantitative determination of the analyte. The use of immuno-based biosensors can be useful to solve some of these

CHAPTER 2

problems. The interaction between an antibody and its target antigen is characterised from a high selectivity, so antibodies appear as an efficient alternative for the detection of single pesticides or small groups of similar molecules. Furthermore, the use of immunosensors is a very well-known procedure, because of their specificity, low costs and versatility and there are a lot of examples that can be found in literature about the determination of many kinds of different molecules, including pesticides [95, 96]. Above all is known that the antibody-antigen complex can be dissociated using an appropriate dissociating reagent and this, concerning the detection of pesticide, gives the possibility to create reusable devices, very useful for continuous monitoring of real samples or on field analysis. Using an immunosensor the experimental procedure can be summarised in two steps: molecular recognition of the target and transduction process. Determination of pesticide is usually carried out making use of a competitive interaction or a displacement between the analyte and a tracer molecule (that can also be a secondary antibody, labelled with a tracer) or using a second recognition step in which a secondary labelled antibody binds the primary antibody-antigen complex. The transduction technique is related to the chosen label or tracer molecule and various examples are reported using e.g. electrochemical, optical, fluorescent or piezoelectric transduction systems [97]. By the way, it is also known that a competitive label dependent detection is more complex to obtain respect to a direct immuno-assay and in the last years, many examples of label-free immunosensors for pesticide detection can be found, due to the advantage given from their rapidity, low cost and real time response [98, 99].

Although many immunosensors have been reported, the development of new antibodies with desired selectivity and high affinity for any different target and the necessity to be developed using a guest in which to stimulate an immune reaction, finds often difficulties due to the toxicity of some classes of pesticides [100]. In the last years, many reports have proved that nanomaterials can improve electrochemical performance of immunosensors. A disposable amperometric immunosensor for sensitive detection of chlorpyrifos-methyl (CM) has been developed by combining dual signal amplification of platinum colloid with an enzymatic catalytic reaction [101]. This method integrated the advantages of nanotechnology, bioconjugation techniques, enzyme amplification and electrochemical detection for monitoring the CM residues.

Many immunosensor for atrazine detection in different format are present in literature.

Tran et al. described a multifunctional conducting polyquinone film coupled with a monoclonal anti-atrazine antibody for label-free electrochemical detection of atrazine using square wave voltammetry [98]. Atrazine has been covalently immobilised on interdigitated μ -electrodes. Detection of free atrazine has been achieved through a competitive reaction with immobilised atrazine for the antibody added in solution. The detection method has been based on the use of antibodies labelled with gold nanoparticles. Their presence amplified the conductive signal. This biosensor has been suitable for the detection of atrazine in red wines since no matrix effect related to red wine samples have been observed. A schematic representation is reported in Figure 2.3 [102, 103]. Impedimetric immunosensor has been developed by immobilising anti-atrazine antibody modified with histidine-tag onto a polypyrrole (PPy)

CHAPTER 2

film N-substituted by nitrilotriacetic acid (NTA) electrogenerated on a gold electrode. In the presence of atrazine, the interaction of the analyte with the immobilised antibody triggered an increase of the charge transfer resistance proportional to the pesticide concentration. The detection limit has been 4.6×10^{-11} M [104].

Piezoelectric immunosensors are devices based on materials such as quartz crystals with bioreceptor, such as antigens or antibodies, immobilised on their surface, which resonate on application of an external alternating electric field. The biospecific reaction between the two interactive molecules, one immobilized on the surface and the other free in solution, can be followed in real time. Several QCM immunosensors for environmental monitoring have been described, but only few of them were developed for the detection of pesticides. Jia et al. reported a cost-effective protocol to fabricate acoustic micro-immunosensors to measure simultaneously carbofuran and atrazine. It was found that the proposed methodology allows sequential specific detection of $4.5 \mu\text{M}$ and $4.6 \mu\text{M}$ atrazine, respectively [105]. A multi-wall carbon nanotube/poly(amidoamine) dendrimer hybrid material and its application in the fabrication of piezoelectric immunosensing platform has been also described. The immunosensor has been used for the determination of amounts of a carbamate pesticide-metolcarb in spiked apple and orange juice samples analysis [106].

Biosensors based on the field effect transistors and carbon nanotubes have become a suitable system for immunosensor applications because they combine the principles of molecular recognition through the recognition layer with the transduction capabilities of the carbon nanotubes. They

have been used to detect various compounds such as the label-free detection of atrazine with potential application in seawater and riverine water analysis [99].

Among the immunosensors, test strips based on ELISA in combination with lateral flow device for pesticide detection have attracted extensive interest in recent years. Thus, we focused the attention on this kind of immunosensors. In contrast to the above methods, lateral-flow sensors (LFSs) have been applied to detect analytes, due to their unique advantages, such as easy operation, low cost and visualized results, that can be judged directly by the naked eye. Colloidal gold or gold nanoparticles (AuNPs) are commonly used in LFSs. The strip tests have the advantages of being efficient and easy to use for on-site testing of food served or in the food industry, allowing the monitoring of the quality of raw food materials at the early stages of food production. Novel technologies have been summarised in a recent review [107]. The test principle involves a flow of fluid containing the analyte through a porous membrane and into an absorbent pad. It is a rapid (within 5 min) and simple immunoassay for qualitative screening, with the advantage of large volumes of samples, but now its application is often restricted by relatively low sensitivity, especially for the analysis of food contaminants such as chemical pesticides. Blažková et al. have reported a strip-based immunoassay for the rapid detection of thiabendazole in a 1% fruit juice matrix with a limit of detection of about 0.08 ng mL^{-1} [108]. Since matrix interference of food sample is always a problem for immunochemical method, another similar test strip that can detect carbaryl in a 10% fruit juice matrix has been developed [109]. The LOD of this strip is about 5 ng mL^{-1} [110].

CHAPTER 2

With the increasing demand for more efficient and more economical tools for screening of pesticides, multi-analyte rapid testing that detects two or more pesticides simultaneously is one of the rational solutions. The recent development of a multianalyte immunoassay has been reviewed by Yan et al. [111]. A semi quantitative strip immunoassay has been developed Xu et al. for the rapid detection of imidacloprid and thiamethoxam in agricultural products using specific nanocolloidal gold-labelled monoclonal antibodies. The conjugates of imidacloprid–bovine serum albumin (BSA), thiamethoxam– bovine serum albumin and goat anti-mouse IgG have been coated on the nitro-cellulose membrane of the strip, serving as test lines and control line, respectively. In the presence of free imidacloprid and thiamethoxam, free imidacloprid and thiamethoxam compete with the immobilised haptens for the binding site of antibodies labelled nanocolloidal gold. The visual LOD for imidacloprid and thiamethoxam of this strip are 0.5 and 2.0 ng mL⁻¹, respectively, in 2% orange extract.

The multi-analyte testing approach make possible to detect a class of pesticides by one antibody or a specific reaction mechanism that reacts with that class of pesticides. This approach aims to screen particular sample with the maximum limit of a class of pesticide, which is the total quantity of pesticides. The major classes of pesticides include organophosphate and carbamate pesticides. In general, the multi-analyte rapid test of OP and CM are based on the irreversible inhibition of acetylcholinesterase. A gold-labelled antibody test strip that can recognize eight OP pesticides by immunoassay in cabbage, apple and greengrocery has been reported [112]. Although the detection principle of this strip is

the same to the single-analyte immunoassay in which free pesticide competes with hapten for the binding to the colloidal gold antibody, this strip is able to detect eight OP pesticides (parathion-methyl, parathion, fenitrothion, EPN, cyanophos, paraoxon-methyl, paraoxon-ethyl, and fenitrooxon) with LODs ranging from 2.7 to 100.2 ng mL⁻¹.

These multi-analyte testing approaches show their potential in the rapid detection of the total pesticide content of OP and CM pesticide. They are suitable for the initial screening of pesticide residues and followed by the confirmation by conventional analytical methods.

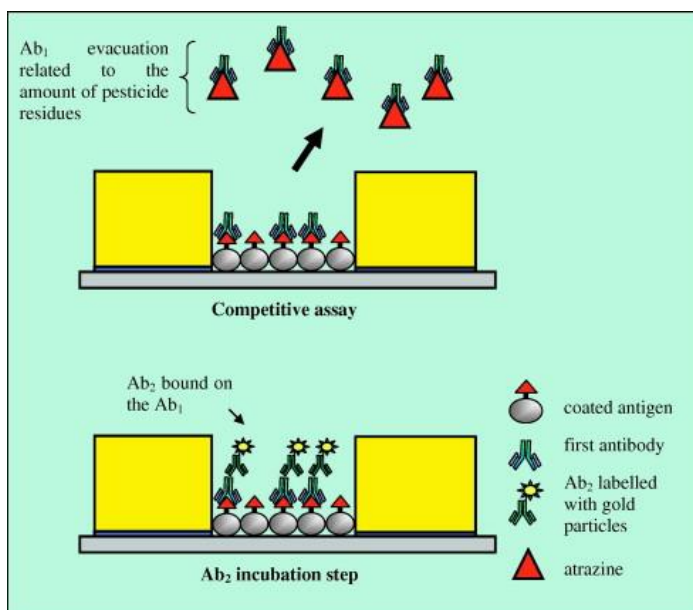


Figure 2.3: Schematic illustration of the conductimetric immunosensor. An amount of the secondary antibody (Ab₂) is bound to the specific antibody (Ab₁). Previously, the amount of Ab₁ bound to the pesticide was evacuated. The amount of gold nanoparticles is indirectly related to the pesticide residue concentration. Reprinted from Food Chemistry, 122, Enrique Valera, Javier Ramón-Azcón, Alejandro Barranco, Begoña Alfaro, Francisco Sánchez-Baeza, M.-P. Marco, Ángel Rodríguez, Determination of atrazine residues in red wine samples. A conductimetric solution, 888-894, 2010, with permission from Elsevier [103].

CHAPTER 2

2.1.4.3 Aptasensors

The main difficulties about the use of bioreceptors in pesticides analysis concern the possibility to isolate biomolecules for targets with high toxicity. In this way, the use of synthetic biomimetic receptors has recently become an interesting alternative in food safety analysis, giving to chemists the possibility to direct synthesise the probe molecule, obtaining high selectivity and specificity [113].

Aptamers are short and single stranded DNA or RNA sequences, selected in vitro using a technique called SELEX (selection evolution of ligands by exponential enrichment) [114, 115] from synthetic oligonucleotides libraries, that are able to bind different kinds of target molecules (e.g. other oligonucleotides, biomarkers or small synthetic molecules such pesticides) with high selectivity and specificity [116]. Compared to antibodies, aptamers show higher detection ranges, a higher stability under different chemical and physical conditions, a prolonged shelf life, and acceptable cross reactivity and can be obtained using efficient and cost effective processes. They can be also easily modified, giving the possibility to obtain various-labelled probe elements [117]. As bio-recognition element, aptamers can be used directly linked to the transducer, both as single [118] or multi [119] target probe (labelled or label-free). Another possible approach is given from the possibility to use aptamer-target interaction to indirectly activate on-off devices in which the interaction with the analyte or the aptamer itself inhibits certain reactivity [120]. Moreover, some studies have shown that aptamers are subjected to significant conformational change caused by the interaction with the analyte that can be used as recognition parameter combining them

with appropriate transducers [121, 122]. Various aptamer-based bioassays including fluorescent, colorimetric, and electrochemical methods have been developed and extensively adopted for an impressively wide variety of applications. A recent review discusses several transduction systems and their principles used in aptamer based nanosensors, which have been developed in the last years [123]. According to our knowledge, at present time, only a few aptamer-based pesticides detection sensors have been developed.

Kwon et al. has recently described a sensitive detection of iprobenfos (IBF) and edifenphos (EDI) by using an aptamer-based colorimetric multi-aptasensor. Both pesticides IBF and EDI can be eventually detected in a range from 10 nM to 5 nM, respectively. This multi-aptasensor has been then implemented in spiked rice samples, obtaining accuracies around 80 and 90% in spiked paddy and polished rice samples, respectively [124]. A schematic representation is reported in Figure 2.4. Recently, a DNA aptamer specific for acetamiprid has been described [125]. A simple aptasensor for sensitive and selective detection of acetamiprid has been developed based on electrochemical impedance spectroscopy. To improve sensitivity of the aptasensor, gold nanoparticles were electrodeposited on the bare gold electrode surface by cyclic voltammetry, which has been employed as a platform for aptamer immobilization. With the addition of acetamiprid, the formation of acetamiprid-aptamer complex on the AuNPs-deposited electrode surface resulted in an increase of electron transfer resistance (R_{et}). A wide linear range was obtained from 5 to 600 nM with a low detection limit of 1 nM. Besides, the applicability of the developed aptasensor has been successfully evaluated by determining acetamiprid in the real samples, wastewater and tomatoes [118]. The same aptamers have been then successfully used with an innovative approach,

CHAPTER 2

developing an electrochemical assay based on a sandwich interaction with the pesticide acetamiprid. The aptasensor has been able to obtain a linear response in the concentration range 0-200 nM in water solution [126].

A simple and selective aptamer-based colorimetric method has also been developed for highly sensitive detection of acetamiprid, taking advantages of the sensitive target-induced colour changes that result from the inter-particle plasmon coupling during the aggregation of Au nanoparticles. The results showed that the established method could be applied to detect acetamiprid in the linear range between 7.5×10^{-6} M to 7.5×10^{-3} M, with a low detection limit of 5×10^{-6} M. The practical application of the colorimetric method has been realised for detecting acetamiprid in real soil samples and monitoring its natural degradation process [127]. New silver dendrites pesticide SERS sensor conjugated with aptamers through silver-thiol bonds that targets isocarbophos, omethoate, phorate and profenofos pesticides has been developed [119]. The silver dendrites are filled with a small blocker molecule to allow the conjugated aptamer to change its 3D conformation during the capture of pesticides and to eliminate non-specific binding on Ag particles. This technique is specific to the four-targeted pesticides and the changes of Raman peak of Ag dendrites can be statistically quantified. The limit of detection of isocarbophos, omethoate, phorate, and profenofos pesticides are 1, 5, 0.1 and 5 ng mL⁻¹, respectively and the total analytical time for six samples is 40 min.

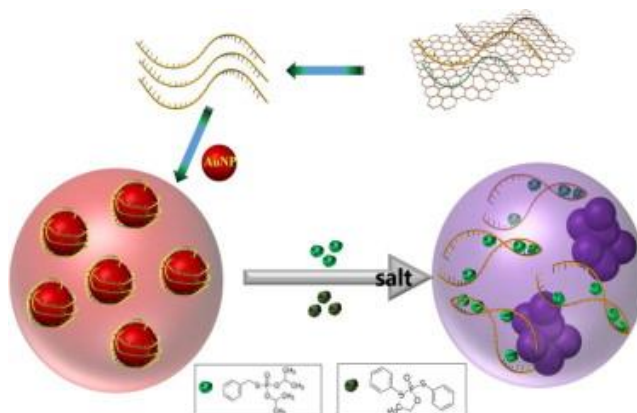


Figure 2.4: Schematic illustration of the aptasensor: sensitive detection of iprobenfos (IBF) and edifenphos (EDI) has been successfully conducted by using a colorimetric method. Reprinted from *Analytica Chimica Acta*, 868, Young Seop Kwon, Van-Thuan Nguyen, Je Gun Park, Man Bock Gu, Detection of Iprobenfos and Edifenphos using a new Multi-aptasensor, 60-66, 2015, with permission from Elsevier [124].

2.1.4.4 Molecularly imprinted polymers

Whereas aptamers are synthetic receptors realised using biological “building blocks”, molecularly imprinted polymers (MIPs) are realised generating specific recognition sites on polymeric nanoparticles in order to mimic a biological receptor [128-130]. MIPs are synthesised using a template-assisted approach: functional monomers form a complex with the template (that will be the analytical target) and then the polymerisation is started, using an appropriate solvent. Removing then the template by extensive washing steps (to break the template-monomers interactions), allows the polymer to maintain specific recognition sites, complementary to the template in size, shape and position of interacting functional groups [131]. The choice of the chemical reagents to synthesise the MIPs must be done in order to create highly specific cavities designed for the template molecule and, for this reason, a computational modelling study is usually carried out to develop the synthesis [132, 133]. At present time, many MIPs-based biosensors have been developed [134]. Even if MIPs are characterised by a high affinity to the target, they show some

CHAPTER 2

disadvantages involving the low binding capacity (and possible low site accessibility) and a slow binding kinetic, given from the rigidity of the polymeric matrix that forms the particles [135]. Recent advances in molecularly imprinted polymers in food analysis are present in literature [136, 137].

Electrochemical sensors based on molecularly imprinted polymers have been developed recently. These sensors show high selectivity towards the target molecules: for this reason, MIPs have been described as artificial locks for target molecules. A variety of MIP-based sensors have been reported such as the amperometric sensor based on metolcarb-imprinted film [138] and molecularly imprinted polymers/sol-gel sensor for methidathion organophosphorous insecticide recognition [139]. To improve the characteristics of MIPs used as biomimetic-recognition agent, nanomaterials are intensively used, as support or signal mediator [140], through electrochemical transducers or in combination with them [139]. Examples of combination between MIPs and enzymes have also been developed [141].

A novel composite of vinyl group-functionalised multiwalled carbon nanotubes molecularly imprinted polymer has been synthesised and applied as recognition element to build an electrochemical sensor for parathion-methyl. The response of the MIP-based sensor has been linearly proportional to the concentration of parathion-methyl over the range of $2.0 \cdot 10^{-7}$ to $1.0 \cdot 10^{-5}$ M with a lower detection limit of $6.7 \cdot 10^{-8}$ M. This sensor has been also successfully applied in the detection of parathion-methyl in pear and cucumber samples [142].

A novel potentiometric sensor with high selectivity in addition to sensitivity has been developed for the determination of lindane, γ -hexachlorocyclohexane (γ -HCCH), based on the modification of MWCNT-imprinted polymer film onto the surface of a Cu electrode. The sensor responds to γ -HCCH in the range $1 \times 10^{-10} - 1 \times 10^{-3} \text{ M}$ and the detection limit has been found to be $1.0 \times 10^{-10} \text{ M}$ [143].

Tan et al. realised a MIP sensor based on glassy carbon electrode decorated by reduced graphene oxide and gold nanoparticles for the detection of carbofuran (CBF). The sensor exhibited high adsorption capacity and good selectivity for CBF and it has been successfully applied to the detection of CBF in real vegetable samples [144].

MIP based-sensor to detect methidathion in wastewater samples has been proposed. The sensing platform has been architected by the combination of a molecularly imprinted technique and sol-gel method on an inexpensive, portable and disposable screen-printed carbon electrode surface. Electrochemical impedimetric detection technique has been employed to perform the label free detection of the target analyte on the designed MIP/sol-gel integrated platform [139].

A rapid, selective, and sensitive double-template imprinted polymer nanofilm-modified pencil graphite electrode has been fabricated for the simultaneous analysis of phosphorus-containing amino acid-type herbicides (glyphosate and glufosinate) in soil and human serum samples [145].

A new biomimetic sensor based on molecularly imprinted polymers for the determination of herbicide hexazinone has been proposed from Taboada Sotomayor et al. [146]. The MIP, containing recognition sites for

CHAPTER 2

hexazinone, has been prepared with a functional monomer selected by means of molecular modelling. A schematic representation is reported in Figure 2.5.

Some piezoelectric sensors using molecularly imprinted polymer have been developed for fast and on-site determination of pesticides in contaminated foods. Liu et al. described a highly selective and sensitive quartz crystal microbalance realised by mixing with polyvinyl chloride and molecularly imprinted polymer microspheres for rapid endosulfan detection. Detection of pesticide in water and milk samples has been observed with recoveries of 96.0 - 104.1% and 101.8 - 108.0% respectively [147]. Özkütük et al. presented a sensor based on the modification of molecular imprinted film for the determination of paraoxon. The study also included the measurement of binding interaction quartz crystal microbalance sensor, selectivity experiments and analytical performance of quartz crystal microbalance [148].

Atrazine detection in wastewater has been reported by imprinted p(HEMA-phenol) film on gold surface of a QCM chip. The developed QCM sensor shows high sensitivity and selectivity for determination of trace ATR in wastewater.

A chemiluminescence sensor for the determination of glyphosate has been made-up based on molecularly imprinted polymer [149].

Wang et al. developed a paper-based, multidisc plate grafted with MIPs for chemiluminescence detection of pesticides. They focused on the challenges e.g. low-cost, portable, fast and easy-to-set up detection for public use, and proposed grafting MIPs onto cellulose fibres in paper

disks. By this approach, they achieved the detection of target pesticide at the femtomolar level under optimised conditions [150].

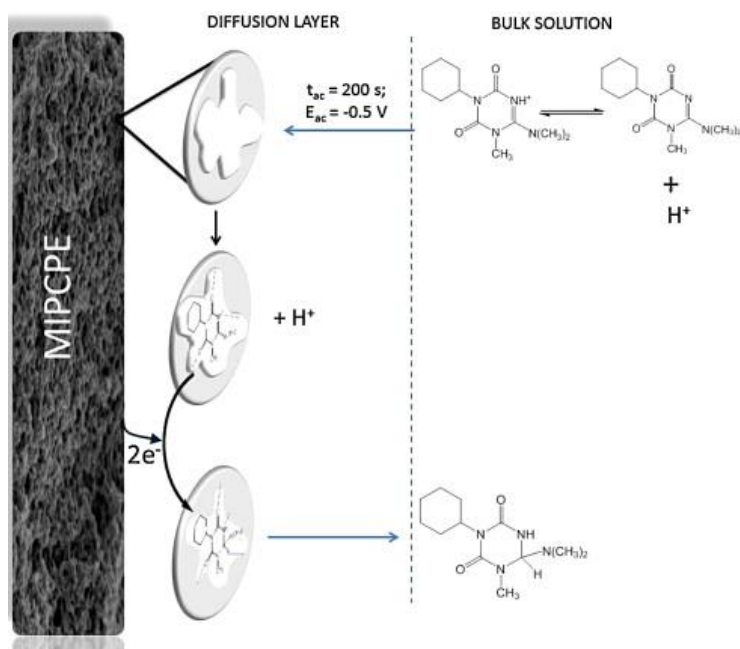


Figure 2.5: Schematic representation of the hexazinone (HXZ) sensor response. In the first step, an accumulation potential (-0.5 V) is used to pre-concentrate HXZ within the MIP cavities of the paste, after which the applied potential resulted in quantitative reduction of HXZ (in an acidic medium) and its return to the solution. Reprinted from *Sensors and Actuators B: Chemical*, 208, Maricely Janette Uria Toro, Luiz Diego Marestoni, Maria Del Pilar, Taboada Sotomayor, A new biomimetic sensor based on molecularly imprinted polymers for highly sensitive and selective determination of hexazinone herbicide, 299-306, 2015, with permission from Elsevier [146].

2.1.5 Conclusions and future perspectives

The widespread application of pesticides in the last decades and the continuous increase of their use nowadays have brought to an enormous diffusion of these compounds in the environment. The variety of their chemical classes and of the degradation processes, in which are they subjected in the environment, make their intrinsic toxicity even more dangerous, because not only the active molecules but also their metabolites can contaminate crops and food, reaching the human food chain. Their toxicity derives from their general stability, mobility,

CHAPTER 2

bioaccumulation and long-term effects on living organisms, including plants, in which pesticides can accumulate and reach mammals. Crops represent the main food source for humans and the quality of the related products is extremely important, in order to protect health consumers. Safe food should contain the less amount possible of dangerous residues from the cultivation and, for this reason, the control of pesticides and their residues for food safety remains one of the most crucial target for analytical chemistry. Monitoring should be constant during the entire food processing chain, from the production of raw ingredients to the sale; however, due to the difficulties related to pesticides detection (mainly caused because of their low concentration in food samples), continuous developments are necessary in order to obtain new and powerful analytical tools. In this way, biosensors represent a valid alternative to classical analytical techniques, due to their low cost, fast response and simplicity of use.

A summary of the recent developments in sensing of pesticide for food safety analysis has been provided. As described, in recent years there has been an intense growth of systems based on bio- or bio-mimetic molecules for pesticides detection, using assays based on biological macromolecules like enzymes or antibodies, synthetic biomolecules like aptamers and artificial macromolecules like MIPs. A great investigation has been made in order to improve the analytical parameters, like sensitivity, selectivity and response, and the chemical and physical ones, like the stability and the number of turnover, using innovative immobilisation approaches, new materials (even nanostructured) and different transducers. Despite the good results achieved, sensing of pesticide via biosensors still shows some

limits in order to become a wide accepted and applicable approach, especially concerning the application in real samples. Nevertheless, their potential for environmental analytical purposes has not been much explored and this makes their development one of the most fascinating targets in analytical chemistry.

2.2 References

- [1] FAO/WHO Joint Meeting on Pesticide Specifications (JMPS), Available only on the Internet (who.int/iris/handle/10665/44527): 2010.
- [2] G.W. Ware, J. Ariz. Acad. Sci., 9: 61-65, 1974.
- [3] N. Verma, A. Bhardwaj, Appl Biochem Biotechnol, 175: 3093-3119, 2015.
- [4] T. Cairns, J. Sherma (Eds.), Emerging strategies for pesticide analysis, CRC Press 1992.
- [5] J. Fenik, M. Tankiewicz, M. Biziuk, TrAC, Trends Anal. Chem., 30: 814-826, 2011.
- [6] M. Tankiewicz, J. Fenik, M. Biziuk, TrAC, Trends Anal. Chem., 29: 1050-1063, 2010.
- [7] Y. Song, Y. Ge, Y. Zhang, B. Liu, Y. Lu, T. Dong, S. Wang, Anal Bioanal Chem, 393: 2001-2008, 2009.
- [8] J. Walker, S. Asher, Anal Chem, 77: 1596-1600, 2005.
- [9] J. Whiteaker, K. Prather, Anal Chem, 75: 49-56, 2003.
- [10] C.E. Handford, C.T. Elliott, K. Campbell, Integr Environ Assess Manag, 11: 525-536, 2015.
- [11] C. Lesueur, P. Knittl, M. Gartner, A. Mentler, M. Fuerhacker, Food Control, 19: 906-914, 2008.
- [12] C. Lesueur, M. Gartner, A. Mentler, M. Fuerhacker, Talanta, 75: 284-293, 2008.
- [13] S. Liu, Z. Zheng, X. Li, Anal Bioanal Chem, 405: 63-90, 2013.
- [14] T.D. Sterling, A.V. Arundel, Scand. J. Work Environ. Health, 12: 161-173, 1986.
- [15] S.K. Hoar, A. Blair, F.F. Holmes, et al., JAMA, 256: 1141-1147, 1986.

- [16] Y. Blume, D.J. Durzan, P. Smertenko (Eds.), Effects of Chlorsulfuron on Early Embryo Development in Norway Spruce Cell Suspensions, in: Cell Biology and Instrumentation: UV Radiation, Nitric Oxide, and Cell Death in Plants IOS Press 2006.
- [17] P. Tchounwou, B. Wilson, A. Ishaque, R. Ransome, M.-J. Huang, J. Leszczynski, *Int. J. Mol. Sci.*, 1: 63-74, 2000.
- [18] M. Abdollahi, A. Ranjbar, S. Shadnia, S. Nikfar, A. Rezaiee, *Med Sci Rev*, 10: RA141-RA147, 2004.
- [19] K. Mwila, M.H. Burton, J.S. Van Dyk, B.I. Pletschke, *Environ Monit Assess*, 185: 2315-2327, 2013.
- [20] M.P. Longnecker, W.J. Rogan, G. Lucier, *Annu. Rev. Public Health*, 18: 211-244, 1997.
- [21] A. Ranjbar, P. Pasalar, M. Abdollahi, *Hum Exp Toxicol*, 21: 179-182, 2002.
- [22] M.V. Kumar, T. Desiraju, *Toxicology*, 75: 13-20, 1992.
- [23] L.G. Costa, G. Giordano, M. Guizzetti, A. Vitalone, *Front Biosci*, 13: 1240-1249, 2008.
- [24] S. Feng, Z. Kong, X. Wang, P. Peng, E.Y. Zeng, *Ecotoxicol Environ Saf*, 61: 239-246, 2005.
- [25] A.Y. Kocaman, M. Topaktas, *Environ. Mol. Mutag.*, 48: 483-490, 2007.
- [26] T. Pastoor, *Toxicol. Sci.*, 86: 56-60, 2005.
- [27] H.P.M. Vijverberg, J. vanden Bercken, *Crit. Rev. Toxicol.*, 21: 105-126, 1990.
- [28] G. Meco, V. Bonifati, N. Vanacore, E. Fabrizio, *Scand. J. Work Environ. Health*, 20: 301-305, 1994.

CHAPTER 2

- [29] L. Gray, J. Ostby, J. Furr, C. Wolf, C. Lambright, L. Parks, D. Veeramachaneni, V. Wilson, M. Price, A. Hotchkiss, *Apmis*, 109: S302-S319, 2001.
- [30] C. Sanfeliu, J. Sebastia, R. Cristofol, E. Rodriguez-Farre, *Neurotox Res*, 5: 283-305, 2003.
- [31] J. Pope, M. Skurky-Thomas, C. Rosen, *Toxicity, Organochlorine Pesticides*, Emedicine, 1994.
- [32] C. De Jong, *Toxicol. Lett.*, 1-206, 1991.
- [33] J.L. Tadeo (Ed.) *Pesticides: classification and properties*, in: *Analysis of pesticides in food and environmental samples* CRC Press, United States of America, 2008.
- [34] K. Lányi, Z. Dinya, *Microchem. J.*, 80: 79-87, 2005.
- [35] J. Bethsass, A. Colangelo, *Int. J. Occup. Environ. Health*, 12: 260-267, 2006.
- [36] P. Jovanov, V. Guzsvany, M. Franko, S. Lazic, M. Sakac, B. Saric, V. Banjac, *Talanta*, 111: 125-133, 2013.
- [37] E. Caldas, M. Conceição, M.C.C. Miranda, L.C.K.R. de Souza, J. Lima, *J. Agric. Food. Chem.*, 49: 4521-4525, 2001.
- [38] R. Noon (Ed.) *New developments in fungicides: 2004 edition*, PJB Publications 2004.
- [39] F.P. Kaloyanova, M.A. El Batawi (Eds.), *Human toxicology of pesticides*, CRC press 1991.
- [40] P.W.T. Poole (Ed.) *FOOD AND NUTRITIONAL ANALYSIS | Pesticide Residues*, in: *Encyclopedia of Analytical Science (Second Edition)* Elsevier, Oxford, 2005.

- [41] P.W.T. Poole (Ed.) FOOD AND NUTRITIONAL ANALYSIS | Sample Preparation, in: Encyclopedia of Analytical Science (Second Edition) Elsevier, Oxford, 2005.
- [42] J. Pan, X.X. Xia, J. Liang, Ultrason. Sonochem., 15: 25-32, 2008.
- [43] A. Juan-Garcia, J. Manes, G. Font, Y. Pico, J. Chromatogr. A, 1050: 119-127, 2004.
- [44] D. Stajnbaher, L. Zupancic-Kralj, J. Chromatogr. A, 1015: 185-198, 2003.
- [45] J.L. Martínez Vidal, P. Plaza-Bolaños, R. Romero-González, A. Garrido Frenich, J. Chromatogr. A, 1216: 6767-6788, 2009.
- [46] E. Sobhanzadeh, N.K.A. Bakar, M.R. Abas, K. Nemati, Mal. J. Fund. Appl. Sci., 5: 2014.
- [47] F.J. Schenck, S.J. Lehotay, J. Chromatogr. A, 868: 51-61, 2000.
- [48] Z. Sharif, Y.B.C. Man, N.S.A. Hamid, C.C. Keat, J. Chromatogr. A, 1127: 254-261, 2006.
- [49] G.G. Birch, G. Campbell-Platt (Eds.), Consumer perceptions of food safety and their impact on food choice, in: Food safety—the challenge ahead Intercept, Andover, 1993.
- [50] A. Wilcock, M. Pun, J. Khanona, M. Aung, Trends Food Sci. Technol., 15: 56-66, 2004.
- [51] A. Amine, H. Mohammadi, I. Bourais, G. Palleschi, Biosens Bioelectron, 21: 1405-1423, 2006.
- [52] J.S. Van Dyk, B. Pletschke, Chemosphere, 82: 291-307, 2011.
- [53] G. Jeanty, A. Wojciechowska, J.L. Marty, M. Trojanowicz, Anal Bioanal Chem, 373: 691-695, 2002.
- [54] A.P. Periasamy, Y. Umasankar, S.M. Chen, Sensors (Basel), 9: 4034-4055, 2009.
- [55] S. Andreescu, J.L. Marty, Biomol. Eng., 23: 1-15, 2006.

CHAPTER 2

- [56] J. Wang, R. Krause, K. Block, M. Musameh, A. Mulchandani, M.J. Schoning, *Biosens Bioelectron*, 18: 255-260, 2003.
- [57] P. Mulchandani, W. Chen, A. Mulchandani, J. Wang, L. Chen, *Biosens Bioelectron*, 16: 433-437, 2001.
- [58] A. Mulchandani, W. Chen, P. Mulchandani, J. Wang, K.R. Rogers, *Biosens Bioelectron*, 16: 225-230, 2001.
- [59] B.G. Choi, H. Park, T.J. Park, M.H. Yang, J.S. Kim, S.-Y. Jang, N.S. Heo, S.Y. Lee, J. Kong, W.H. Hong, *ACS nano*, 4: 2910-2918, 2010.
- [60] J.H. Lee, J.Y. Park, K. Min, H.J. Cha, S.S. Choi, Y.J. Yoo, *Biosensors Bioelectron.*, 25: 1566-1570, 2010.
- [61] D. Du, W. Chen, W. Zhang, D. Liu, H. Li, Y. Lin, *Biosensors Bioelectron.*, 25: 1370-1375, 2010.
- [62] Y. Zhao, W. Zhang, Y. Lin, D. Du, *Nanoscale*, 5: 1121-1126, 2013.
- [63] A. Amine, F. Arduini, D. Moscone, G. Palleschi, *Biosensors Bioelectron.*, 76: 180-194, 2016.
- [64] V. Scognamiglio, F. Arduini, G. Palleschi, G. Rea, *TrAC, Trends Anal. Chem.*, 62: 1-10, 2014.
- [65] W.Y. Zhang, A.M. Asiri, D.L. Liu, D. Du, Y.H. Lin, *TrAC, Trends Anal. Chem.*, 54: 1-10, 2014.
- [66] G. Marrazza, *Biosensors (Basel)*, 4: 301-317, 2014.
- [67] Y. Liu, G. Wang, C. Li, Q. Zhou, M. Wang, L. Yang, *Mater Sci Eng C Mater Biol Appl*, 35: 253-258, 2014.
- [68] K.A. Hassall (Ed.) *Biochemistry and uses of pesticides*, Macmillan Press Ltd 1990.
- [69] A. Simonian, E. Efremenko, J. Wild, *Anal Chim Acta*, 444: 179-186, 2001.

- [70] F. Berti, L. Lozzi, I. Palchetti, S. Santucci, G. Marrazza, *Electrochim. Acta*, 54: 5035-5041, 2009.
- [71] F. Berti, C. Eisenkolbl, D. Minocci, P. Nieri, A.M. Rossi, M. Mascini, G. Marrazza, *J. Electroanal. Chem.*, 656: 55-60, 2011.
- [72] L. Rotariu, L.-G. Zamfir, C. Bala, *Anal Chim Acta*, 748: 81-88, 2012.
- [73] C. Zhai, X. Sun, W. Zhao, Z. Gong, X. Wang, *Biosensors Bioelectron.*, 42: 124-130, 2013.
- [74] D. Du, M. Wang, J. Cai, A. Zhang, *Sensors Actuators B: Chem.*, 146: 337-341, 2010.
- [75] D. Du, M. Wang, J. Cai, Y. Qin, A. Zhang, *Sensors Actuators B: Chem.*, 143: 524-529, 2010.
- [76] R.-S. Saberi, S. Shahrokhian, G. Marrazza, *Electroanalysis*, 25: 1373-1380, 2013.
- [77] Z. Taleat, A. Ravalli, M. Mazloun-Ardakani, G. Marrazza, *Electroanalysis*, 25: 269-277, 2013.
- [78] Z. Taleat, A. Khoshroo, M. Mazloun-Ardakani, *Microchimica Acta*, 181: 865-891, 2014.
- [79] D. Du, X. Ye, J. Cai, J. Liu, A. Zhang, *Biosensors Bioelectron.*, 25: 2503-2508, 2010.
- [80] Z.-j. Shang, Y.-l. Xu, Y. Wang, D.-x. Wei, L.-l. Zhan, *Procedia Eng.*, 15: 4480-4485, 2011.
- [81] Y. Li, Y. Bai, G. Han, M. Li, *Sensors Actuators B: Chem.*, 185: 706-712, 2013.
- [82] R. Xue, T.-F. Kang, L.-P. Lu, S.-Y. Cheng, *Anal. Lett.*, 46: 131-141, 2013.
- [83] L. Yang, G. Wang, Y. Liu, M. Wang, *Talanta*, 113: 135-141, 2013.
- [84] P. Nayak, B. Anbarasan, S. Ramaprabhu, *J. Phys. Chem. C*, 117: 13202-13209, 2013.

CHAPTER 2

- [85] A. Ravalli, G.P. dos Santos, M. Ferroni, G. Faglia, H. Yamanaka, G. Marrazza, *Sensors Actuators B: Chem.*, 179: 194-200, 2013.
- [86] Y. Wang, S. Zhang, D. Du, Y. Shao, Z. Li, J. Wang, M.H. Engelhard, J. Li, Y. Lin, *J. Mater. Chem.*, 21: 5319-5325, 2011.
- [87] L. Zhang, L. Long, W. Zhang, D. Du, Y. Lin, *Electroanalysis*, 24: 1745-1750, 2012.
- [88] Y. Yang, A.M. Asiri, D. Du, Y. Lin, *Analyst*, 139: 3055-3060, 2014.
- [89] T. Liu, H. Su, X. Qu, P. Ju, L. Cui, S. Ai, *Sensors Actuators B: Chem.*, 160: 1255-1261, 2011.
- [90] J. Dong, T. Liu, X. Meng, J. Zhu, K. Shang, S. Ai, S. Cui, *J. Solid State Electrochem.*, 16: 3783-3790, 2012.
- [91] X. Meng, J. Wei, X. Ren, J. Ren, F. Tang, *Biosensors Bioelectron.*, 47: 402-407, 2013.
- [92] A. Hatefi-Mehrjardi, *Electrochim. Acta*, 114: 394-402, 2013.
- [93] T.M. Oliveira, M.F. Barroso, S. Morais, M. Araújo, C. Freire, P. de Lima-Neto, A.N. Correia, M.B. Oliveira, C. Delerue-Matos, *Bioelectrochemistry*, 98: 20-29, 2014.
- [94] C. Tortolini, P. Bollella, R. Antiochia, G. Favero, F. Mazzei, *Sensors Actuators B: Chem.*, 224: 552-558, 2016.
- [95] D. Ying, W. JiHua, H. Ping, M. Shuai, F. XiaoYuan, *JFSQ*, 6: 2976-2980, 2015.
- [96] G. Liu, W. Guo, D. Song, *Biosens Bioelectron*, 52: 360-366, 2014.
- [97] R. Toonika (Ed.) *Impedimetric Immunosensor for Pesticide Detection*, in: *State of the Art in Biosensors - Environmental and Medical Applications InTech* 2013.

- [98] H.V. Tran, R. Yougnia, S. Reisberg, B. Piro, N. Serradji, T.D. Nguyen, L.D. Tran, C.Z. Dong, M.C. Pham, *Biosens Bioelectron.*, 31: 62-68, 2012.
- [99] N. Belkhamssa, C.I.L. Justino, P.S.M. Santos, S. Cardoso, I. Lopes, A.C. Duarte, T. Rocha-Santos, M. Ksibi, *Talanta*, 146: 430-434, 2016.
- [100] B. Van Dorst, J. Mehta, K. Bekaert, E. Rouah-Martin, W. De Coen, P. Dubruel, R. Blust, J. Robbens, *Biosensors Bioelectron.*, 26: 1178-1194, 2010.
- [101] W. Wei, X. Zong, X. Wang, L. Yin, Y. Pu, S. Liu, *Food Chem.*, 135: 888-892, 2012.
- [102] E. Valera, D. Muñiz, Á. Rodríguez, *Microelectron. Eng.*, 87: 167-173, 2010.
- [103] E. Valera, J. Ramón-Azcón, A. Barranco, B. Alfaro, F. Sánchez-Baeza, M.-P. Marco, Á. Rodríguez, *Food Chem.*, 122: 888-894, 2010.
- [104] R.E. Ionescu, C. Gondran, L. Bouffier, N. Jaffrezic-Renault, C. Martelet, S. Cosnier, *Electrochim. Acta*, 55: 6228-6232, 2010.
- [105] K. Jia, P.-M. Adam, R.E. Ionescu, *Sensors Actuators B: Chem.*, 188: 400-404, 2013.
- [106] M. Pan, L. Kong, B. Liu, K. Qian, G. Fang, S. Wang, *Sensors Actuators B: Chem.*, 188: 949-956, 2013.
- [107] J. Chiou, A.H.H. Leung, H.W. Lee, W.-t. Wong, *J. Integr. Agric.*, 14: 2243-2264, 2015.
- [108] M. Blažková, P. Rauch, L. Fukal, *Biosensors Bioelectron.*, 25: 2122-2128, 2010.
- [109] B. Holubová-Mičková, M. Blažková, L. Fukal, P. Rauch, *Eur. Food Res. Technol.*, 231: 467-473, 2010.

CHAPTER 2

- [110] W. Zheng, GB 2763-2014: Translated English PDF of Chinese Standard GB2763-2014: National food safety standard - Maximum Residue Limits for Pesticides in Food, chinesestandard.net, 2015.
- [111] X. Yan, H. Li, Y. Yan, X. Su, *Anal. Methods*, 6: 3543-3554, 2014.
- [112] X. Hua, J. Yang, L. Wang, Q. Fang, G. Zhang, F. Liu, *PLoS One*, 7: e53099, 2012.
- [113] D.P. Nikolelis, A. Erdem, G.-P. Nikoleli, T. Varzakas (Eds.), *Portable Biosensing of Food Toxicants and Environmental Pollutants*, CRC Press 2013.
- [114] C. Tuerk, L. Gold, *Science*, 249: 505-510, 1990.
- [115] A.D. Ellington, J.W. Szostak, *Nature*, 346: 818-822, 1990.
- [116] J.H. Lee, M.V. Yigit, D. Mazumdar, Y. Lu, *Adv Drug Deliv Rev*, 62: 592-605, 2010.
- [117] T. Tang, J. Deng, M. Zhang, G. Shi, T. Zhou, *Talanta*, 146: 55-61, 2016.
- [118] L. Fan, G. Zhao, H. Shi, M. Liu, Z. Li, *Biosens Bioelectron*, 43: 12-18, 2013.
- [119] S. Pang, T.P. Labuza, L. He, *Analyst*, 139: 1895-1901, 2014.
- [120] P. Weerathunge, R. Ramanathan, R. Shukla, T.K. Sharma, V. Bansal, *Anal Chem*, 86: 11937-11941, 2014.
- [121] T. Hermann, D.J. Patel, *Science*, 287: 820-825, 2000.
- [122] D.J. Patel, A.K. Suri, *J. Biotechnol.*, 74: 39-60, 2000.
- [123] R. Sharma, K. Ragavan, M. Thakur, K. Raghavarao, *Biosensors Bioelectron.*, 74: 612-627, 2015.
- [124] Y.S. Kwon, V.T. Nguyen, J.G. Park, M.B. Gu, *Anal Chim Acta*, 868: 60-66, 2015.

- [125] J. He, Y. Liu, M. Fan, X. Liu, *J Agric Food Chem*, 59: 1582-1586, 2011.
- [126] R. Rapini, G. Marrazza, DNA technology for small molecules sensing: a new approach for Acetamiprid detection, Trento, 2015.
- [127] H. Shi, G. Zhao, M. Liu, L. Fan, T. Cao, *J Hazard Mater*, 260: 754-761, 2013.
- [128] R.V. Shutov, A. Guerreiro, E. Moczko, I.P. de Vargas-Sansalvador, I. Chianella, M.J. Whitcombe, S.A. Piletsky, *Small*, 10: 1086-1089, 2014.
- [129] T. Panasyuk, V. Campo Dall'Orto*, G. Marrazza, A. El'skaya, S. Piletsky**, I. Rezzano, M. Mascini**, *Anal. Lett.*, 31: 1809-1824, 1998.
- [130] F. Berti, S. Todros, D. Lakshmi, M.J. Whitcombe, I. Chianella, M. Ferroni, S.A. Piletsky, A.P. Turner, G. Marrazza, *Biosensors Bioelectron.*, 26: 497-503, 2010.
- [131] A. Poma, A. Guerreiro, M.J. Whitcombe, E.V. Piletska, A.P. Turner, S.A. Piletsky, *Adv. Funct. Mater.*, 23: 2821-2827, 2013.
- [132] D. Lakshmi, M. Akbulut, P.K. Ivanova-Mitseva, M.J. Whitcombe, E.V. Piletska, K. Karim, O. Güven, S.A. Piletsky, *Ind. Eng. Chem. Res.*, 52: 13910-13916, 2013.
- [133] P.S. Sharma, F. D'Souza, W. Kutner, *TrAC, Trends Anal. Chem.*, 34: 59-77, 2012.
- [134] D.P. Nikolelis, A. Erdem, G.-P. Nikoleli, T. Varzakas (Eds.), *Molecularly Imprinted Polymer-Based Biosensors Portable Biosensing of Food Toxicants and Environmental Pollutants*, in: *Portable Biosensing of Food Toxicants and Environmental Pollutants* CRC Press 2013.
- [135] C. Xie, B. Liu, Z. Wang, D. Gao, G. Guan, Z. Zhang, *Anal Chem*, 80: 437-443, 2008.
- [136] X.L. Song, S.F. Xu, L.X. Chen, Y.Q. Wei, H. Xiong, *J. Appl. Polym. Sci.*, 131: 2014.

CHAPTER 2

- [137] V. Suryanarayanan, C.T. Wu, K.C. Ho, *Electroanalysis*, 22: 1795-1811, 2010.
- [138] M.-F. Pan, G.-Z. Fang, B. Liu, K. Qian, S. Wang, *Anal Chim Acta*, 690: 175-181, 2011.
- [139] I. Bakas, A. Hayat, S. Piletsky, E. Piletska, M.M. Chehimi, T. Noguer, R. Rouillon, *Talanta*, 130: 294-298, 2014.
- [140] Y. Zhao, Y. Ma, H. Li, L. Wang, *Anal Chem*, 84: 386-395, 2012.
- [141] B.O. Najwa, B. Idriss, I. Georges, A.-I. Ihya, A.-A. Elhabib, R. Régis, N. Thierry, *Science*, 2: 1-6, 2014.
- [142] D. Zhang, D. Yu, W. Zhao, Q. Yang, H. Kajiura, Y. Li, T. Zhou, G. Shi, *Analyst*, 137: 2629-2636, 2012.
- [143] T.S. Anirudhan, S. Alexander, *Biosensors Bioelectron.*, 64: 586-593, 2015.
- [144] X. Tan, Q. Hu, J. Wu, X. Li, P. Li, H. Yu, X. Li, F. Lei, *Sensors Actuators B: Chem.*, 2015.
- [145] B.B. Prasad, D. Jauhari, M.P. Tiwari, *Biosensors Bioelectron.*, 59: 81-88, 2014.
- [146] M.J.U. Toro, L.D. Marestoni, M.D.P.T. Sotomayor, *Sensors Actuators B: Chem.*, 208: 299-306, 2015.
- [147] N. Liu, J. Han, Z. Liu, L. Qu, Z. Gao, *Anal. Methods*, 5: 4442-4447, 2013.
- [148] E.B. Özkütük, S.E. Diltemiz, E. Özalp, R. Say, A. Ersöz, *Mater. Sci. Eng., C*, 33: 938-942, 2013.
- [149] P. Zhao, M. Yan, C. Zhang, R. Peng, D. Ma, J. Yu, *Spectrochim. Acta, Pt. A: Mol. Biomol. Spectrosc.*, 78: 1482-1486, 2011.
- [150] S. Wang, L. Ge, L. Li, M. Yan, S. Ge, J. Yu, *Biosensors Bioelectron.*, 50: 262-268, 2013.

CHAPTER 3

3.1 Electrochemical aptasensors for contaminants detection in crops and food and environment: recent advances

Rapini, R, Marrazza G – review in preparation.

3.1.1 Abstract

The growing number of contaminants requires the development of new analytical tools that are precise, sensitive, specific, rapid, and easy-to-use to meet the increasing demand for legislative actions on environmental pollution control. Electrochemical biosensors, as a powerful alternative to conventional analytical techniques, enable the highly sensitive, real-time, and high-frequency monitoring of pollutants without extensive sample preparation. Aptamers are synthetic nucleic acid sequences or peptide capable to bind a target with affinity and selectivity comparable of those of monoclonal antibodies. Due to their advantages respect to antibodies (such as high stability, chemical synthesis, low dimension, affinity for small molecules, etc.) aptamers were successfully applied as bioreceptors in sensor technology. This article reviews important advances in electrochemical aptasensor biosensors for contaminants detection that have been realised over the last two years.

Keywords: aptamer, biosensor, pollutants, contaminants

3.1.2 Introduction

The development of sensitive, reliable and easy-to-use bioanalytical tools to detect contaminants (e.g. pesticides, toxins, drugs and metal ions) is a main purpose in many fields, like health care, forensic analysis, environmental, agricultural and food safety.

CHAPTER 3

Nevertheless, obtaining selective, stable and sensible probes for those kind of analytes, based on most diffused bioreceptors, antibodies, creates difficulties that concern the necessity to induce controlled immunoreactions even against molecules characterised by a low immunogenicity or a high toxicity, or, in general, against small size targets (e.g. metal ions). The recent developments in the use of biomimetic synthetic receptors such as nucleic acid-based aptamers provide an interesting alternative [1].

Nucleic acid-based aptamers are single stranded DNA or RNA short sequences, isolated in vitro from a synthetic oligonucleotides library using an automated technique named SELEX (selection evolution of ligands by exponential enrichment), first described in 1990 [2, 3]. Oligonucleotides from the library are selected according to their affinity toward a target molecule looking for the best selectivity and specificity [4]. Selected aptamers show high values of dissociation constants (K_d), often within nanomolar and picomolar range. Furthermore, their stability can be improved via chemical modifications [5].

A biosensors using aptamer as recognition element is called aptasensor. Compared to immunoassays, the use of aptasensors gives many advantages: biomimetic probe molecules are more thermally stable and eventually reusable, they show higher detection ranges, a prolonged shelf life, a low cross reactivity and they can be obtained using efficient and cost effective processes [6-8]. Moreover aptamers are easy to be modified adding functional groups, useful for their labelling (e.g. with enzymes, fluorophores and electrochemical mediator), or for their surface immobilisation. They can be directly linked to the active surface, as single

[9] or multi [10] target probes, showing high packing density [11]. A growing number of aptamer-based biosensors based on fluorescent, colorimetric, and electrochemical methods were proposed and compared to more classical approaches, testing them even in complex matrices [12, 13]. A recent review discusses last developments that were proposed in recent years for small molecules-binding aptamers selection strategies [14]. Moreover, some studies showed that aptamers are subjected to significant conformational change caused by the interaction with the analyte that can be used as recognition parameter combining them with appropriate transducers [15, 16]. These characteristics make easier the detection of small molecules target, enfolding them in the DNA secondary structure, both for the development of label free aptasensors and molecular switches [17]. In the last years, a great variety of aptamers were selected, able to bind different targets, such as pesticides, toxins [14, 18], antibiotics [19, 20] and biomarkers [21], and their versatility make them particularly suitable for environmental analysis.

In the last years, assays using aptamers coupled with electrochemical transducers were realised and their number is continuously growing due to the simplicity, rapidity and cost effectiveness as well as the possibility to modify probe aptamers adding a great variety of functional groups that help to integrate them in the electrochemical platforms [22].

Electrochemical techniques also give to scientists the possibility to take advantage of nanostructured electrode surfaces, e.g. modifying working electrodes by metal electrodeposition or conductive polymeric layers growth, or simply depositing carbon based nanomaterials [12, 23, 24].

This review provides a summary about trends and highlights in aptamer-based electrochemical biosensors for contaminants analysis in crops and

CHAPTER 3

food and environment over the last two years. The research was focused on substances of heterogeneous chemical classes that have in common the toxicity and can contaminate food production chain or water supplying. Traditional analytical methods used for these issues are based on chromatographic techniques, able to provide sensitive, selective and quantitative detections [25, 26]. Despite these advantages, the use of chromatographic instruments still remain an expensive alternative, that requires high skilled technicians to be set up and unable to be used for on situ rapid screening analysis. In this way, the need to develop rapid and cost-effective devices for environmental monitoring, including in situ analysis is continuously growing because of the potential strong influence of pollution on human life [18, 27].

3.1.3 Aptasensors Format

Many different designs were applied to develop electrochemical aptasensors but usually scheme an aptasensor is a device composed of a DNA (or RNA) oligonucleotide, used as molecular probe and able to recognise the analyte and an electrochemical transducer, used to convert the chemical reaction resulting from the interaction of the target with the aptamer probe (production of electroactive molecules, conformational changes, electrochemical mediator releases) into an electronic signal that can be elaborated by a computer. Different electrochemical techniques, such as cyclic voltammetry, potentiometry, and electrochemical impedance spectroscopy can be applied. Aptamer can be easily modified using electroactive probes, enzymes (able to generate an electroactive product or to catalyse a proper reaction) or used label free. Intensity of the analytical signal can be directly or inversely proportional to target

concentration. Recently, modification of electrochemical transducer with nanocomposite functional materials (e.g. carbon nanotubes, graphene, metal nanoparticles or conductive polymeric layers) has shown to be one of the most promising development to increase analytical performances of electrochemical biosensors in general, including aptasensors [28].

3.1.4 *Pesticides*

The term pesticide indicates any substance used to control the growth of infesting species (e.g. insect, weeds, little mammals, fungi, etc.-) that can affect the agricultural production. Total worldwide consumption of pesticide has been estimated around 2 million ton per year, about 45% of which used in Europe, 25% in the USA and 25% in the remaining countries: their application is crucial, considering that more or less one third of the agricultural production would be lost without it [29, 30]. Moreover, molecules used as pesticide represent some of the most toxic, stable and mobile substances released in the environment and we know that they can have toxic effects also against non-target organisms, including humans: for this reason, uncontrolled diffusion trough environment and also human food chain is extremely dangerous [31]. In the last years, there has been an increasing interest in biosensor technology for fast pesticide detection using easy and rapid procedures [8]. Aptasensor represent probably the most promising alternative, and many interesting application of their combination with electrochemistry have shown how to simplify or eliminate sample preparation to make in situ screening testing easier and faster with significant decrease in cost per analysis.

Several biosensors were reported describing pesticides detection. Acetamiprid is one of the most interesting analyte and the development of

CHAPTER 3

an efficient and reliable analytical method for its detection in food samples remains an important target in order to prevent potential risk for human health. Acetamiprid is a neuro-active widespread pesticide of the neonicotinoid class, synthetic derivatives of nicotine that act as nicotinic acetylcholine receptor agonist, causing to the contaminated organism paralysis followed by death [32]. It has shown a high toxicity, causing potential risk to humans who are exposed to the contaminated environment [33-35]. Fei et al. described a label-free approach for its detection based on a gold nanoparticles/multi-walled carbon nanotubes/reduced graphene oxide nanoribbons composite as sensor platform. The selective aptamer was immobilised using Au-S interaction and acetamiprid concentration was evaluated via EIS measurements, obtaining a LOD of 1.7×10^{-14} M. Real water samples were also tested [36]. Also Jiang et al. proposed a selective aptasensor for acetamiprid detection based on Ag nanoparticles-decorated nitrogen doped graphene deposited onto a glassy carbon electrode. Aptamer was immobilised onto Ag NPs and interaction with the target was evaluated with EIS, obtaining a LOD of 3.3×10^{-14} M. Real sample analysis was carried out in waste water samples, cucumber and tomato [37].

3.1.5 Pollutants

The term pollutant refers to any kind of substance that, once introduced into the environment, shows undesired effects, or adversely affects the usefulness of a natural resource. A polluting chemical can cause long- or short-term damages, e.g. by changing the growth rate of plant or animal species, or by interfering with human health, contaminating water supplies or food production chain. Some pollutants are (bio)degradable and

therefore do not persist in the environment in the long term, nonetheless degradation products of some pollutants are themselves polluting agents. Environmental pollution has become one of the most acute problems and captured attentions because the amount of toxic chemicals released into the environment has grown enormously due to growing human activity. These chemicals in air, water and soil can cause serious health problems [38]. Increase of these public health problems and relative consequences caused by environmental contaminants led to the necessity of developing reliable, cost effective and field suitable technologies for in situ screening analysis and monitoring of environmental pollutants. As well as other analysed chemical classes, development of aptasensors results particularly suitable for these purposes [39].

The term “pollutant” can be related to many different chemical classes of compounds. Those that will be highlighted in this paragraph will be introduced, shortly describing the known toxic effects for human health.

Bisphenol-A, is a diffused industrial compound involved in the production of polycarbonate plastics and epoxy resins. It can be found in many plastic consumer products, it is non-biodegradable and highly resistant to chemical degradation, resulting in that bisphenol-A is abundant in the environment and enters human body by ingestion or adsorption [40, 41]. As endocrine disrupting compounds, bisphenol-A could increase cancer rate, decrease semen quality and reduce immune function [41, 42]. Liu et al. proposed an aptasensor for bisphenol-A based on a gold-modified glassy carbon electrode on which the specific aptamer was immobilised. The analyte and a complementary DNA oligonucleotide sequence labelled with methylene blue competed for the binding site, resulting in a signal off sensor. Using SWV a LOD of 0.6 pM was obtained. Tap water was also

tested as real sample [43]. Another bisphenol-A aptasensor was described by Yu et al., immobilising a specific aptamer onto the surface of a gold electrode, via Au-S interaction. The aptamer is labelled with ferrocene, while a complementary DNA oligonucleotide sequence, labelled with methylene blue, competed with the analyte for the interaction with the aptamer. The two labels acted as a dual amplification system: the more analyte is present, the lower is the signal given from methylene blue and the higher is the signal given by ferrocene (both used as electrochemical probe). Measurements were carried out using SWV and the reported LOD is 0.19 pM. Real sample analysis was carried out on tap water samples [44]. Considering label free approaches, Derikvand et al. have also described an aptasensor for bisphenol-A detection. Highly dispersed Pt nanoparticles/acid-oxidised carbon nanotubes, functionalised with polyethyleneimine were deposited on a glassy carbon electrode. An amine-capped DNA oligonucleotide, complementary to the specific aptamer, was bound to the nanostructured surface, in order to bind the aptamer forming a double strand structure. DPV measurements, using $[\text{Fe}(\text{CN})_6]^{3-/4-}$ as electrochemical mediator were carried out, observing a decrease of the signal in presence of the analyte. The obtained LOD was 210 pM. Real spiked samples of environmental water were also analysed (Figure 3.1) [45]. Zhou et al. reported an aptasensor for detection of bisphenol-A in milk samples based on a glassy carbon electrode modified with Au-dotted graphene. Specific aptamer was immobilised onto Au nanoparticles and its interaction with the target was measured using DPV, obtaining a LOD of 5 nM and testing also milk samples [46].

Even if it is not commonly considered a pollutant, detection of 2, 4, 6-trinitrotoluene (TNT) is an interesting topic, because its extensive use has led to contamination of soil and groundwater [47, 48]. The environmental protection agency (EPA) considers TNT toxic because it showed diffused carcinogenic and mutagenic effects [48, 49]. Shorie et al. presented an approach for selection and utilisation specific aptamers for explosives detection, TNT included. The probe aptamer was immobilised on a gold electrode, and SWV was used to measure direct reduction of TNT nitro-groups, obtaining a LOD of 1 ppb in buffer. Spiked soil samples were also analysed [50].

Heavy metals are an important class of pollutants with both lethal and sub-lethal effects on organisms, because most of them can be toxic to all forms of life at high concentrations due to formation of complex compounds within the cell. An essential difference with organic pollutant concern the fact that heavy metals introduced into the environment cannot be biodegraded, persisting indefinitely and accumulating in air, water and soil. Industrial growth has led to a massive diffusion of these compounds, sometimes determining high exposure even through dietary intake of plant-derived food and beverages, drinking water, or air. Heavy metal ions can have long-term effects on human health, going from nervous system damage to renal dysfunction or lung disease and respiratory system damages. In some cases they were related to lung cancer [51, 52]. For these reasons they are receiving a growing attention as crucial parameter to evaluate environmental pollution. Hg^{2+} ion is reported as one of the most toxic heavy metal ions, seriously involved in environmental pollution. The exposure to mercury can lead to a series of harmful effects to health, such as brain damage, kidney failure, nervous system damage and immune system damage [53, 54]. Wu et al. proposed an aptamer-

based biosensor for its detection by immobilising streptavidin modified magnetic beads ($\text{Fe}_3\text{O}_4\text{-SA}$) onto a magnetic glassy carbon electrode. The biotin-labelled thymine-rich DNA aptamer has then been bound to the beads, capturing Hg^{2+} ions and forming a secondary structure able to intercalate thionine (used as signal mediator). By means of DPV a LOD of 0.33 nM was obtained. Tap and river water were tested as spiked real samples [55]. An enzyme-based approach for Hg^{2+} detection was reported by Bao et al., in which a DNA oligonucleotide was immobilised on a gold electrode. Oligo DNA binds the specific thymine-rich aptamer and its interaction with the target allows exonuclease III to digest the double strand-like structure containing Hg^{2+} , then available for a new cycle. Remaining DNA is used to form a long double strand chain using two auxiliary DNA sequences. An electrochemical mediator ($[\text{Ru}(\text{NH}_3)_6]^{3+}$) was able to intercalate this conformation, increasing the signal. Using DPV a LOD of 0.12 pM was achieved. Spiked lake water samples were also analysed [56]. Li et al. proposed an interesting aptamer-based biosensor for Hg^{2+} detection based on a self-assembly of thiolated β -cyclodextrins on a gold electrode. Orderly arranged molecularly layer showed interspaces among β -cyclodextrins that let electrochemical probe $[\text{Fe}(\text{CN})_6]^{3-/4-}$ to reach electrode surface. Thionine labelled aptamer was then linked to β -cyclodextrins and hybridised with a DNA oligonucleotide, letting interspaces free. Interaction with the target brought to the formation of a secondary structure that closed interspaces, lowering the signal. Using DPV, a LOD of 5.0×10^{-15} M was achieved. Real samples analysis was also carried out on tap and river water samples (Figure 3.2) [57]. The sensor reported by Gao et al. is based on the immobilisation of a specific Hg^{2+} aptamer onto the surface of a gold electrode. Secondary

structure of aptamer-target adduct was able to bind natural red, used as electrochemical mediator. By means of DPV a LOD of 1.5×10^{-12} M was obtained. Spiked samples of tap and river water were used to test the aptasensor [58].

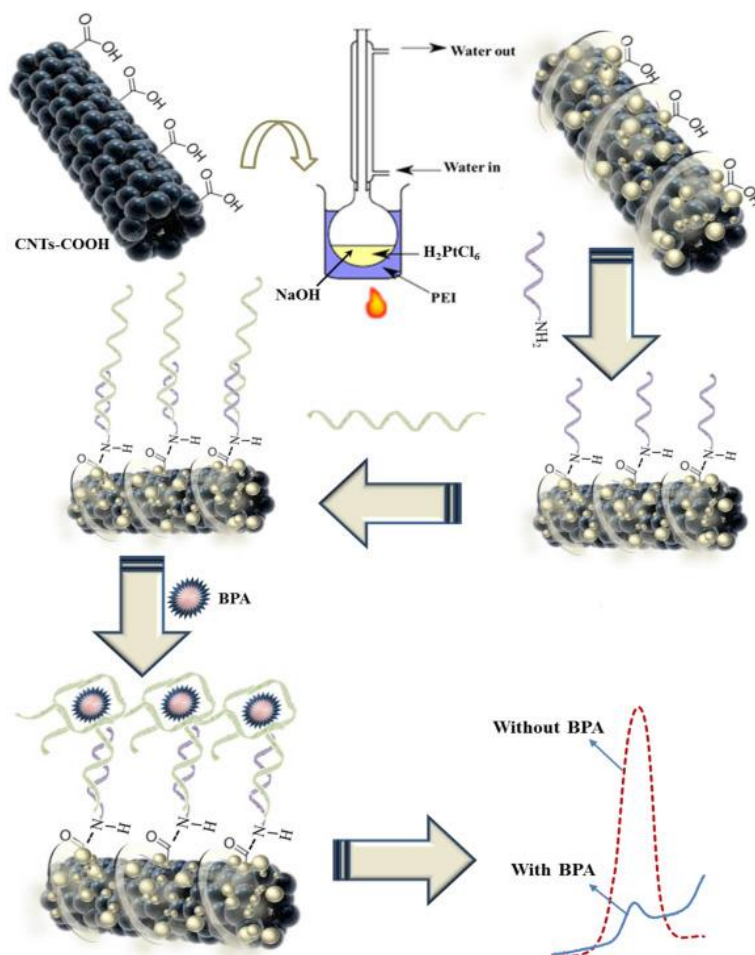


Figure 3.1: Scheme of the proposed aptasensor for bisphenol-A detection. Highly dispersed Pt nanoparticles/acid-oxidised carbon nanotubes, functionalised with polyethyleneimine were deposited on a glassy carbon electrode. An amine-capped DNA oligonucleotide, complementary to the specific aptamer, was bound to the nanostructured surface, in order to bind the aptamer forming a double strand structure. DPV measurements, using $[\text{Fe}(\text{CN})_6]^{3-/4-}$ as electrochemical mediator were carried out, observing a decrease of the signal in presence of the analyte. Reprinted with permission of Elsevier [45].

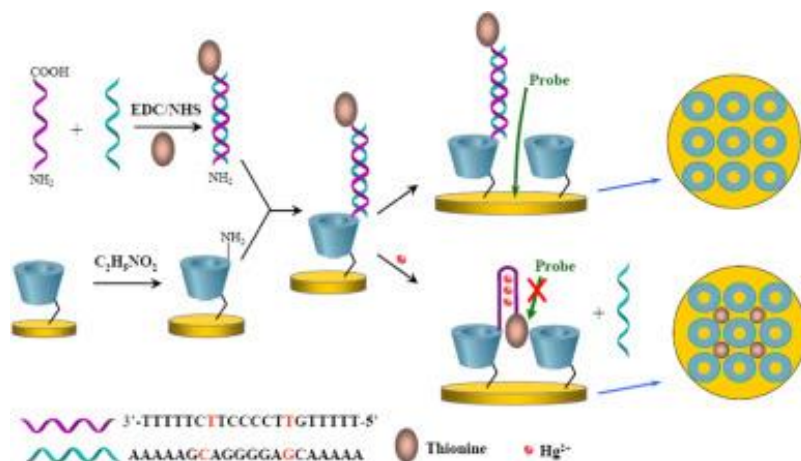


Figure 3.2: Scheme of the proposed aptasensor for Hg^{2+} detection based on a self-assembly of thiolated β -cyclodextrins on a gold electrode. Orderly arranged molecular layer showed interspaces among β -cyclodextrins that let electrochemical probe $[\text{Fe}(\text{CN})_6]^{3-/4-}$ to reach electrode surface. Thionine labelled aptamer was then linked to β -cyclodextrins and hybridised with a DNA oligonucleotide, letting interspaces free. Interaction with the target brought to the formation of a secondary structure that closed interspaces, lowering the DPV signal. Reprinted with permission of Elsevier [57].

3.1.6 Drugs

The term antibiotic indicates any natural or synthetic molecule showing a toxic and selective action on single-cell organism like bacteria [59]. Antibiotics represent more than 70% of all consumed pharmaceuticals in veterinary medicine and they are diffused also in human medicine (around 6% of all prescription) [60]. A certain amount of these antibiotics remains unmetabolised and can be spread into the environment in many ways (including human medical waste), but the main source remains breeding in which they are used to increase animal growth (mixed with feed) in addition to therapeutic reasons. In this case, antibiotics are diffused into environment via food production or directly via excreted faeces (used also as fertilizer) and urines [60, 61]. Final fate of these molecules depends from their physical-chemical properties, environmental conditions, pH,

soil type: all these parameters can influence their chemical behaviour, their mobility and, most importantly, their persistence and bioaccumulation [61]. One of the worst effects caused from the intake of antibiotics in human food chain is antibiotic resistance of bacteria: for this reason they still represent one of the most interesting targets for bioanalytical chemistry. Chloramphenicol is an antibiotic used for the treatment of bacterial infections like meningitis, plague, cholera, and typhoid fever but its use is only recommended when safer antibiotics cannot be used because many potential lethal side effects on humans, such as leukaemia, aplastic anaemia and grey baby syndrome were observed [62]. Chen et al proposed a sensor for simultaneous detection of chloramphenicol and polychlorinated biphenyl-72 (PCB72) based on the displacement of quantum dots (CdS and ZnS) labelled dendritic nanotracers given by the interaction of the analyte with aptamer labelled magnetic nanoparticles ($\text{Fe}_3\text{O}_4@\text{Au}$). Square wave stripping voltammetry (SWSV) was applied to detect the amount of released nanotracers, obtaining a LOD of 0.33 pg/mL for chloramphenicol and 0.35 pg/mL for PCB72. Spiked fish samples were also analysed [63]. Pilehvar et al. proposed an impedimetric label-free aptasensor able to detect chloramphenicol based on a gold electrode on which the specific aptamer was immobilised. Increasing the concentration of the target brought to an increased electronic transfer resistance from the solution to the electrode surface using $[\text{Fe}(\text{CN})_6]^{3-/4-}$ as redox probe. A LOD of 1.76 nM was obtained [64]. A multiplex electrochemical aptasensor was developed for simultaneous detection of two antibiotics (chloramphenicol and oxytetracycline) by Yan et al., using high-capacity magnetic metal encoded hollow porous nanotracers coupled with exonuclease-assisted target recycling to increase sensitivity. A glassy carbon electrode was

CHAPTER 3

modified by electrodeposition of gold nanoparticles on which two DNA oligonucleotide chains, respectively complementary to the two selected aptamers, were immobilised. In presence of the targets the double strand interaction was broken, and metal ions incorporated nanotracers were able to bind the again available oligonucleotide: amount of metal ions (Cd^{2+} and Pb^{2+}) was proportional to the targets and were determined by means of SWV, obtaining a LOD of 0.15 ng/mL for chloramphenicol and 0.10 ng/mL for oxytetracycline. The proposed aptasensor was also tested on spiked milk samples [65]. Rapid analytical methods for the detection of tetracyclines, broad-spectrum class of antibiotic of the polyketide type, that act inhibiting protein synthesis, are gaining interest because their excessive use can led to antibiotic-resistance [61]: multi walled carbon nanotubes were also used by Guo et al. in combination with chitosan and chitosan-prussian blue-graphene nanoparticles to increase conductivity of a glassy carbon electrode on which a selective aptamer against tetracycline was immobilised. By means of DPV, the sensor was able to detect tetracycline in buffered samples obtaining a LOD of 0.56×10^{-11} M and milk samples were also analysed [66]. Shen et al proposed a label-free aptasensor for detection of tetracycline modifying a glassy carbon electrode by fixing a prussian blue-chitosan-glutaraldehyde layer on which gold nanoparticles were attached to immobilise the selective aptamer. Tetracycline was detected by the signal off sensor using DPV and obtaining a LOD of 3.2×10^{-10} M. Spiked milk samples were also analysed [67]. An enzyme-amplified approach was proposed by Taghdisi et al. for tetracycline determination, based on a M-shape structure complex given from the probe aptamer with different complementary DNA strands, using exonuclease I on a gold electrode. Using cyclic voltammetry (CV) the

80

method was able to reach a LOD 450 pM in buffered solution and was tested in real samples too: milk (LOD 740 pM) and serum (LOD 710 pM) [68]. Wang et al. developed an electrochemical aptasensor for sensitive detection of ampicillin, a broad spectrum antibiotic active against many Gram-positive and Gram-negative bacteria [69], combining polymerase-assisted target recycling amplification with strand displacement amplification using polymerase and nicking endonuclease. The sensor worked as a signal-off assay and the DPV electrochemical signal was generated using methylene-blue as label, obtaining a detection limit (LOD) of 1.09 pM. Spiked milk samples were also analysed to test aptasensor response [70]. An enzyme-based detection scheme was also been applied: Wang et al. proposed an aptasensor for detection of ampicillin based on target-induced and T7 exonuclease-assisted dual recycling signal amplification strategy. By means of differential pulse voltammetry (DPV) on a negatively charged indium tin oxide electrode the sensor reached a LOD of 4.0 pM, being tested also in milk samples [71]. Many reported examples describe label-free approaches, like the work reported by Chen et al., that described an aptasensor able to detect ractopamine, clenbuterol, salbutamol, phenylethanolamine and procaterol, molecules acting as β -agonists (medications able to relax airways muscles) that can accumulate in body tissues causing acute or chronic poisoning in case of exceeding consumption [72, 73]. The sensor was obtained immobilising the aptamer on a gold electrode and performing electrochemical impedance spectroscopy measurements (EIS). The obtained LOD were 0.04 ng/mL ractopamine, 0.35 pg/mL clenbuterol, 0.53 pg/mL salbutamol, 1.0 pg/mL phenylethanolamine and 1.73 pg/mL procaterol. Spiked pork samples were also analysed [74]. Yang et al. also studied ractopamine detection using a nanocomposite immobilisation

CHAPTER 3

support based on gold nanoparticles/poly-dimethyl-diallyl ammonium chloride-graphene to improve conductivity on which the aptamer was immobilised. Recording peak currents obtained via DPV from the signal-off assay, they obtained a LOD of 5.0×10^{-13} M. Real sample analysis were carried out in spiked swine urine [75]. Streptomycin is a broad-spectrum antibiotic used in human and veterinary medicine against gram-negative bacterial infections [76, 77]. Its uncontrolled application may result in a spread diffusion in foodstuffs and serious side effects on human health, such as nephrotoxicity and ototoxicity [77, 78]. Danesh et al. described an enzyme-based assay for its detection based on a gold electrode, on which a specific streptomycin aptamer and a DNA oligonucleotide were immobilised. The two sequences are able to form a secondary arch-shape structure that inhibits electron transfer from $[\text{Fe}(\text{CN})_6]^{3-/4-}$, used as redox probe. Interaction with the target breaks the secondary structure, letting exonuclease I to degrade the available DNA oligonucleotide, increasing the signal. Measurement performed via DPV brought to a LOD of 14.1 nM in buffered samples. Real samples (rat serum and milk) were also tested [79]. Quin et al. developed, instead a signal amplification strategy to detect kanamycin, an aminoglycoside bactericidal antibiotic: residual amounts of this molecule in food products may lead to antibiotic resistance from pathogenic bacterial strains and the molecule itself has shown side effects like nephrotoxicity and ototoxicity [80]. Aptasensor was developed using thionine functionalised graphene and hierarchical nanoporous PtCu alloy as support for aptamer immobilisation to increase conductivity, obtaining a LOD of 0.42 pg/mL in buffer via DPV. Real matrixes analyses were also tested, spiking animal derived food [81]. Kanamycin was also studied by Zhou et al. that proposed a simple and

label-free assay based on the immobilisation of a specific kanamycin aptamer onto the surface of a gold electrode: the more is the concentration of the target interacting with the probe, the lower is the SWV signal recorded, with a LOD of 0.014 nM. The sensor was also tested on milk samples [82]. A nanoporous PtTi alloy-modified glassy carbon electrode was used by Guo et al. as support for aptamer immobilisation in the assay they proposed for kanamycin, combining the nanostructured surface with a film composed by multi walled carbon nanotubes and a ionic liquid (1-hexyl-3-methylimidazolium hexafluorophosphate) to increase surface conductivity. A LOD of 3.7 pg/mL was obtained using DPV in buffered solution and the assay was also tested in milk samples [83]. A similar approach was used by Qin et al. that also proposed a selective aptasensor for kanamycin. The surface of a glassy carbon electrode was modified using a composite film formed by multi walled carbon nanotubes and a ionic liquid (1-butyl-3-methylimidazolium hexafluorophosphate). After that amino-functionalised graphene was formed by oxidation onto the nanocomposite film to increase conductivity. The specific aptamer has then been immobilised and the interaction with the target was evaluated by means of DPV obtaining a LOD of 0.87 nM. Real milk samples were also tested [84]. Enzyme-amplified detection schemes were also been reported: Xu et al. proposed a sensor for the detection of kanamycin. The assay is based on a label-free and signal-on square wave voltammetric (SWV) measurement: a complementary DNA sequence is immobilised onto gold electrode surface and able to hybridise kanamycin specific aptamer. In presence of the analyte, the combination of kanamycin and its aptamer block the cleavage process catalysed by exonuclease III, and remained complementary DNA is proportional to the concentration of the target, which is electrochemically quantified via absorption of $\text{Ru}(\text{NH}_3)_6$.

CHAPTER 3

Reported LOD was 1 pM and the sensor was tested also on milk samples [85]. An aptasensor based on the contributions of chitosan-gold nanoparticles, graphene-gold nanoparticles and multi-walled carbon nanotubes cobalt phthalocyanine nanocomposites was proposed by Sun et al. for kanamycin detection. A gold electrode was modified with the nanocomposite structures to increase its conductivity and a primary aptamer was immobilised. A secondary aptamer, linked to the target and labelled with horseradish peroxidase (HRP) was used to form a sandwich structure with the immobilised one. Reduction current of H_2O_2 catalysed by HRP was recorded by means of DPV obtaining a LOD of 5.8×10^{-9} M. Milk spiked samples have also been analysed [86]. Xu et al. also proposed a sandwich approach by assembling graphene-polyaniline and polyamidoamine dendrimer-Au nanoparticle (PAMAM-Au) nanocomposites on the surface of a glassy carbon electrode used as support to immobilise an anti-kanamycin antibody that bound the target. The sandwich interaction was completed using an aptamer specific for the analyte labelled with biotin on which HRP was linked via streptavidin-biotin interaction. Current given from electro-reduction reaction of H_2O_2 catalysed by HRP was recorded via DPV obtaining a LOD of 4.6×10^{-6} $\mu\text{g/mL}$. Aptasensor was also tested in milk spiked samples [87].

As well as antibiotics, indiscriminate diffusion other drugs also represents a potential menace for environmental health, considering their bioaccumulation [88-90]. Due to their persistence in environmental waters, pharmaceuticals compounds have become important emerging contaminants also because of their massive diffusion in commercial products: more than 3000 different substances are used as ingredients in

many products like painkillers, antidiabetics, betablockers, contraceptives, lipid regulators, antidepressants and impotence drugs [91]. Finally we also reported latest electrochemical aptasensors against some kind of illicit drugs (mainly cocaine). These compounds and their metabolites form another interesting group of emerging pollutants and their residues appears to be widespread at very low concentrations in all populated zones. Determination of these targets in environmental samples can be an indirect tool to detect the amount of their illegal consumption in a certain area and can help to evaluate impact and risks given from a chronic low level exposure [92]. Ibuprofen is a nonsteroidal anti-inflammatory drug derivative of propionic acid. It is commonly used for relieving pain (even after surgery), for alleviating fever and in case of inflammatory diseases. A long term overuse of this drug could double the risk of heart attack [93, 94] and even other toxic effects given from overdose are reported [95]. Roushani et al. proposed a methylene blue label-based aptasensor modifying a glassy carbon electrode with a multiwalled carbon nanotubes/ionic liquid/chitosan nanocomposite and successively immobilising the ibuprofen specific aptamer via covalent bond. Intercalated methylene blue was used as electrochemical redox marker. Measurements of different concentration of ibuprofen were carried out via DPV obtaining a LOD of 20 pM in buffered solution. The assay was also tested in real samples, spiking pharmaceutical formulations, human serum and waste water [96]. Cocaine is an illicit drug which abuse causes physiological and psychosocial health problems, but, as well as other illicit drugs, it is also gaining attention as contaminant because of the potential risks for human health given by its diffusion in the environment [97-100]. Roushani et al. proposed a similar approach to the previous one to realise an aptasensor based on a multi-walled carbon nanotubes/ionic

CHAPTER 3

liquid/chitosan nanocomposite-modified glassy carbon electrode for detection of cocaine. The selective aptamer was immobilised on the nanocomposite material and labelled with gold nanoparticles, DPV was used to perform measurement in presence of $[\text{Fe}(\text{CN})_6]^{3-/4-}$ as electrochemical probe. Obtained LOD was 100 pM, and analysis on human serum were also performed [101]. Another aptasensor for the detection of cocaine was described by Taghdisi et al.: the assay was based on a selective aptamer, bound to a complementary DNA sequence immobilised on a gold electrode: in presence of the target the double strand interaction was broken and the single strand oligonucleotide was able to bound single-walled carbon nanotubes, in order to increase electrochemical response. Measurement were performed using DPV and obtaining a LOD of 105 pM. The assay was also tested on real rat serum samples [102]. An enzyme-based approach has also been presented by Shen et al. based on the use of a supramolecular aptamer, rolling circle DNA amplification, and multiple binding of the enzyme alkaline-phosphatase. Selective cocaine aptamer was cleaved in two fragments: one fragment was immobilised on a gold electrode, while the second one was labelled with biotin: in the presence of cocaine, the two strands form a supramolecular structure that conjugates to streptavidin for anchoring of biotinylated circular DNA. Using phi29 DNA polymerase, it was possible to produce micrometer-long single-strand DNA which contained hundreds of tandem-repeat sequences able to bind many biotinylated detection probes. Alkaline phosphatase linked to streptavidin has then been bound and the hydrolysis of the synthetic enzyme substrate α -naphthylphosphate was measured via DPV obtaining a LOD of 1.3 nM. Spiked complex matrixes (urine samples) were also tested [103].

3.1.7 *Toxins*

Mycotoxins represent the most diffused group of toxins that can affect food products. They are secondary metabolites of filamentous fungi, and they are formed by many different substances produced by different mycotoxigenic species (molds). The infection of agricultural crops can happen at any production stage: during crop growth, harvest, storage or processing [104]. They showed several adverse impacts on human health, such as gastrointestinal diseases, kidney damage and immune suppression, in general defined as mycotoxicosis. The severity of which depends on the toxicity of the mycotoxin, the extent of exposure, age and nutritional status of the individual and possible synergistic effects of other chemicals to which the individual is exposed. The chemical structures of mycotoxins are various, but they are all relatively low molecular mass compounds [105]. Algal toxins (mostly cyanobacterial toxins produced from bluegreen algae) represent another group on which interest is continuously growing. Massive discharges of nutrients (mainly from agricultural wastewater) have led to increased algal bloom and toxins produced by these algae were implicated adverse effects against sea wildlife and also humans. Most common algal toxins are microcystins, nodularins, anatoxins, cylindrospermopsin, and saxitoxins and toxic effect can affect liver and nervous system. All the countries using surface water as a drinking water source have to face up with contamination given by these compounds [91]. Ochratoxin-A is a low molecular weight mycotoxin which is characterised by high toxicity at very low concentrations. It was suggested to contribute to the development of cancer by the International Agency for Research on Cancer (Group 2B) and was considered nephrotoxic, teratogenic and immunosuppressive [106, 107]. A label free approach for ochratoxin-A detection was reported by Mejri-Omrani et al.,

CHAPTER 3

that realised an impedimetric aptasensor based on a gold electrode covered with a film layer of modified polypyrrole (PPy), covalently bound to polyamidoamine dendrimers. A specific DNA aptamer was covalently linked and interaction with different concentration of the analyte was evaluated, obtaining a LOD of 2 ng/L. Wine samples were also tested as real matrices [108]. An enzyme amplification-based assay was proposed by Tan et al. using a negatively charged indium/tin oxide electrode and a non-immobilised selective aptamer. A competitive interaction between a complementary DNA sequence labelled with methylene blue and the analyte for aptamer binding make the two DNA chains available for recJ_f exonuclease (that can catalyse the removal of deoxy-nucleotide monophosphates from DNA in the 5'→3' direction) degradation, increasing electrochemical signal given from free methylene blue. Using DPV a LOD of 0.004 ng/mL was obtained and real samples (corn) were also tested [109]. Yang et al. proposed an aptamer-based sensor in which a capture DNA oligonucleotide was immobilised on a gold electrode. It is able to bind the ochratoxin-A aptamer that form a double strand structure with reporter DNA bound gold nanoparticles. A guanine-rich DNA oligonucleotide was also able to bind the unoccupied chains on the nanoparticles' surface: the more target is present, the less labelled nanoparticles are bound. Methylene blue is used to intercalate the guanine-rich sequence and used as electrochemical probe via DPV measurements obtaining a LOD of 0.75 pM [110]. Aflatoxin-B1 is a strongly toxic metabolite produced by several molds, specially diffused in crops [111]. It was described as a carcinogenic substance (first hazard class in accordance with the classification of the International Agency for Research on Cancer) [112, 113]. Zheng et al. reported an aptasensor for aflatoxin-B1

detection by adopting a telomerase and exonuclease III based two-round signal amplification strategy. A DNA oligonucleotide was immobilised onto Au-NPs. Modified particles were able to interact with the aflatoxin-B1 aptamer immobilised onto a gold electrode. Telomerase was used to elongate unbound DNA oligonucleotide sequence. The analyte competed then for the binding site while methylene blue has then been added as electrochemical mediator. Then, exonuclease III was used to hydrolyse the 3'-end of the aptamer-target adduct, causing the release of bounded aflatoxin-B1 into the sensing system, available for the following recognition-sensing cycle. By means of SWV, a LOD of 0.6×10^{-4} ppt was obtained and spiked corn samples were also analysed [114]. Evtugyn et al. realised an assay for aflatoxin-B1 detection based on a glassy carbon electrode on which neutral red and polycarboxylated macrocyclic ligands were electropolymerised for covalent aptamer immobilisation. Interaction with the analyte was evaluated using both cyclic voltammetry (CV) and EIS, obtaining, respectively a LOD of 0.1 nM and 0.05 nM. Real matrixes (peanuts, cashew nuts, soy sauce, wine) have also been analysed [115]. Staphylococcal enterotoxin-B is one of the most epidemic super-antigens that can cause serious immunosuppression and give lethal effects even at low concentration [116, 117]. Deng et al. described an electrochemical aptamer-based sensor for its detection based on a gold electrode, modified with a nanocomposite adduct of gold nanoparticles, zirconia nanoparticles, and chitosan. A DNA capture probe was immobilised onto the modified surface in order to bind the specific aptamer for staphylococcal enterotoxin-B. In presence of the target, the aptamer is released and a detection probe marked with biotin is captured. Streptavidin-horseradish peroxidase is then bound to the biotinylated DNA and reduction of H_2O_2 is measured via DPV. Obtained LOD was 0.24 ng/mL and serum samples

CHAPTER 3

were also tested [118]. Saxitoxin, one of the most harmful marine toxins, and its analogues, such as neosaxitoxin and gonyautoxins, are potent neurotoxins that can block mammalian voltage-gated sodium channels and result in death [119, 120]. Saxitoxin can enter in the marine food chain, causing the “paralytic shellfish poisoning” via contaminated seafood or water intake [121, 122]. Hou et al. proposed an aptasensor for its detection based on a gold electrode modified with carbon nanotubes containing electrostatically anchored methylene blue, used as electrochemical probe. The specific aptamer was bound on the previously described self-assembled monolayer and its interaction with the analyte was evaluated using DPV and oxidation of methylene blue. The assay worked as a signal off sensor, and the obtained LOD was 0.38 nM in buffered solution. Sensor was also tested on real matrixes (mussel samples) [123]. Fumonisin B1 is a diffused toxin of the fumonisin class produced by *fusarium moniliforme*, mostly found in maize, in processed maize products and animal feeds [124, 125]. Its detection remains important because it is considered a possible carcinogen (Group 2B) by the International Agency for Research on Cancer, being related with esophageal and liver cancers in some countries [126-128]. Chen et al. described a simple label-free impedimetric aptasensor based on a glassy carbon electrode on which gold nanoparticles were electrodeposited for aptamer immobilisation via Au-S interaction. EIS was applied to detect interaction with the analyte, obtaining a LOD of 2 pM. Spiked real matrixes (maize) have also been tested [129]. Brevetoxins are potent cyclic polyether neurotoxins produced by the marine “red tide” dinoflagellates *karenia brevis* and accumulate in shellfish. Human exposure to these substances can occur through food (contaminated shellfish) and even through aerosol exposure in marine

zones; brevetoxins are neurotoxic and can cause mortality [130, 131]. A label-free aptamer-based competitive electrochemical assay for brevetoxin-2 detection was proposed by Eissa et al. by covalently immobilising brevetoxin-2 on a gold electrode. Solutions containing the specific aptamer and different concentrations of free brevetoxin-2 have then been incubated onto the modified surface. Free and bound analyte competed for the interaction and the amount of surface bound aptamer was evaluated by means of EIS, obtaining a LOD of 106 pg/mL. Spiked shellfish samples have also been analysed [132]. Ricin is a toxin derived from the castor bean plant *ricinus communis*. Poisoning can occur via ingestion, inhalation, or injection and can have symptoms similar to gastroenteritis or respiratory illnesses, its effects kill eukaryotic cells by inactivating ribosomes and blocking protein synthesis [133, 134]. Du et al. described an interesting competitive assay based on kinetic competition between a specific ricin toxin A-chain aptamer, a short DNA sequence used as blocker and a molecular beacon labelled with a fluorophore and a quencher. The more was the target, the more blocker bound the beacon increasing fluorescence. Obtained LOD was 30nM. The work describes also an electrochemical approach based on the same sequences. The kinetic competition was carried out between a DNA oligonucleotide with the same sequence as the molecular beacon, immobilised on a gold electrode, the same blocker labelled with methylene blue and the aptamer. Even in this case, the assay worked as a signal on sensor, obtaining a LOD of 3nM. Measurements in human serum and human saliva were also carried out (Figure 3.3) [135]. Fetter et al. proposed a simple strategy for the detection of ricin toxin and botulinum, a bacterial neurotoxin common in soil and water causing a potential fatal disease named botulism [136]. The assay is based on a gold electrode on which surface specific aptamers

CHAPTER 3

for ricin and botulinum are respectively immobilised using Au-S interaction. Aptamers are labelled with methylene blue and SWV was used for analytes detection [137]. Cylindrospermopsin is one of the most hazardous cyanotoxins in freshwater sources, showing strong cytotoxicity, developmental toxicity and carcinogenic activity; its assumption can also bring to multiple organ dys-function syndrome [138-141]. Zhao et al. realised a label-free impedimetric aptasensor by covalently grafting a specific aptamer onto a thionine/graphene-modified glassy carbon electrode using glutaraldehyde as crosslinker. The sensor was able to capture the analyte from buffered solution. By means of EIS a LOD of 0.117 ng/mL was obtained and lake water samples were also analysed [142]. Elshafey et al. realised an impedimetric aptasensor for anatoxin-A, another compound of the cyanotoxins class that can contaminate drinking water [143, 144]. The assay was based on a gold electrode, on which anatoxin-a aptamer was immobilised via Au-S interaction. Using $[\text{Fe}(\text{CN})_6]^{3-/4-}$ as redox probe for EIS measurements a reduction of electronic transfer resistance was observed in presence of the target and used as analytical signal, resulting in a LOD of 0.5 nM. Measurements were also carried out in spiked drinking water samples [145]. Elshafey et al. also proposed an impedimetric aptasensor for this group of toxins starting from the selection of the high affinity aptamer, which was subsequently immobilised via Au-S interaction on a gold electrode. Using $[\text{Fe}(\text{CN})_6]^{3-/4-}$ as redox probe for EIS measurements, they obtained a LOD of 100 pM. Real samples (spiked tap water) were also analysed [146]. *Clostridium difficile* is a pathogen often involved in nosocomial intestinal infections and toxin-A is a lethal enterotoxin produced by this organism. *Clostridium difficile* was also isolated from different environmental

sources, like soil and various water environments (seawater and freshwater) [147-149]. Luo et al. described an aptamer-based biosensor for toxin-A detection using gold nanoparticles synthesised by *bacillus stearothermophilus*. A complementary DNA oligonucleotide sequence was immobilised on the nafion/thionine/AuNPs-modified screen-printed electrode via Au-S interaction in order to bind the horseradish peroxidase-labelled selective aptamer. In presence of the analyte the duplex interaction was broken, leading to a lower current signal in CV measurements. Obtained LOD was 1nM [150].

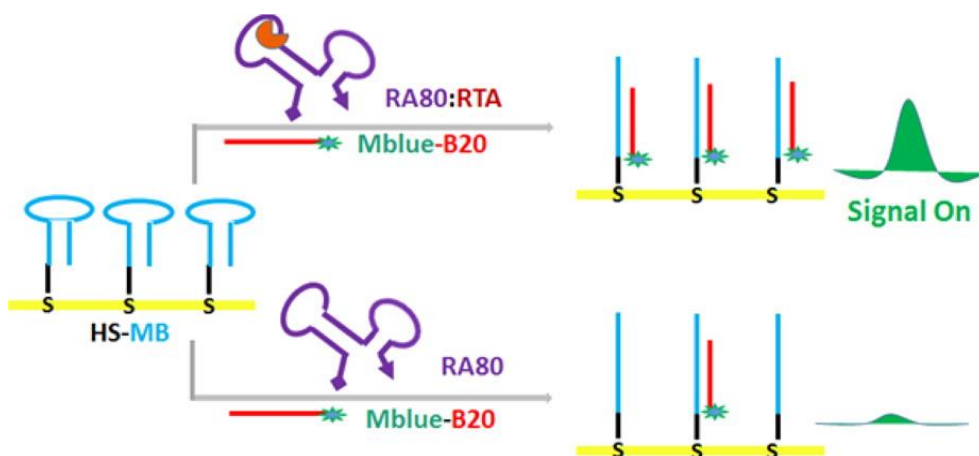


Figure 3.3: Scheme of the proposed aptasensor for ricin toxin. The competitive assay is based on a kinetic competition between a specific ricin toxin A-chain aptamer, a short DNA sequence used as blocker and a molecular beacon labelled with a fluorophore and a quencher. The more was the target, the more blocker bound the beacon increasing fluorescence. The work describes also an electrochemical approach based on the same sequences. The kinetic competition was carried out between a DNA oligonucleotide with the same sequence as the molecular beacon, immobilised on a gold electrode, the same blocker labelled with methylene blue and the aptamer. Even in this case, the assay worked as a signal on sensor. Reprinted with permission from: Y. Du, S.J. Zhen, B. Li, M. Byrom, Y.S. Jiang, A.D. Ellington, *Anal. Chem.*, 88: 2250-2257, 2016. Copyright 2016 American Chemical Society [135].

3.1.8 New approaches for electrochemical aptasensors based on screen printed transducers

The combination between aptamers and electrochemistry offers the possibility to develop a large amount of simple-to-use devices with low costs, fast and sensitive response and high selectivity (Figure 3.4). For these reasons, they are particularly suitable for on field screening analysis, being easily coupled with portable devices. In this way, sensors based on screen printed electrodes (SPEs) have been highlighted separately, at the end of this review, being many of the SPEs-based devices proposed as portable analytical tools. Utilisation of SPEs also showed to be an advantageous alternative respect to classical bare electrodes. Screen printing technology is based on a layer by layer deposition of a special ink mixed with conductive powder (that can be composed by graphite, or a metal like gold, silver or platinum) on a polymeric support, using a proper screen or mesh, in order to define size and shape the disposable electrochemical cell (usually they are produced in a three electrodes configuration). This technology has advantages given from design flexibility, process automation, good reproducibility, and a wide choice of materials, which determine selectivity, sensitivity and adequacy for the use in a certain analysis [151]. SPEs low costs and ease of mass production, combined with their dimensions that give the possibility to miniaturise the electrochemical cell and to lower sample volumes, are their main advantages, especially developing small and portable devices, particularly suited for on field screening analysis [152-154]. Even for laboratory analysis, SPEs can solve some of the disadvantages given from classical solid electrodes, like memory effect or cleaning procedures (that can also affect measurements reproducibility) [155]. Some limitation can

be observed in case of use of organic solvents, that can dissolve printing insulating inks damaging SPE, structure [156], even if examples of organic solvents-compatible SPEs are reported [157]. Moreover, in some cases small dimensions can cause insensitivity, due to the low rate electron transfer [155, 158, 159]. Anyway, even if some work using unmodified SPEs is reported [160], electrochemical and biochemical modification can increase their performances: modifications of SPEs are simpler if compared with ordinary electrodes, which need several polishing, preparation and refreshment steps. Many kind of modifications were reported, fitting SPEs to multiple characteristics required by different classes of analytes [151, 155]. Last reported developments are connected with the use of nanostructured materials, which represent the most potential field in SPEs functionalisation [24, 28, 161].

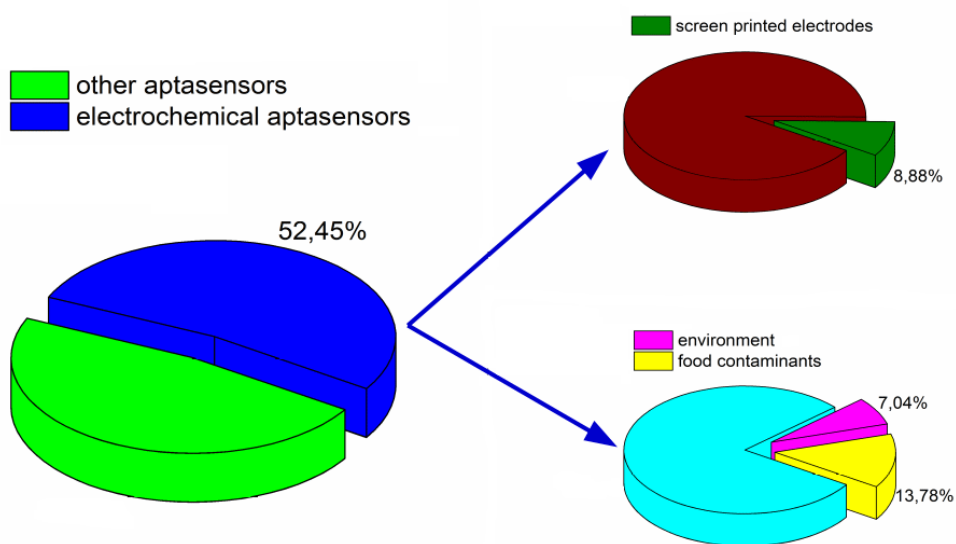


Figure 3.4: Per cent relevance of electrochemical aptasensors, with particular focus on screen printed electrodes utilisation and environmental and food contaminants analysis. Source: Scifinder 2016.

CHAPTER 3

Rapini et al. reported an enzyme based aptasensor for acetamiprid detection, based on a graphite SPE modified with electrochemical deposition of a conductive layer of polyaniline and gold nanoparticles, used for aptamer immobilisation via Au-S interaction. A competitive approach was used, incubating the analyte and a complementary DNA oligonucleotide labelled with biotin, which competed for the aptamer binding site. Streptavidin-labelled alkaline phosphatase was then bound to the biotinylated oligonucleotide and current generated by the oxidation of 1-naphtyl-phosphate was used as analytical signal via DPV measurements. Reported LOD of the proposed signal off sensor was 0.086 μM . Real samples analysis on spiked fruit juices was also carried out [162].

Environmental arsenic contamination can cause a series of health problems, including systemic disease and carcinogenic effects [163-166]. Toxicity and mobility of As depend on its oxidation state: the trivalent As(III) is more mobile and toxic than As(V) also respect to organic arsenic compounds [167], because of its ability to form complexes with certain co-enzymes. Cui et al. proposed an aptasensor for arsenite ion detection based on a graphite SPE on which gold nanoparticles were deposited for aptamer immobilisation via Au-S interaction. Free aptamer could absorb cationic polydiallyl-dimethyl-ammonium that is removed by the interaction with the target: aptamer-target adduct could absorb more $[\text{Ru}(\text{NH}_3)_6]^{3+}$, used as electrochemical mediator, increasing signal recorded by means of DPV. A LOD of 0.15 nM was obtained, and spiked tap and lake water were tested as real samples [168].

Bagheri Hashkavayi et al. reported a label-free aptasensor for chloramphenicol detection, based on a graphite SPE that was modified with a dendritic nanostructure based on mesoporous silica (SBA-15) functionalised with 1,4-diazabicyclo[2,2,2]octane (DABCO) in order to increase Au nanoparticles immobilisation, enhancing surface conductivity. The specific chloramphenicol aptamer was then bound via Au-S interaction, and analyte capturing was monitored via DPV, using hemin as electrochemical indicator and achieving a LOD of 4.0 nM. Real sample analysis in spiked human serum were also performed (Figure 3.5) [169]. Bagheri Hashkavayi et al. also described a previous electrochemical aptasensor for chloramphenicol detection, based on a gold nanocubes/cysteine-modified gold SPE. Specific aptamer was immobilised on the nanostructured surface and interaction with the target was measured by means of SWV, obtaining a LOD of 4.0 nM [170]. Feng et al. proposed an electrochemiluminescent aptasensor for chloramphenicol detection using a particular homemade graphite SPE, consisting of a common Ag/AgCl reference electrode a carbon counter electrode and two spatial-resolved carbon working electrodes (WE1 and WE2). Luminol/gold nanoparticles were deposited onto WE1 as signal tags, while CdS quantum dots were placed onto WE2 as internal reference. NPs on WE1 were functionalised with a DNA oligonucleotide sequence complementary to chloramphenicol aptamer, tagged with chlorogenic acid (used as luminol/gold NPs quencher), that was successively hybridised to it. Adding the analyte, the duplex interaction is broken, leading to the formation of the aptamer-target adduct and releasing chlorogenic acid. This increased WE1 electrochemiluminescence, while its ratio with WE2 electrochemiluminescence was used to reduce environmental matrix effect.

CHAPTER 3

Performing one-cycle voltammetric measurement, a LOD of 0.03 nM was obtained, performing also measurements on real fish samples [171]. A similar approach was previously reported by Feng et al., for simultaneous detection of chloramphenicol and malachite green. Using the same double-working electrodes graphite SPE, WE1 was modified CdS quantum dots on which a DNA oligonucleotide, complementary to malachite green aptamer, was immobilised, while WE2 was modified with luminol/gold nanoparticles on which a DNA oligonucleotide, complementary to chloramphenicol aptamer, was immobilised. The two selective aptamers have then been hybridised, respectively labelled with cysteine-5 and chlorogenic acid as electrochemiluminescence quenchers. In presence of the two analytes, aptamers bound their targets releasing the quenchers and increasing electrochemiluminescence. By means of one-cycle voltammetry, a LOD of 0.03 nM for malachite green and 0.07 nM for chloramphenicol were detected. Real samples were also tested [172]. Another SPE-based aptasensor for chloramphenicol detection was presented by Hamidi-Asl et al., combining a selective aptamer with different type-B gelatines, dropped onto the surface of a gold SPE. By means of DPV, a LOD of 1.83×10^{-10} M was obtained and spiked milk samples were analysed [173]. The sensor proposed by Zhan et al. is also based on a graphite SPE that was modified using a composite material consisting of reduced graphene oxide, magnetite (Fe_3O_4) and sodium alginate, used as tetracycline aptamer support. By means of the electrochemical probe thionine, DPV measurements were performed, obtaining a LOD of 6nM [174].

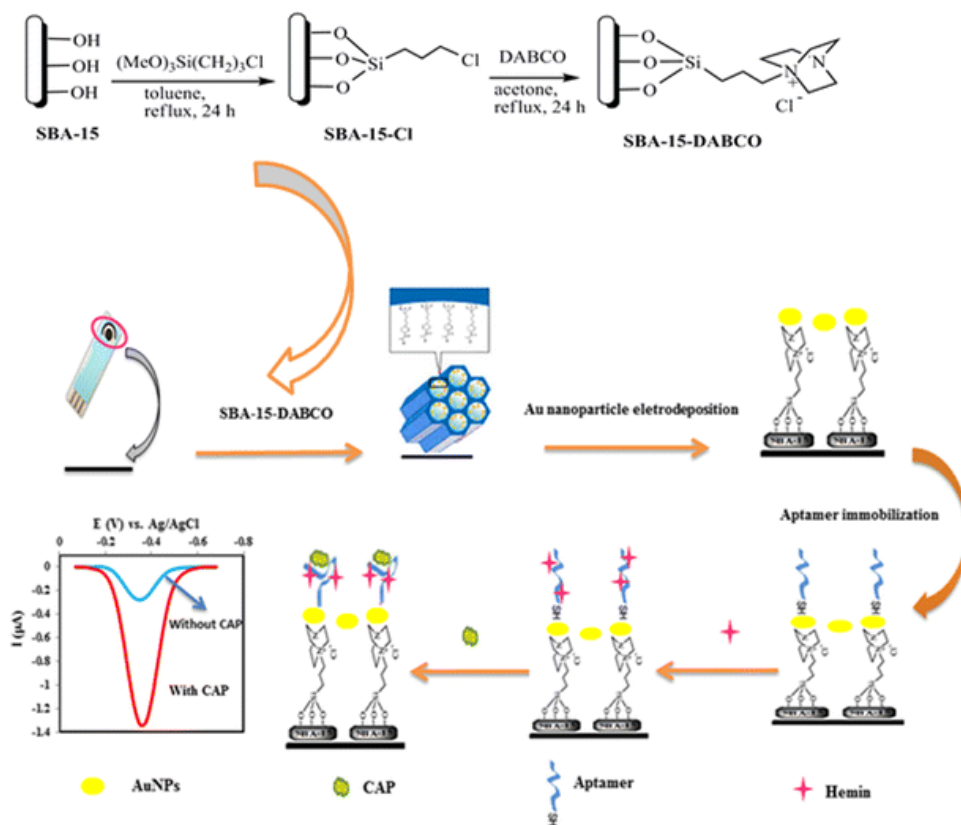


Figure 3.5: Scheme of the proposed label-free aptasensor for chloramphenicol detection. A graphite SPE was modified with a dendritic nanostructure based on mesoporous silica (SBA-15) functionalised with 1,4-diazabicyclo[2,2,2]octane (DABCO) in order to increase Au nanoparticles immobilisation, enhancing surface conductivity. The specific aptamer was bound via Au-S interaction, and analyte capturing was monitored via DPV, using hemin as electrochemical. Reprinted with Springer permission [169].

Catanante et al. reported an ochratoxin-A aptasensor based on a methylene blue-labelled selective aptamer, immobilised on a graphite SPE. Several aptamer immobilisation methods were tested, and best results were obtained by grafting hexamethylenediamine on electrode surface as aptamer linker. Interaction with the analyte brought to a conformational change, approaching methylene blue to working electrode surface and increasing the signal recorded by DPV. A LOD of 0.01 ng/mL was obtained and real samples (cocoa) were tested [175]. A graphite SPE DPV-based aptasensor was reported by Mishra et al. for ochratoxin-A

CHAPTER 3

detection. The system was based on a competitive interaction between free and biotin-labelled target with a covalently immobilised aptamer onto electrode surface. Signal was amplified binding avidin-alkaline phosphatase to labelled target-aptamer adduct and measuring current obtained by oxidation of 1-naphthyl-phosphate, inversely proportional to free ochratoxin-A concentration. A LOD of 0.07 ng/mL was obtained and real samples were also tested (cocoa beans) [176]. Mishra et al. previously reported another aptasensor for ochratoxin-A detection, based on a label-free approach. Specific aptamer was covalently bound onto the surface of a graphite SPE and interaction with the analyte was measured via EIS, using $[\text{Fe}(\text{CN})_6]^{3-/4-}$ as redox probe. A LOD of 0.15 ng/mL was obtained and analyses on cocoa beans were also carried out [177]. Bulbul et al proposed an assay based on a non-enzymatic nanoceria (CeO_2) tag, depositing graphene oxide onto the surface of a graphite SPE and immobilising a specific ochratoxin-A aptamer on it. The assay is based on the competition between free and nanoceria-labelled target: the more free target interact with the probe, the lower is the signal. By means of cyclic voltammetry (CV), oxidation of H_2O_2 (catalysed by nanoceria) was measured, obtaining a LOD of 0.1 nM. Real corn samples were also tested [178]. Rivas et al. reported a label-free impedimetric aptasensor for ochratoxin-A detection, modifying a graphite SPE with a thin film of electrodeposited polythionine and IrO_2 nanoparticles, on which the probe aptamer was electrostatically immobilised. The sensor was able to detect the target in buffered samples by means of EIS, using $[\text{Fe}(\text{CN})_6]^{3-/4-}$ as redox probe. A LOD of 14 pM was obtained, testing also real wine samples (Figure 3.) [179]. Another aptasensor for ochratoxin-A was described by Sun et al., attaching a thionine-labelled probe aptamer to the

surface of graphene nanosheets via non-covalent interaction and suspending the nanocomposite adduct in a buffered solution. Interaction with the target released aptamer-target adduct, that was cleaved by DNase I: free target was used to trigger again aptamer release, while free thionine was used as electrochemical mediator being measured by means of a negatively charged graphite SPE via DPV. A LOD of 5.6 pg/mL was obtained and real samples were also tested, using spiked and naturally contaminated wheat [180]. Istamboulié et al. developed an impedimetric aptasensor for aflatoxin-M1 detection, based on a graphite SPE on which a hexaethyleneglycol-tailored specific aptamer was immobilised via carbodiimide binding. Aptamer-target interaction induced an increase in electron-transfer resistance, measured by means of EIS, using $[\text{Fe}(\text{CN})_6]^{3-}/4-$ as redox probe. A LOD of 1.15 ng/L was obtained and spiked milk samples were also analysed [181]. Yugender Goud et al. reported a label free aptasensor for aflatoxin-B1 detection based on graphite SPEs on which two different probe aptamers (seqA and seqB) were separately linked via covalent bond. Interaction with the target brought to an increase of electron transfer resistance that was monitored by means of EIS, using $[\text{Fe}(\text{CN})_6]^{4-/3-}$ as redox probe. Obtained LOD were 0.12 ng/mL for seqA and 0.25 ng/mL for seqB, and real matrices were also tested, spiking beer and wine samples [182].

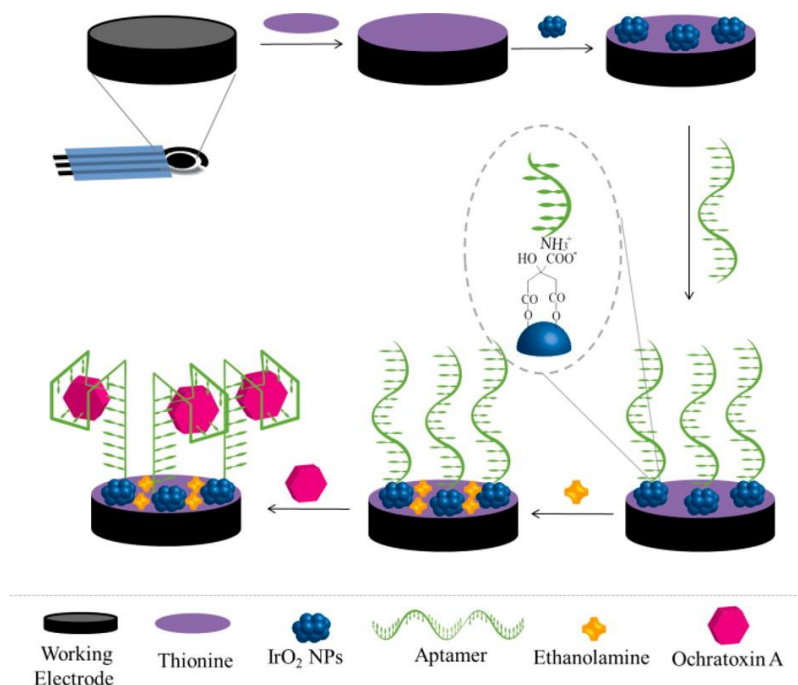


Figure 3.6: Scheme of the label-free impedimetric aptasensor for ochratoxin-A detection. A graphite SPE was modified with a thin film of electrodeposited polythionine and IrO₂ nanoparticles, on which the probe aptamer was electrostatically immobilised. The sensor was able to detect the target in buffered samples by means of EIS, using [Fe(CN)₆]^{3-/4-} as redox probe. Reprinted with permission from: L. Rivas, C.C. Mayorga-Martinez, D. Quesada-González, A. Zamora-Gálvez, A. de la Escosura-Muñiz, A. Merkoçi, *Anal. Chem.*, 87: 5167-5172, 2015. Copyright 2015 American Chemical Society [179].

3.1.9 Conclusions

In recent years many works were proposed, describing advances in aptamer sequences realisation, as well as combination of probe sequences with nanomaterials in order to improve detection procedures. Compared to other techniques, electrochemical transduction showed some advantages, like the possibility to integrate different signal amplification schemes (e.g. using catalytic or bio-catalytic amplification) simply adding a proper label to the probe sequence or to the aptamer-target adduct. Apart from this,

many assays were developed using a label free approach, in order to simplify step-by-step procedure for the realisation of the analytical tool.

Works presented in this review show that aptamer based devices still represent one of the most promising approach for biosensor development; moreover it can be noticed that their application in environmental analysis is one of the less explored field, being the majority of the summarised works about clinical targets.

Despite of this attractive advantages, aptamers for environmental and food security monitoring are still under development phase, if compared to immunoassays. The primary limit is the limited number of available probe sequences (even if SELEX continuous improvements will help scientists from this point of view). Another potentially growing field concerns development in aptamer immobilisation strategies, especially in combination with nanomaterials. These limits certify that exciting improving opportunities still exist in the field of aptasensors. Future growth could be focused on the design of aptamers against unexplored target analyte, and then their subsequent integration in well-known and reliable electrochemical platform to perform analysis.

CHAPTER 3

3.1.10 Summary tables

Table 3.1: Summary of reported works about pesticides and pollutants

Analyte	Electrochemical technique	Reported LOD	Tested matrix	Ref.
bisphenol-A	SWV	0.6 pM	tap water	[43]
	SWV	0.19 pM	tap water	[44]
	DPV	210 pM	environmental water	[45]
	DPV	5 nM	milk	[46]
acetamiprid	EIS	1.7×10^{-14} M	water	[36]
	EIS	3.3×10^{-14} M	waste H ₂ O, vegetables	[37]
	DPV (on SPEs)	0.086 μ M	fruit juice	[162]
2, 4, 6- trinitrotoluene (TNT)	SWV	1 ppb	soil	[50]
	DPV	0.33 nM	tap water, river water	[55]
	DPV	0.12 pM	lake water	[56]
mercury (Hg ²⁺ ion)	DPV	5×10^{-15} M	tap water, river water	[57]
	DPV	1.5×10^{-12} M	tap water, river water	[58]
arsenic (arsenite ion)	DPV (on SPEs)	0.15 nM	tap water, lake water	[168]
polychlorinated biphenyl-72	SWSV	0.35 pg/mL	fish	[63]
malachite green	CV (on SPEs)	0.07 nM	fish	[172]

Table 3.2: Summary of reported works about drugs

Analyte	Electrochemical technique	Reported LOD	Tested matrix	Ref.
chloramphenicol	SWSV	0.33 pg/mL	fish	[63]
	EIS	1.76 nM	-	[64]
	SWV	0.15 ng/mL	milk	[65]
	DPV (on SPEs)	4.0 nM	hum. serum	[169]
	SWV (on SPEs)	4.0 nM	hum. serum	[170]
	CV (on SPEs)	0.03 nM	fish	[171]
	CV (on SPEs)	0.03 nM	fish	[172]
	DPV (on SPEs)	1.83×10^{-10} M	milk	[173]
	DPV (on SPEs)	6 nM	-	[174]
tetracyclines	SWV (oxytetracycline)	0.10 ng/mL	milk	[65]
	DPV (tetracycline)	0.56×10^{-11} M	milk	[66]
	DPV (tetracycline)	3.2×10^{-10} M	milk	[67]
	CV	150 pM	milk, serum	[68]
ampicillin	DPV	1.09 pM	milk	[70]
	DPV	4.0 pM	milk	[71]
ractopamine	EIS	0.04 ng/mL	pork	[74]
	DPV	5.0×10^{-13} M	swine urine	[75]
clenbuterol		0.35 pg/mL		
salbutamol		0.53 pg/mL		
phenylethanolamine	EIS	1.0 pg/mL	pork	[74]
procaterol		1.73 pg/mL		
streptomycin	DPV	14.1 nM	rat serum, milk	[79]
	DPV	0.42 pg/mL	animal derived food	[81]
	SVW	0.014 nM	milk	[82]
	DPV	3.7 pg/mL	milk	[83]
kanamycin	DPV	0.87 nM	milk	[84]
	SWV	1 pM	milk	[85]
	DPV	5.8×10^{-9} M	milk	[86]
	DPV	4.6×10^{-6} µg/mL	milk	[87]
			pharmaceutical formulations, hum. serum, waste water	
ibuprofen	DPV	20 pM		[96]
cocaine	DPV	100 pM	hum. serum	[101]
	DPV	105 pM	rat serum	[102]
	DPV	1.3 nM	urine	[103]

CHAPTER 3

Table 3.3: Summary of reported works about toxins

Analyte	Electrochemical technique	Reported LOD	Tested matrix	Ref.
ochratoxin-A	EIS	2 ng/L	wine	[108]
	DPV	0.004 ng/mL	corn	[109]
	DPV	0.75 pM	wine	[110]
	DPV (on SPEs)	0.01 ng/mL	cocoa	[175]
	DPV (on SPEs)	0.07 ng/mL	cocoa beans	[176]
	EIS (on SPEs)	0.15 ng/mL	cocoa beans	[177]
	CV (on SPEs)	0.1 nM	corn	[178]
	EIS (on SPEs)	14 pM	wine	[179]
	DPV (on SPEs)	5.6 pg/mL	wheat	[180]
aflatoxins	SWV (aflatoxin-B1)	0.6x10 ⁻⁴ ppt	corn	[114]
	CV, EIS* (aflatoxin-B1)	0.1 nM, 0.05 nM	nuts, soy, wine	[115]
	EIS (aflatoxin-M1)	1.15 ng/L	milk	[181]
	EIS (aflatoxin-B1)	0.12; 0.25 ng/mL*	beer, wine	[182]
staphylococcal enterotoxin-B	DPV	0.24 ng/mL	serum	[118]
saxitoxin	DPV	0.38 nM	mussel	[123]
fumonisin-B1	EIS	2 pM	maize	[129]
brevetoxin-2	EIS	106 pg/mL	shellfish	[132]
ricin	fluorescence, SWV**	30; 3nM	hum. serum, saliva	[135]
	SWV	-	-	[137]
botulinum	SWV	-	-	[137]
	EIS (cylindrospermopsin)	0.117 ng/mL	lake water	[142]
cyanotoxins	EIS (anatoxin-A)	0.5 nM	drinking water	[145]
	EIS	100pM	tap water	[146]
toxin-A (from <i>clostridium difficile</i>)	CV	1 nM	-	[150]

*The reported paper describes two approaches based on two different probe aptamers.

**The reported paper describes two approaches based on same probe aptamer.

3.2 References

- [1] D.P. Nikolelis, A. Erdem, G.-P. Nikoleli, T. Varzakas (Eds.), *Portable Biosensing of Food Toxicants and Environmental Pollutants*, CRC Press 2013.
- [2] C. Tuerk, L. Gold, *Science*, 249: 505-510, 1990.
- [3] A.D. Ellington, J.W. Szostak, *Nature*, 346: 818-822, 1990.
- [4] J.H. Lee, M.V. Yigit, D. Mazumdar, Y. Lu, *Adv Drug Deliv Rev*, 62: 592-605, 2010.
- [5] C. Yao, T. Zhu, Y. Qi, Y. Zhao, H. Xia, W. Fu, *Sensors*, 10: 5859-5871, 2010.
- [6] T. Tang, J. Deng, M. Zhang, G. Shi, T. Zhou, *Talanta*, 146: 55-61, 2016.
- [7] T. Mairal, V.C. Özalp, P.L. Sánchez, M. Mir, I. Katakis, C.K. O'Sullivan, *Anal. Bioanal. Chem.*, 390: 989-1007, 2008.
- [8] V. Scognamiglio, G. Rea, F. Arduini, G. Palleschi (Eds.), *Biosensor potential in pesticide monitoring*, in: *Biosensors for Sustainable Food - New Opportunities and Technical Challenges*, 1st Edition Elsevier 2016.
- [9] L. Fan, G. Zhao, H. Shi, M. Liu, Z. Li, *Biosens Bioelectron*, 43: 12-18, 2013.
- [10] S. Pang, T.P. Labuza, L. He, *Analyst*, 139: 1895-1901, 2014.
- [11] R. White, N. Phares, A. Lubin, Y. Xiao, K. Plaxco, *Langmuir*, 24: 10513-10518, 2008.
- [12] C.I. Justino, A.C. Freitas, R. Pereira, A.C. Duarte, T.A.R. Santos, *TrAC Trends in Analytical Chemistry*, 68: 2-17, 2015.
- [13] R. Sharma, K. Ragavan, M. Thakur, K. Raghavarao, *Biosensors Bioelectron.*, 74: 612-627, 2015.
- [14] A. Ruscito, M.C. DeRosa, *Frontiers in Chemistry*, 4: 2016.
- [15] N. Seeman, *Annu. Rev. Biochem*, 79: 65-87, 2010.

CHAPTER 3

- [16] T. Hermann, D.J. Patel, *Science*, 287: 820-825, 2000.
- [17] C.J. Yang, W. Tan (Eds.), *Molecular Aptamer Beacons*, in: *Molecular Beacons* Springer 2013.
- [18] A. Hayat, J.L. Marty, *Frontiers in Chemistry*, 2: 41, 2014.
- [19] J. Daprà, L.H. Lauridsen, A.T. Nielsen, N. Rozlosnik, *Biosensors Bioelectron.*, 43: 315-320, 2013.
- [20] L.R. Schoukroun-Barnes, S. Wagan, R.J. White, *Anal. Chem.*, 86: 1131-1137, 2014.
- [21] S.N. Topkaya, M. Azimzadeh, M. Ozsoz, *Electroanal*, 28: 1402–1419 2016.
- [22] S. MacKay, D. Wishart, J.Z. Xing, J. Chen, *IEEE Transactions on Biomedical Circuits and Systems*, 8: 4-14, 2014.
- [23] L. Reverté, B. Prieto-Simón, M. Campàs, *Anal. Chim. Acta*, 908: 8-21, 2016.
- [24] M. Trojanowicz, *TrAC Trends in Analytical Chemistry*, 84: 22-47, 2016.
- [25] J. Aceña, S. Stampachiachiere, S. Pérez, D. Barceló, *Anal. Bioanal. Chem.*, 407: 6289-6299, 2015.
- [26] Liang, H.C. Liang, N. Bilon, M. Hay, *Water Environ. Res*, 87: 1923-1937, 2015.
- [27] N. Duan, S. Wu, S. Dai, H. Gu, L. Hao, H. Ye, Z. Wang, *Analyst*, 141: 3942-3961, 2016.
- [28] F. Arduini, S. Cinti, V. Scognamiglio, D. Moscone, *Microchimica Acta*, 1-21, 2016.
- [29] N. Verma, A. Bhardwaj, *Appl Biochem Biotechnol*, 175: 3093-3119, 2015.

- [30] T. Cairns, J. Sherma (Eds.), *Emerging strategies for pesticide analysis*, CRC Press 1992.
- [31] J. Fenik, M. Tankiewicz, M. Biziuk, *TrAC, Trends Anal. Chem.*, 30: 814-826, 2011.
- [32] K. Matsuda, S.D. Buckingham, D. Kleier, J.J. Rauh, M. Grauso, D.B. Sattelle, *Trends Pharmacol. Sci.*, 22: 573-580, 2001.
- [33] A.M.J. Ragas, R. Oldenkamp, N.L. Preeker, J. Wernicke, U. Schlink, *Environ. Int.*, 37: 872-881, 2011.
- [34] A.Y. Kocaman, M. Topaktas, *Environ. Mol. Mutag.*, 48: 483-490, 2007.
- [35] A. Aagaard, T. Brock, E. Capri, S. Duquesne, M. Filipic, A. Hernandez-Jerez, K. Ildico Hirsch-Ernst, S. Hougaard Bennekou, M. Klein, T. Kuhl, R. Laskowski, M. Liess, A. Mantovani, C. Ockleford, B. Ossendorp, D. Pickford, R. Smith, P. Sousa, I. Sundh, A. Tiktak, T. Van Der Linden, *EFSA Journal*, 11: 2013.
- [36] A. Fei, Q. Liu, J. Huan, J. Qian, X. Dong, B. Qiu, H. Mao, K. Wang, *Biosens Bioelectron.*, 70: 122-129, 2015.
- [37] D. Jiang, X. Du, Q. Liu, L. Zhou, L. Dai, J. Qian, K. Wang, *Analyst*, 140: 6404-6411, 2015.
- [38] X. Wang, X. Lu, J. Chen, *Trends in Environmental Analytical Chemistry*, 2: 25-32, 2014.
- [39] A. Sett, S. Das, P. Sharma, U. Bora, *Open Journal of Applied Biosensor*, Vol.01No.02: 11, 2012.
- [40] L. Vandenberg, R. Hauser, M. Marcus, N. Olea, W. Welshons, *Reprod. Toxicol.*, 24: 139-177, 2007.
- [41] H. Hiroi, O. Tsutsumi, M. Momoeda, Y. Takai, Y. Osuga, Y. Taketani, *Endocr. J.*, 46: 773-778, 1999.
- [42] S.H. Safe, *Environ. Health Perspect.*, 108: 487, 2000.

CHAPTER 3

- [43] Y. Liu, X. Zhang, J. Yang, E. Xiong, X. Zhang, J. Chen, *Can. J. Chem.*, 94: 509-514, 2016.
- [44] P. Yu, Y. Liu, X. Zhang, J. Zhou, E. Xiong, X. Li, J. Chen, *Biosensors Bioelectron.*, 79: 22-28, 2016.
- [45] Z. Derikvand, A.R. Abbasi, M. Roushani, Z. Derikvand, A. Azadbakht, *Anal. Biochem.*, 512: 47-57, 2016.
- [46] L. Zhou, J. Wang, D. Li, Y. Li, *Food Chem.*, 162: 34-40, 2014.
- [47] J.C. Spain (Ed.) Basic knowledge and perspectives on biodegradation of 2, 4, 6-trinitrotoluene and related nitroaromatic compounds in contaminated soil, in: *Biodegradation of nitroaromatic compounds* Plenum Press, New York, 1995.
- [48] J.M. Conder, T.W. La Point, J.A. Steevens, G.R. Lotufo, *Environ. Toxicol. Chem.*, 23: 141-149, 2004.
- [49] P. Gong, B.-M. Wilke, S. Fleischmann, *Arch. Environ. Contam. Toxicol.*, 36: 152-157, 1999.
- [50] M. Shorie, V. Bhalla, P. Pathania, C.R. Suri, *Chem. Commun.*, 50: 1080-1082, 2014.
- [51] M. Saghir Khan, A. Zaidi, R. Goel, J. Musarrat (Eds.), *Heavy Metal Pollution: Source, Impact, and Remedies*, in: *Bio management of Metal-Contaminated Soils* 2011.
- [52] R.S. Boyd, *J. Chem. Ecol.*, 36: 46-58, 2010.
- [53] A. Bhan, N. Sarkar, *Reviews on environmental health*, 20: 39-56, 2005.
- [54] D.W. Boening, *Chemosphere*, 40: 1335-1351, 2000.
- [55] D. Wu, Y. Wang, Y. Zhang, H. Ma, X. Pang, L. Hu, B. Du, Q. Wei, *Biosensors Bioelectron.*, 82: 9-13, 2016.

- [56] T. Bao, W. Wen, X. Zhang, Q. Xia, S. Wang, *Biosensors Bioelectron.*, 70: 318-323, 2015.
- [57] J. Li, M. Sun, X. Wei, L. Zhang, Y. Zhang, *Biosensors Bioelectron.*, 74: 423-426, 2015.
- [58] C. Gao, Q. Wang, F. Gao, F. Gao, *Chem. Commun.*, 50: 9397-9400, 2014.
- [59] D.M. Whitacre (Ed.) *Reviews of Environmental Contamination and Toxicology*, Springer New York, New York, NY, 2012.
- [60] A. Puckowski, K. Mioduszevska, P. Łukaszewicz, M. Borecka, M. Caban, J. Maszkowska, P. Stepnowski, *J. Pharm. Biomed. Anal.*, 127: 232-255, 2016.
- [61] A.K. Sarmah, M.T. Meyer, A.B.A. Boxall, *Chemosphere*, 65: 725-759, 2006.
- [62] J. Wang, J.D. MacNeil, J.F. Kay (Eds.), *Chemical analysis of antibiotic residues in food*, John Wiley & Sons 2011.
- [63] M. Chen, N. Gan, H. Zhang, Z. Yan, T. Li, Y. Chen, Q. Xu, Q. Jiang, *Microchimica Acta*, 183: 1099-1106, 2016.
- [64] S. Pilehvar, T. Dierckx, R. Blust, T. Breugelmans, K. De Wael, *Sensors*, 14: 12059-12069, 2014.
- [65] Z. Yan, N. Gan, T. Li, Y. Cao, Y. Chen, *Biosensors Bioelectron.*, 78: 51-57, 2016.
- [66] Y. Guo, G. Shen, X. Sun, X. Wang, *IEEE Sens. J.*, 15: 1951-1958, 2015.
- [67] G. Shen, Y. Guo, X. Sun, X. Wang, *Nano-Micro Letters*, 6: 143-152, 2014.
- [68] S.M. Taghdisi, N.M. Danesh, M. Ramezani, K. Abnous, *Biosensors Bioelectron.*, 85: 509-514, 2016.

CHAPTER 3

- [69] G. Suleyman, M.J. Zervos, *Expert Opin. Drug Saf.*, 15: 153-167, 2016.
- [70] H. Wang, Y. Wang, S. Liu, J. Yu, W. Xu, Y. Guo, J. Huang, *Chem. Commun.*, 51: 8377-8380, 2015.
- [71] X. Wang, S. Dong, P. Gai, R. Duan, F. Li, *Biosensors Bioelectron.*, 82: 49-54, 2016.
- [72] D.H. Au, J.R. Curtis, N.R. Every, M.B. McDonell, S.D. Fihn, *Chest*, 121: 846-851, 2002.
- [73] W.O. Spitzer, S. Suissa, P. Ernst, R.I. Horwitz, B. Habbick, D. Cockcroft, J.-F. Boivin, M. McNutt, A.S. Buist, A.S. Rebuck, *New Engl. J. Med.*, 326: 501-506, 1992.
- [74] D. Chen, M. Yang, N. Zheng, N. Xie, D. Liu, C. Xie, D. Yao, *Biosensors Bioelectron.*, 80: 525-531, 2016.
- [75] F. Yang, P. Wang, R. Wang, Y. Zhou, X. Su, Y. He, L. Shi, D. Yao, *Biosensors Bioelectron.*, 77: 347-352, 2016.
- [76] N. Zhou, J. Wang, J. Zhang, C. Li, Y. Tian, J. Wang, *Talanta*, 108: 109-116, 2013.
- [77] R.H. Granja, A.M.M. Niño, R.A. Zucchetti, R.E.M. Niño, R. Patel, A.G. Salerno, *Anal. Chim. Acta*, 637: 64-67, 2009.
- [78] R.C. de Oliveira, J.A.R. Paschoal, M. Sismotto, F.P. da Silva Airoldi, F.G.R. Reyes, *J. Chromatogr. Sci.*, 47: 756-761, 2009.
- [79] N.M. Danesh, M. Ramezani, A.S. Emrani, K. Abnous, S.M. Taghdisi, *Biosensors Bioelectron.*, 75: 123-128, 2016.
- [80] O.n.W. Guthrie, *Toxicology*, 249: 91-96, 2008.
- [81] X. Qin, Y. Yin, H. Yu, W. Guo, M. Pei, *Biosensors Bioelectron.*, 77: 752-758, 2016.

- [82] N. Zhou, J. Luo, J. Zhang, Y. You, Y. Tian, *Anal. Methods*, 7: 1991-1996, 2015.
- [83] W. Guo, N. Sun, X. Qin, M. Pei, L. Wang, *Biosensors Bioelectron.*, 74: 691-697, 2015.
- [84] X. Qin, W. Guo, H. Yu, J. Zhao, M. Pei, *Anal. Methods*, 7: 5419-5427, 2015.
- [85] Y. Xu, L. Sun, X. Huang, Y. Sun, C. Lu, *Anal. Methods*, 8: 726-730, 2016.
- [86] X. Sun, F. Li, G. Shen, J. Huang, X. Wang, *Analyst*, 139: 299-308, 2014.
- [87] W. Xu, Y. Wang, S. Liu, J. Yu, H. Wang, J. Huang, *New J. Chem.*, 38: 4931-4937, 2014.
- [88] O.A.H. Jones, N. Voulvoulis, J.N. Lester, *Crit. Rev. Toxicol.*, 34: 335-350, 2004.
- [89] O.A. Jones, J.N. Lester, N. Voulvoulis, *Trends Biotechnol.*, 23: 163-167, 2005.
- [90] T. Malchi, Y. Maor, G. Tadmor, M. Shenker, B. Chefetz, *Environ. Sci. Technol.*, 48: 9325-9333, 2014.
- [91] S.D. Richardson, T.A. Ternes, *Anal. Chem.*, 86: 2813-2848, 2014.
- [92] R. Pal, M. Megharaj, K.P. Kirkbride, R. Naidu, *Sci. Total Environ.*, 463: 1079-1092, 2013.
- [93] M. Cleuvers, *Ecotoxicol. Environ. Saf.*, 59: 309-315, 2004.
- [94] S. Adams, E. Cliffe, B. Lessel, J. Nicholson, *J. Pharm. Sci.*, 56: 1686-1686, 1967.
- [95] S. Halpern, R. Fitzpatrick, G. Volans, *Adverse Drug React. Toxicol. Rev.*, 12: 107, 1993.
- [96] M. Roushani, F. Shahdost-fard, *Materials Science and Engineering: C*, 68: 128-135, 2016.

CHAPTER 3

- [97] S. Castiglioni, E. Zuccato, R. Fanelli (Eds.), *Illicit drugs in the environment: occurrence, analysis, and fate using mass spectrometry*, John Wiley & Sons 2011.
- [98] C. Balducci, M. Perilli, P. Romagnoli, A. Cecinato, *Environmental Science and Pollution Research*, 19: 1875-1884, 2012.
- [99] A. Cecinato, C. Balducci, E. Guerriero, F. Sprovieri, F. Cofone, *Sci. Total Environ.*, 412–413: 87-92, 2011.
- [100] M. Parolini, A. Pedriali, C. Riva, A. Binelli, *Sci. Total Environ.*, 444: 43-50, 2013.
- [101] M. Roushani, F. Shahdost-fard, *Anal. Chim. Acta*, 853: 214-221, 2015.
- [102] S.M. Taghdisi, N.M. Danesh, A.S. Emrani, M. Ramezani, K. Abnous, *Biosensors Bioelectron.*, 73: 245-250, 2015.
- [103] B. Shen, J. Li, W. Cheng, Y. Yan, R. Tang, Y. Li, H. Ju, S. Ding, *Microchimica Acta*, 182: 361-367, 2015.
- [104] M.L. Fernández-Cruz, M.L. Mansilla, J.L. Tadeo, *Journal of Advanced Research*, 1: 113-122, 2010.
- [105] M. Peraica, B. Radic, A. Lucic, M. Pavlovic, *Bull. W.H.O.*, 77: 754-766, 1999.
- [106] S. Amézqueta, E. González-Peñas, M. Murillo-Arbizu, A. López de Cerain, *Food Control*, 20: 326-333, 2009.
- [107] A. Pfohl-Leszkowicz, R.A. Manderville, *Mol. Nutr. Food Res.*, 51: 61-99, 2007.
- [108] N. Mejri-Omrani, A. Miodek, B. Zribi, M. Marrakchi, M. Hamdi, J.-L. Marty, H. Korri-Youssoufi, *Anal. Chim. Acta*, 920: 37-46, 2016.
- [109] Y. Tan, X. Wei, Y. Zhang, P. Wang, B. Qiu, L. Guo, Z. Lin, H.-H. Yang, *Anal. Chem.*, 87: 11826-11831, 2015.

- [110] X. Yang, J. Qian, L. Jiang, Y. Yan, K. Wang, Q. Liu, K. Wang, *Bioelectrochemistry*, 96: 7-13, 2014.
- [111] I.Y.S. Rustom, *Food Chem.*, 59: 57-67, 1997.
- [112] M.E. Smela, S.S. Currier, E.A. Bailey, J.M. Essigmann, *Carcinogenesis*, 22: 535-545, 2001.
- [113] J.H. Do, D.-K. Choi, *Biotechnology and Bioprocess Engineering*, 12: 585-593, 2007.
- [114] W. Zheng, J. Teng, L. Cheng, Y. Ye, D. Pan, J. Wu, F. Xue, G. Liu, W. Chen, *Biosensors Bioelectron.*, 80: 574-581, 2016.
- [115] G. Evtugyn, A. Porfireva, V. Stepanova, R. Sitdikov, I. Stoikov, D. Nikolelis, T. Hianik, *Electroanal*, 26: 2100-2109, 2014.
- [116] J. White, A. Herman, A.M. Pullen, R. Kubo, J.W. Kappler, P. Marrack, *Cell*, 56: 27-35, 1989.
- [117] M. Labib, M. Hedström, M. Amin, B. Mattiasson, *Anal. Bioanal. Chem.*, 393: 1539-1544, 2008.
- [118] R. Deng, L. Wang, G. Yi, E. Hua, G. Xie, *Colloids Surf. B. Biointerfaces*, 120: 1-7, 2014.
- [119] A. Hoehne, D. Behera, W.H. Parsons, M.L. James, B. Shen, P. Borgohain, D. Bodapati, A. Prabhakar, S.S. Gambhir, D.C. Yeomans, *J. Am. Chem. Soc.*, 135: 18012-18015, 2013.
- [120] K.D. Cusick, G.S. Sayler, *Mar. Drugs*, 11: 991-1018, 2013.
- [121] J.R. Deeds, J.H. Landsberg, S.M. Etheridge, G.C. Pitcher, S.W. Longan, *Mar. Drugs*, 6: 308-348, 2008.
- [122] S.M. Etheridge, *Toxicon*, 56: 108-122, 2010.
- [123] L. Hou, L. Jiang, Y. Song, Y. Ding, J. Zhang, X. Wu, D. Tang, *Microchimica Acta*, 183: 1971-1980, 2016.
- [124] A. Visconti, M.B. Doko, M. Solfrizzo, M. Pascale, A. Boenke, *Microchimica Acta*, 123: 55-61, 1996.

CHAPTER 3

- [125] P.E. Nelson, A.E. Desjardins, R.D. Plattner, *Annu. Rev. Phytopathol.*, 31: 233-252, 1993.
- [126] I.W.G.o.t.E.o.C.R.t. Humans, W.H. Organization, I.A.f.R.o. Cancer (Eds.), Fumonisin B1, in: Some traditional herbal medicines, some mycotoxins, naphthalene and styrene IARCPress, Lyon (France), 2002.
- [127] T. Yoshizawa, A. Yamashita, Y. Luo, *Appl. Environ. Microbiol.*, 60: 1626-1629, 1994.
- [128] G.S. Shephard, L. van der Westhuizen, P.M. Gatyeni, N.I. Somdyala, H.-M. Burger, W.F. Marasas, *J. Agric. Food. Chem.*, 53: 9634-9637, 2005.
- [129] X. Chen, Y. Huang, X. Ma, F. Jia, X. Guo, Z. Wang, *Microchimica Acta*, 182: 1709-1714, 2015.
- [130] D.G. Baden, A.J. Bourdelais, H. Jacocks, S. Michelliza, J. Naar, *Environ. Health Perspect.*, 621-625, 2005.
- [131] L.J. Flewelling, J.P. Naar, J.P. Abbott, D.G. Baden, N.B. Barros, G.D. Bossart, M.-Y.D. Bottein, D.G. Hammond, E.M. Haubold, C.A. Heil, *Nature*, 435: 755-756, 2005.
- [132] S. Eissa, M. Siaj, M. Zourob, *Biosensors Bioelectron.*, 69: 148-154, 2015.
- [133] J. Audi, M. Belson, M. Patel, J. Schier, J. Osterloh, *Jama*, 294: 2342-2351, 2005.
- [134] J. Wesche, A. Rapak, S. Olsnes, *J. Biol. Chem.*, 274: 34443-34449, 1999.
- [135] Y. Du, S.J. Zhen, B. Li, M. Byrom, Y.S. Jiang, A.D. Ellington, *Anal. Chem.*, 88: 2250-2257, 2016.
- [136] J. Sobel, *Clin. Infect. Dis.*, 41: 1167-1173, 2005.

- [137] L. Fetter, J. Richards, J. Daniel, L. Roon, T.J. Rowland, A.J. Bonham, *Chem. Commun.*, 51: 15137-15140, 2015.
- [138] B. Poniedziałek, P. Rzymiski, M. Kokociński, *Environ. Toxicol. Pharmacol.*, 34: 651-660, 2012.
- [139] I. Ohtani, R.E. Moore, M.T. Runnegar, *J. Am. Chem. Soc.*, 114: 7941-7942, 1992.
- [140] I. Falconer, A. Humpage, *Environ. Toxicol.*, 16: 192-195, 2001.
- [141] F.M. Young, J. Micklem, A.R. Humpage, *Reprod. Toxicol.*, 25: 374-380, 2008.
- [142] Z. Zhao, H. Chen, L. Ma, D. Liu, Z. Wang, *Analyst*, 140: 5570-5577, 2015.
- [143] J.A. Camargo, Á. Alonso, *Environ. Int.*, 32: 831-849, 2006.
- [144] J. Osswald, S. Rellán, A. Gago, V. Vasconcelos, *Environ. Int.*, 33: 1070-1089, 2007.
- [145] R. Elshafey, M. Siaj, M. Zourob, *Biosensors Bioelectron.*, 68: 295-302, 2015.
- [146] R. Elshafey, M. Siaj, M. Zourob, *Anal. Chem.*, 86: 9196-9203, 2014.
- [147] V. Pasquale, V.J. Romano, M. Rupnik, S. Dumontet, I. Čižnár, F. Aliberti, F. Mauri, V. Saggiomo, K. Krovacek, *Folia Microbiol.*, 56: 431-437, 2011.
- [148] V. Pasquale, V. Romano, M. Rupnik, F. Capuano, D. Bove, F. Aliberti, K. Krovacek, S. Dumontet, *Food Microbiol.*, 31: 309-312, 2012.
- [149] D.D. DePestel, D.M. Aronoff, *Journal of pharmacy practice*, 26: 464-475, 2013.
- [150] P. Luo, Y. Liu, Y. Xia, H. Xu, G. Xie, *Biosensors Bioelectron.*, 54: 217-221, 2014.

CHAPTER 3

- [151] M. Alonso-Lomillo, O. Domínguez-Renedo, M. Arcos-Martínez, *Talanta*, 82: 1629-1636, 2010.
- [152] O.D. Renedo, M. Alonso-Lomillo, M.A. Martínez, *Talanta*, 73: 202-219, 2007.
- [153] M. Tudorache, C. Bala, *Anal. Bioanal. Chem.*, 388: 565-578, 2007.
- [154] J. Wang, *TrAC Trends in Analytical Chemistry*, 21: 226-232, 2002.
- [155] Z. Taleat, A. Khoshroo, M. Mazloun-Ardakani, *Microchimica Acta*, 181: 865-891, 2014.
- [156] F. Lucarelli, L. Authier, G. Bagni, G. Marrazza, T. Baussant, E. Aas, M. Mascini, *Anal. Lett.*, 36: 1887-1901, 2003.
- [157] S. Kröger, A.P.F. Turner, *Anal. Chim. Acta*, 347: 9-18, 1997.
- [158] P. Fanjul-Bolado, D. Hernández-Santos, P.J. Lamas-Ardisana, A. Martín-Pernía, A. Costa-García, *Electrochim. Acta*, 53: 3635-3642, 2008.
- [159] J. Wang, B. Tian, V.B. Nascimento, L. Angnes, *Electrochim. Acta*, 43: 3459-3465, 1998.
- [160] K.C. Honeychurch, J.P. Hart, *TrAC Trends in Analytical Chemistry*, 22: 456-469, 2003.
- [161] F. Arduini, F. Di Nardo, A. Amine, L. Micheli, G. Palleschi, D. Moscone, *Electroanal*, 24: 743-751, 2012.
- [162] R. Rapini, A. Cincinelli, G. Marrazza, *Talanta*, 161: 15-21, 2016.
- [163] C.O. Abernathy, Y.-P. Liu, D. Longfellow, H.V. Aposhian, B. Beck, B. Fowler, R. Goyer, R. Menzer, T. Rossman, C. Thompson, *Environ. Health Perspect.*, 107: 593, 1999.
- [164] T. Yoshida, H. Yamauchi, G.F. Sun, *Toxicol. Appl. Pharmacol.*, 198: 243-252, 2004.
- [165] S. Kapaj, H. Peterson, K. Liber, P. Bhattacharya, *Journal of Environmental Science and Health Part A*, 41: 2399-2428, 2006.

- [166] P.B. Tchounwou, A.K. Patlolla, J.A. Centeno, *Toxicol. Pathol.*, 31: 575-588, 2003.
- [167] W. Cullen, K. Reimer, *Chem Rev*, 89: 713-764, 1989.
- [168] L. Cui, J. Wu, H. Ju, *Biosensors Bioelectron.*, 79: 861-865, 2016.
- [169] A. Bagheri Hashkavayi, J. Bakhsh Raoof, R. Azimi, R. Ojani, *Anal. Bioanal. Chem.*, 408: 2557-2565, 2016.
- [170] A. Bagheri Hashkavayi, J. Bakhsh Raoof, R. Ojani, E. Hamidi Asl, *Electroanal*, 27: 1449-1456, 2015.
- [171] X. Feng, N. Gan, S. Lin, T. Li, Y. Cao, F. Hu, Q. Jiang, Y. Chen, *Sensors Actuators B: Chem.*, 226: 305-311, 2016.
- [172] X. Feng, N. Gan, H. Zhang, Q. Yan, T. Li, Y. Cao, F. Hu, H. Yu, Q. Jiang, *Biosensors Bioelectron.*, 74: 587-593, 2015.
- [173] E. Hamidi-Asl, F. Dardenne, R. Blust, K. De Wael, *Sensors*, 15: 7605-7618, 2015.
- [174] X. Zhan, G. Hu, T. Wagberg, S. Zhan, H. Xu, P. Zhou, *Microchimica Acta*, 183: 723-729, 2016.
- [175] G. Catanante, R.K. Mishra, A. Hayat, J.-L. Marty, *Talanta*, 153: 138-144, 2016.
- [176] R.K. Mishra, A. Hayat, G. Catanante, G. Istamboulie, J.-L. Marty, *Food Chem.*, 192: 799-804, 2016.
- [177] R.K. Mishra, A. Hayat, G. Catanante, C. Ocaña, J.-L. Marty, *Anal. Chim. Acta*, 889: 106-112, 2015.
- [178] G. Bulbul, A. Hayat, S. Andreescu, *Nanoscale*, 7: 13230-13238, 2015.
- [179] L. Rivas, C.C. Mayorga-Martinez, D. Quesada-González, A. Zamora-Gálvez, A. de la Escosura-Muñiz, A. Merkoçi, *Anal. Chem.*, 87: 5167-5172, 2015.

CHAPTER 3

- [180] A.-L. Sun, Y.-F. Zhang, G.-P. Sun, X.-N. Wang, D. Tang, *Biosensors Bioelectron.*, 89: 659-665, 2015.
- [181] G. Istamboulié, N. Paniel, L. Zara, L.R. Granados, L. Barthelmebs, T. Noguer, *Talanta*, 146: 464-469, 2016.
- [182] K. Yugender Goud, G. Catanante, A. Hayat, S. M, K. Vengatajalabathy Gobi, J.L. Marty, *Sensors Actuators B: Chem.*, 235: 466-473, 2016.

CHAPTER 4

4.1 Electrochemical techniques

4.1.1 Cyclic voltammetry

Cyclic voltammetry (CV) is a simple and largely applied electrochemical technique, used for the determination of the thermodynamic and kinetic parameters of a redox process [1-3].

CV can be also applied for surface electrode characterisation, fast determination of redox potential of electroactive targets and comparisons between different media effects on redox process. CV measurements are carried out applying a triangular potential waveform (Figure 4.1) to the working electrode and measuring the resulting current variations, at rest. Cyclic potential scan can be applied once as well as many times, depending on the experimental setup. Measurement results are commonly reported in form of potential (E) vs. current (i), a plot called voltammogram.

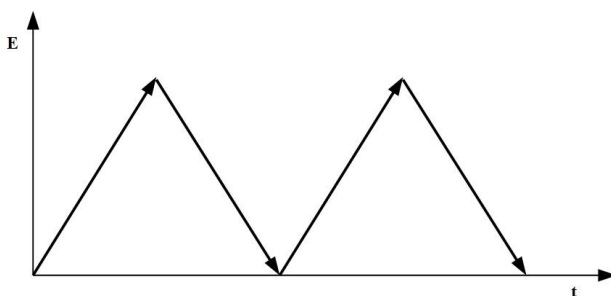


Figure 4.1: Potential vs. time scan applied in CV.

Analysing a voltammogram (Figure 4.2), it is possible to determine the cathodic peak potential, indicated as E_{pc} and related to the reduction process ($Ox + ne^- \rightarrow Red$) and the anodic peak potential, indicated as E_{pa}

CHAPTER 4

and related to the oxidation process ($\text{Red} \rightarrow \text{Ox} + ne^-$). Both processes define their characteristic peak current, indicated as i_{pc} (for the cathodic peak) and i_{pa} (for the anodic peak). All this information helps to characterise the reversibility of the redox process in order to compare it with the Nernstian behaviour. In an ideal Nernstian system at $T = 25^\circ\text{C}$, i_{pc} and i_{pa} ratio should have value = 1 and the difference between cathodic and anodic peak potential ($\Delta E_p = E_{pa} - E_{pc}$) should be = $0.059/n$ (n is the number of electrons involved in the half-reaction).

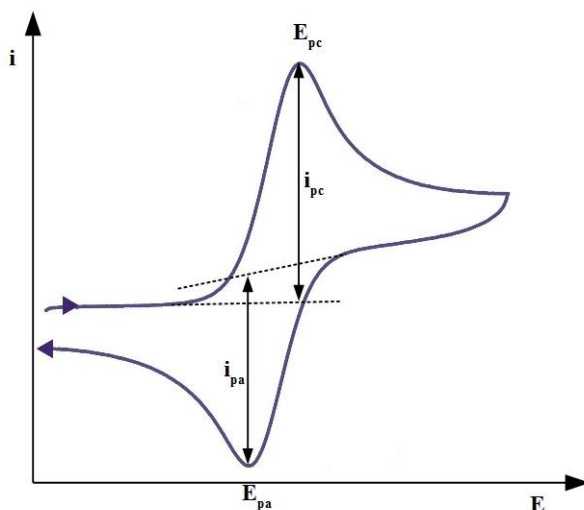


Figure 4.2: Example of voltammogram for a reversible redox process.

The Randles-Sevcik equation, which can be written at $T = 25^\circ\text{C}$ in the form:

$$i_p = (2.69 \times 10^{-5}) n^{3/2} A D^{1/2} C v^{1/2}$$

can provide other information, being i_p the peak current, n the number of electrons, A the electrode area (expressed in cm^2), C the concentration (expressed in mol/cm^3), D the diffusion coefficient (expressed in cm^2/s) and v the potential scan rate (expressed in V/s).

4.1.2 *Electrochemical impedance spectroscopy*

Electrochemical impedance spectroscopy is an analysis method that can provide information about electrodes surface characteristics and about changes of bulk solution properties [4].

Measurements in the electrochemical cell are generally carried out using two different modes: the potentiostatic mode, in which a sinusoidal AC voltage is superimposed to a selected DC potential (response sampled signal is formed by an AC current), and the galvanostatic mode, in which an AC current is superimposed to a selected DC current (response sampled signal is formed by an AC voltage).

Impedance value (called Z) is determined by the ratio between the time dependent function of the applied AC potential $E(t)$ and the related shifted AC current $I(t)$:

$$Z = E(t)/I(t) = E_0 \sin(2\pi\nu t)/i_0 \sin(2\pi\nu t + \Phi) = Z_0 \sin(2\pi\nu t)/\sin(2\pi\nu t + \Phi)$$

where E_0 and I_0 are, respectively, potential and current at $t = 0$ (from which is possible to write $Z_0 = E_0/I_0$), ν is the frequency of the sinusoidal potential and Φ is the phase shift between the potential- and current-time functions (Figure 4.3).

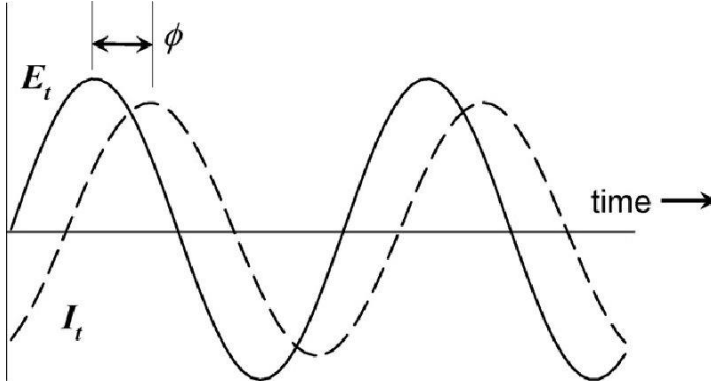


Figure 4.3: Typical EIS alternate applied potential (E_t) and relative current response (I_t), separated by the phase-shift Φ [5].

Because of the fact that current and potential differ both in phase than in amplitude, impedance Z is a complex value, so, considering Euler's rule:

$$e^{(j\Phi)} = \cos\Phi + j\sin\Phi,$$

where j is a complex number, and expressing:

$$2\pi\nu = \omega,$$

it is possible to write:

$$E(t) = E_0 e^{(j\omega t)}$$

and

$$I(t) = I_0 e^{(j\omega t + \Phi)}.$$

Thus, impedance Z can be expressed as a complex number:

$$Z(\omega) = E(t)/I(t) = Z_0 e^{(j\Phi)} = Z_0 (\cos\Phi + j\sin\Phi).$$

Impedance function is then formed by a real part (Z_r or Z') and an imaginary one (Z_j or Z''): results of EIS measurements can be plotted using the Bode plot (where $\log|Z|$ and Φ are plotted vs. $\log\nu$) or using

the Nyquist plot (where Z_r is plotted vs. Z_j). In this work Nyquist plot will be used so only this representation will be explained (Figure 4.4).

Raw data of EIS measurements in form of Nyquist plot are fitted using an equivalent circuit, properly selected to better approximate experimental values. The circuit used in this work is called equivalent Randles circuit (Figure 4.5) and it is realised with ideal impedance elements: two ohmic resistances (R_{el} – that depends from ion concentration and electrochemical cell geometry - and R_{ct} – that depends from the current flow produced by the redox reaction at the interface), a capacitor (C – related to the charge double layer at electrode interface), a constant phase element (CPE) and a Warburg impedance (W – related to the diffusion from the bulk to the interface) arranged in series or in parallel in order to “translate” experimental data. The Warburg element (W) can be avoided if non-faradic processes can be neglected (in presence of a redox probe, where non-faradic capacitance methods are not applied).

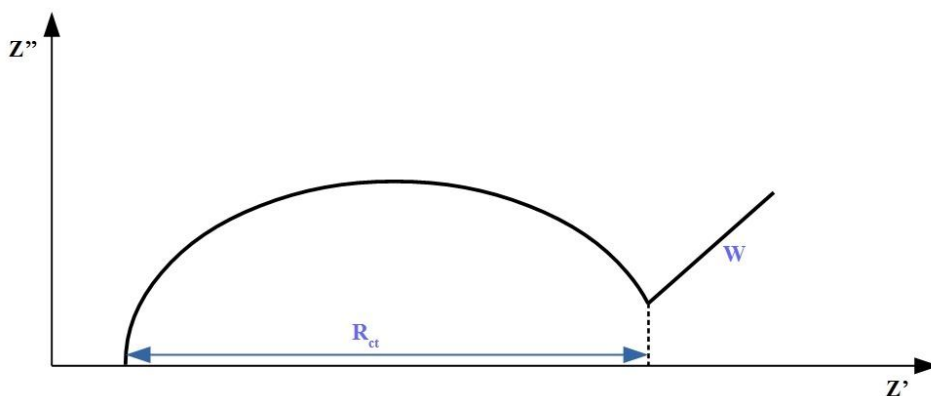


Figure 4.4: Example of Nyquist plot.

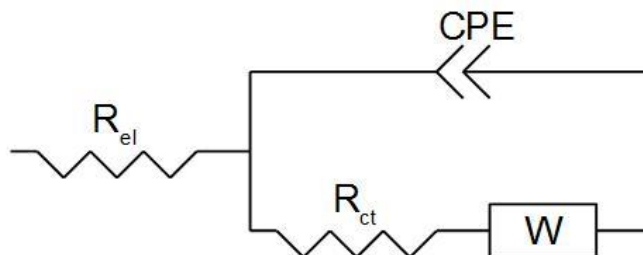


Figure 4.5: Equivalent Randles circuit.

In biosensor application, EIS spectroscopy can be used as well to characterise every electrode modification step (e.g. surface conductivity modification, self-assembly of monolayers, probe immobilisation) than to obtain label-free quantitative measurements (e.g. interaction between the immobilised probe and the target, enzymatic production of an insoluble molecule [6, 7]).

In this work $[\text{Fe}(\text{CN})_6]^{3-/4-}$ was used as redox probe to generate current flow from bulk solution to electrode surface and an AC potential, superimposed to the formal DC redox potential of the chosen redox couple, was applied, taking charge transfer resistance (R_{ct}) or ΔR_{ct} as analytical signal.

4.1.3 Differential pulse voltammetry

In differential pulse voltammetry (DPV) a pulsed potential (with a defined magnitude) is superimposed to a linear potential sweep at the working electrode of an electrochemical cell (Figure 4.6).

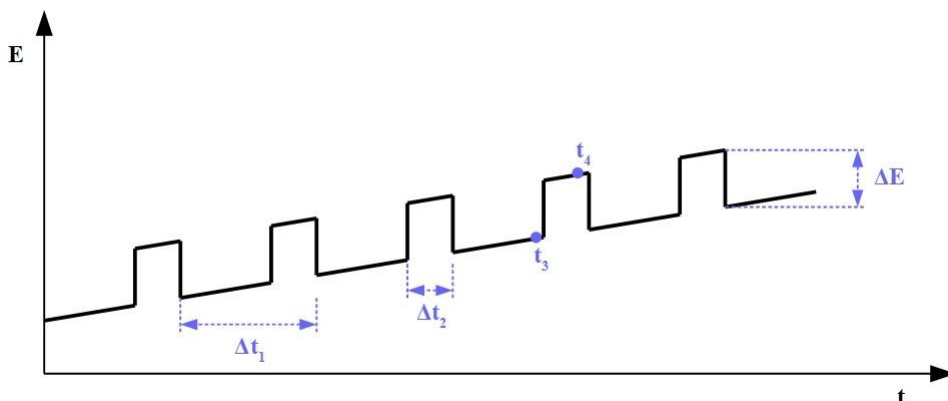


Figure 4.6: Typical potential-time waveform of a DPV measurement.

Applied potential is defined by the pulse amplitude (ΔE – usually within the range 25-50 mV), interval time (Δt_1 – usually within the range 0.5-5 s) and pulse time (Δt_2 – usually below 50 ms). The current is sampled twice: before the pulse application (t_3), and approximately 40 ms later in the pulse time (t_4); the difference between the two sampled currents (Δi) is then plotted against potential, obtaining a peak shaped voltammogram where peak height and area are directly proportional to analyte concentration while peak position (defined by peak potential) is related to different electroactive species oxidation potential (Figure 4.7) [1].

Main advantages of DPV (as well as other pulsed voltammetric techniques) consist in increasing signal/noise ratio because of the reduction of background currents. Furthermore, plotting current difference Δi helps to reduce capacitive current interference, because capacitive current decay is faster than faradic current one.

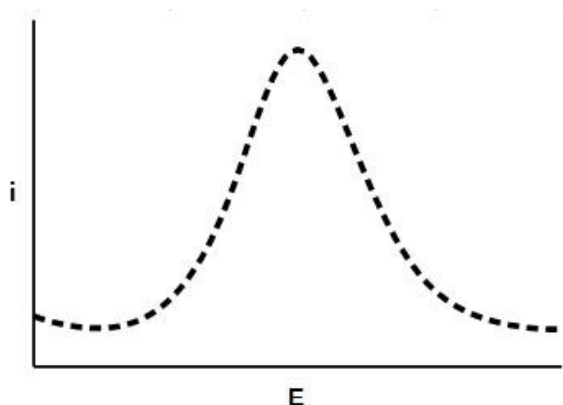


Figure 4.7: Typical DPV voltammogram.

High sensibility and low detection limits are achieved respect to others non-pulsed voltammetries. Moreover this peak-shaped response allows the determination of species with little differences in their redox potential (down to $\Delta E \approx 50$ mV), making this technique particularly useful for mixture analysis [1-3].

4.1.4 Multi-pulsed amperometry

Amperometric detection is suitable for any analyte that can be oxidised or reduced [8]. In simple amperometric detection a fixed DC potential is applied at the working electrode of an electrochemical cell. The measured current depends from oxidation at anode or reduction at cathode of the electroactive analyte. Specificity is achieved adjusting the applied potential in order to maximise the response for the analyte of interest while minimising the response for interfering analytes (in case of measurements in a mixture of electroactive molecule). The current signal obtained with conventional amperometric detection is determined by the rate of electroactive material transport. An increase of the thickness of the diffusion layer of a chemically modified electrode can slow down the transport resulting small amperometric signal [9]. Another problem can be

given by electroactive analytes that give electrode fouling, that reduce signal intensity and make necessary electrode cleaning.

In this sense, an upgrade of DC potential amperometry is multi-pulsed amperometry (MPA), in which a DC working potential (or more than one, in case of a multi-analyte mixture) is applied for a short time (approx. a few hundred ms), followed by a higher or lower potential (or potentials) that is used to clean the electrode or simply applied as resting potential (Figure 4.8).

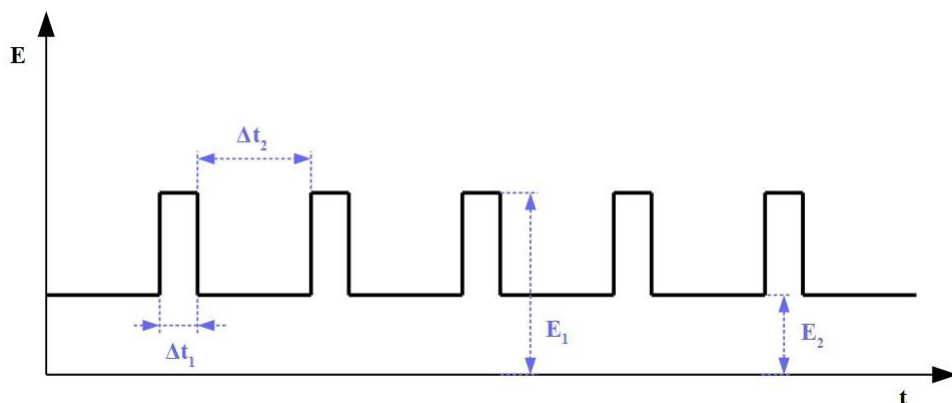


Figure 4.8: Typical potential-time waveform of a multi-pulsed amperometry measurement (single pulsed potential).

A square shaped potential wave is applied switching the potential of the working electrode continuously between the working potential pulse (E_1), and the cleaning or resting potential one (E_2), for defined application times, respectively Δt_1 (typically in the order of hundreds of ms) and Δt_2 (typically bigger than Δt_1 , from hundreds of millisecond to seconds).

Current is measured only while the working potential is applied, then sequential current measurements (collected in a defined time interval that depends from cell stabilisation and analyte addition time) are processed by

CHAPTER 4

the detector to produce a smooth output. The current vs. time resulting plot is called chronoamperogram (Figure 4.9).

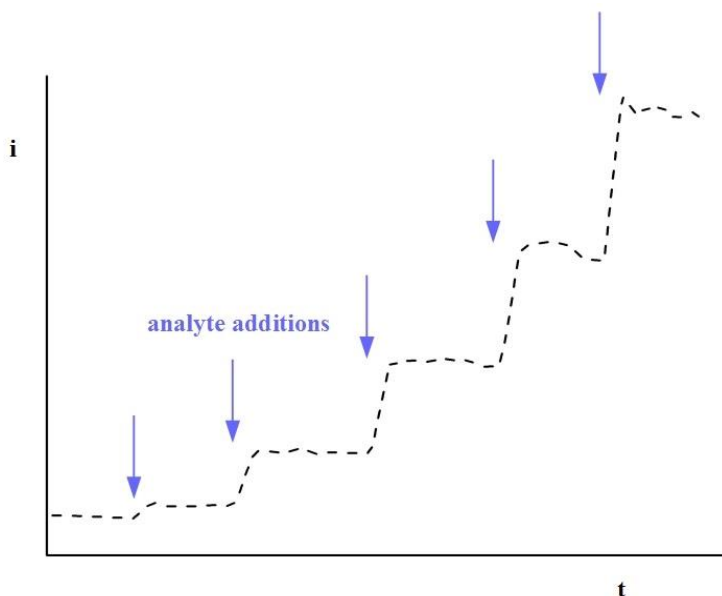


Figure 4.9: Typical MPA chronoamperogram.

In this work, measurements are performed immersing a screen printed cell in an electrochemical cell under stirring in order to allow time for the diffusion-lead mass transfer to reload the depleted layer at the electrode surface during the resting period after the oxidising potential pulse; concentration of electroactive molecule is increased directly in the electrochemical cell by subsequent addition, measuring current changes continuously.

4.2 References

- [1] Analytical electrochemistry, John Wiley & Sons 2006.
- [2] D.A. Skoog, F.J. Holler, T.A. Nieman, Inc.: Toronto, ON, 1998.
- [3] Fundamentals of analytical chemistry, Nelson Education 2013.
- [4] E. Katz, I. Willner, *Electroanal*, 15: 913-947, 2003.
- [5] R. Toonika (Ed.) *Impedimetric Biosensors for Label-Free and Enzymless Detection*, InTech 2013.
- [6] A. Ravalli, G.P. dos Santos, M. Ferroni, G. Faglia, H. Yamanaka, G. Marrazza, *Sensors Actuators B: Chem.*, 179: 194-200, 2013.
- [7] F. Lucarelli, G. Marrazza, M. Mascini, *Biosensors Bioelectron.*, 20: 2001-2009, 2005.
- [8] D.C. Johnson, W.R. LaCourse, *Anal. Chem.*, 62: 589A-597A, 1990.
- [9] A. Takátsy, B. Csóka, L. Nagy, G. Nagy, *Talanta*, 69: 281-285, 2006.

CHAPTER 5

5.1 DNA technology for small molecules sensing: a new approach for acetamiprid detection

Published in: *Rapini R, Marrazza G DNA technology for small molecules sensing: a new approach for Acetamiprid detection. In: AISEM Annual Conference, 2015 XVIII, Trento, 3-5 Feb. 2015. pp 1-4. doi:10.1109/aisem.2015.7066768*

5.1.1 Abstract

In this work, an electrochemical DNA aptasensor for acetamiprid is presented. The aptasensor is based on a dual signal amplified strategy by employing a gold-polyaniline modified screen-printed electrode as sensor platform and an enzyme-linked label for sensitive detection. The polyaniline-gold nanocomposite modified electrodes were firstly modified with a mixed monolayer of a thiol-tethered DNA aptamer and 6-mercapto-1-hexanol. The acetamiprid solution was then incubated with the aptasensor. An enzyme-amplified detection scheme, based on the coupling of a streptavidin-alkaline phosphatase conjugate and secondary biotinylated aptamer was then applied. The enzyme catalysed the hydrolysis of the electroinactive 1-naphthyl-phosphate to 1-naphthol. This electroactive product was detected by means of differential pulse voltammetry. A calibration curve between 0-200 nM acetamiprid concentration range was obtained.

Keywords

pesticide, acetamiprid, aptamer, electrochemical, nanoparticles

CHAPTER 5

5.1.2 *Introduction*

The use of pesticides to control the growth of different types of infesting organisms in order to limit the possible loss of productivity is a diffused and necessary practice in modern agriculture. Acetamiprid belongs to the neonicotinoid class of pesticide that includes neuro-active substances structurally derived from nicotine that act as nicotinic acetylcholine receptor agonists, causing paralysis and then death. The acetamiprid structural formula is reported in Figure 5.1. The intensive use of neonicotinoids has led to an increasing interest about the toxic effects caused on not infesting insects like natural pollinators. Neonicotinoids have recently been identified as a potential contributing factor to the sudden decline in adult honeybee population, commonly known as colony collapse disorder (CCD) [1]. Mainly diffused pesticide detection methods include high pressure liquid chromatography (HPLC) [2], gas chromatography (GC) [3], mass spectrometry (MS) [4]. All these techniques produce satisfactory analytical performances, but they generally require skilled technicians, they are time consuming. In addition, they have high costs and for all these reasons, they result impractical for on field screening analysis and constant environment monitoring. In recent years, there has been an increasing interest in biosensor technology for fast pesticide detection using easy and rapid procedures. The biosensors have the potential to complement or replace the classical analytical methods by simplifying or eliminating sample preparation and making field-testing easier and faster with significant decrease in cost per analysis [5, 6]. As many pesticides are designed to inhibit various enzymes within insects and other pests, utilising these enzymes for detection purposes seemed a logical route. In this manner, many biosensors are based on enzymes such as acetylcholinesterase, butyrylcholinesterase and others for their ability to

detect pesticides in environment [7]. The use of aptamer-based biosensors has emerged as an interesting alternative to enzymatic and immunosensors, giving the possibility to combine low realisation costs of the artificial receptors and good analytical performances, especially for small molecules such as pesticides, with simple and rapid detection procedures [8]. In this study, an electrochemical single-use aptasensor based on gold-polyaniline graphite screen-printed electrode for acetamiprid detection is proposed. Two different aptamers (Apt1 and Apt2) have been used to perform the sandwich aptassay. Both aptamers have been developed by Zhao et al. [9] and possess the ability to bind selectively to acetamiprid molecules. Graphite screen-printed electrodes (GSPE) have been firstly modified with gold-polyaniline film by electrosynthesis. A mixed monolayer of a primary thiolated DNA aptamer (Apt1SH) and a spacer thiol, 6-mercapto-1-hexanol (MCH) has then been formed on gold nanoparticles. Acetamiprid has then been incubated and the aptasensor developed. An enzyme-amplified detection scheme, based on the coupling of streptavidin-alkaline phosphatase conjugate and secondary biotinylated DNA aptamer (Apt2biot) has then been applied. The enzyme catalysed the hydrolysis of the electroinactive 1-naphthyl-phosphate to 1-naphthol. This electroactive product has been detected by means of differential pulse voltammetry (DPV). A calibration curve of acetamiprid samples has been obtained over a concentration range 0 - 200 nM.

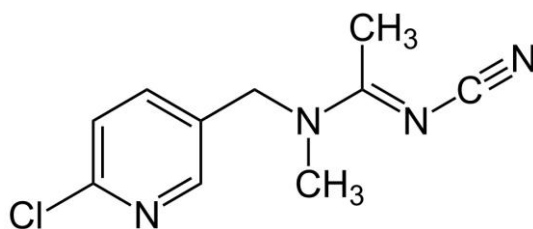


Figure 5.1: Acetamiprid structural formula

CHAPTER 5

5.1.3 *Materials and methods*

A. Chemicals

Perchloric acid (HClO_4), sulfuric acid (H_2SO_4), aniline, streptavidin - alkaline phosphatase enzyme, have been purchased from Merck (Milan, Italy). Tetrachloroauric acid (HAuCl_4), 6-mercapto-1-hexanol (MCH), KCl, NaCl, MgCl_2 , Bovine Serum Albumin (BSA), diethanolamine, Trizma[®] hydrochloride and DL-dithiothreitol (DTT) have been purchased from Sigma-Aldrich (Milan, Italy). Sodium acetate has been purchased from Carlo Erba (Milan). Thiol-tethered DNA aptamer 1 (Apt1SH) [5'-(SH)-(CH₂)₆-

TGTAATTTGTCTGCAGCGGTTCTTGATCGCTGACACCATATTATG AAGA-3'], biotinylated DNA aptamer 2 (Apt2biot) [5'-(biot)-TTTTTTTTTTTTTTTTTATTGGACTAGCTGCAGCGATTCTTAATCGCT ATGCTCCGCCCAATACTG-3'] have been purchased from Eurofins MWG Operon, Ebersberg, Germany. All reagents have been purchased at analytical grade. Milli-Q water has been used throughout the work.

B. Instrumentation and electrochemical measurements

Differential pulse and cyclic voltammetric measurements have been performed with the portable potentiostat/galvanostat PalmSens electrochemical analyser (PalmSens, The Netherlands). Electrochemical impedance spectroscopy measurements have been performed in a digital potentiostat/galvanostat AUTOLAB PGSTAT 30(2)/FRA2 controlled with General Purpose Electrochemical System (GPES) and Frequency Response Analyser (FRA2) 4.9 software (Eco Chemie, Utrecht, the Netherlands). The aptasensor has been built using screen-printed cells formed by a graphite working electrode (diameter 2.5 mm), a silver pseudo-reference electrode and a graphite counter electrode. The screen-

printed cells have been self-produced using a DEK 248 screen-printing machine (DEK, Weymouth, UK). The printing has been performed on a polyester film (Autostat CT5) from Autotype (Milan, Italy) using the polymeric inks Electrodag PF-410 (silver) and Electrodag 423 SS (graphite) that have been purchased from Acheson (Milan, Italy). Vinylfast 36-100, obtained from Agron (Lodi, Italy) has been used as insulating ink. Faradic impedance measurements were carried out in the presence of $[\text{Fe}(\text{CN})_6]^{3-/4-}$ redox probe (5 mM equimolecular mixture in TRIS buffer). A voltage of 10mV in amplitude (peak-to-peak), within the frequency range 100 kHz – 10 mHz, was superimposed to the applied bias potential. The dc potential was set up to +0.13 V, the formal potential of $[\text{Fe}(\text{CN})_6]^{3-/4-}$ redox probe. Experimental spectra, presented in the Nyquist plots, were fitted with proper equivalent circuits using the facilities of the FRA2 software. DPV scans were performed from 0 V to +0.6 V (vs. Ag/AgCl pseudo-silver reference), using the following parameters: modulation time 0.05 s, interval time 0.15 s, step potential 5 mV, modulation amplitude 0.07 V.

5.1.4 Experimental procedure

In this work an aptasensor for the detection of Acetamiprid has been developed following the scheme reported in Figure 5.2. Firstly electropolymerisation of polyaniline has been performed with 50 μL of 2.5 mM aniline solution in 50 mM HClO_4 for 10 cycles in the potential range from -0.4 V to +0.8 V and 50 mVs^{-1} scan rate. After washing with H_2O Milli-Q, the gold nanoparticles have been electro-deposited on the surface of polyaniline modified graphite screen-printed electrode (GSPE) with 50 μL of 0.5 mM HAuCl_4 solution in H_2SO_4 0.5 M for 15 cycles in the potential range from -0.2 V to +1.2 V and a scan rate of 100 mVs^{-1} . 7 μL

of 0.1 μM primary thiolated aptamer (Apt1SH) solution prepared in TRIS buffer, have been placed on gold nanoparticle-modified graphite screen-printed electrodes (AuNPs/GSPEs). Chemisorption has been allowed to proceed overnight (≈ 16 h). The immobilisation step has been followed by a mixed SAM formation by incubation with 6-mercapto-1-hexanol (MCH). A 7 μL drop of the 1 mM aqueous solution of 6-mercapto-1-hexanol has been placed onto the DNA-modified electrode surface for 1 h. Finally, the modified sensors have been washed 3 times with TRIS buffer. The procedures have been applied as reported in previous works of the authors [10-12]. To perform the calibration curve, the aptasensor has been incubated with 7 μL of acetamiprid at various concentrations prepared in buffer solution for 40 minutes at 25 $^{\circ}\text{C}$. Then, the sensor has been washed 3 times with buffer in order to remove the unbound acetamiprid molecules. To complete the sandwich assay, the aptasensor has been incubated with 7 μL of 1 μM secondary biotinylated aptamer (Apt2biot), for 5 minutes. After a washing step performed with DEA buffer, streptavidin-alkaline phosphates prepared in DEA buffer has been added to the system and incubated for 20 minutes. Finally, the aptasensor has been washed three times with DEA buffer. The 1-naphtyl-phosphate enzyme substrate has then been added using a buffered solution in DEA pH=9.6 and the detection of the obtained enzyme product 1-naphtol has been carried out via differential pulse voltammetry (DPV).

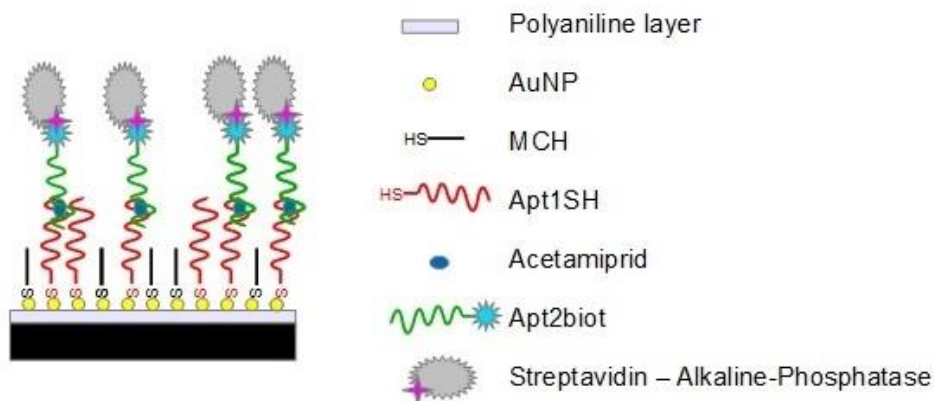


Figure 5.2: Enzyme-amplified detection scheme of the aptasensor.

5.1.5 Results and discussion

Each surface modification step has been studied via electrochemical impedance spectroscopy (EIS) measurements. The electron transfer resistance (R_{ct}), which values have been reported in form of Nyquist plots, has been used as parameter to evaluate modified working electrodes conductivity (Figure 5.3). Polyaniline modified screen-printed electrodes (SPEs) presented a decrease of the charge transfer resistance (R_{ct} 2.00 ± 0.50 k Ω) in comparison with bare SPE (R_{ct} 6.00 ± 0.50 k Ω). When the polyaniline screen-printed electrodes have been modified with AuNPs, the R_{ct} had a further decrease (R_{ct} 0.50 ± 0.02 k Ω). These results are related to the increased conductivity of the modified electrodes surfaces. Calibration curve for the determination of acetamiprid in optimised conditions by aptasensor is reported in Figure 5.4. A linear response has been obtained in the range of 0 – 200 nM which is also an important range from the agricultural and analytical point of view.

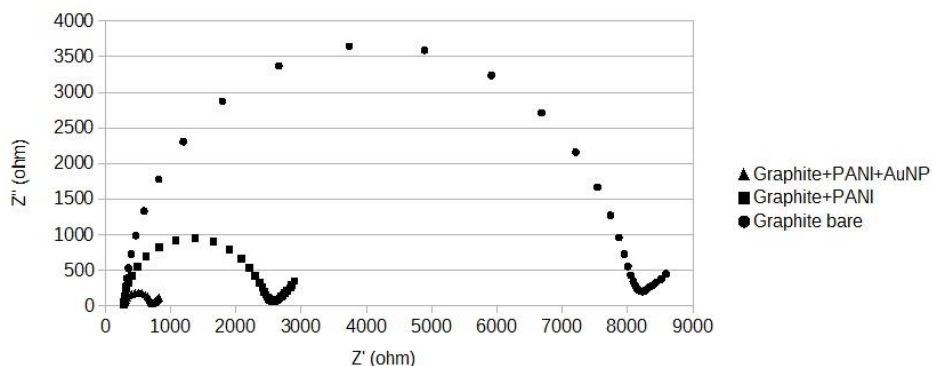


Figure 5.3: Typical Nyquist plots from bare graphite, polyaniline and gold-polyaniline modified screen-printed electrodes, obtained in 5 mM $K_3Fe(CN)_6/K_4Fe(CN)_6$, 0.1 M KCl.

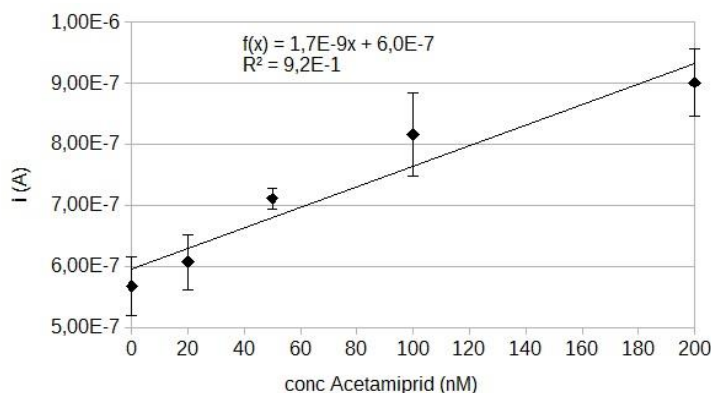


Figure 5.4: Calibration curve obtained of acetamiprid buffered solutions. Each point was repeated at least 3 times.

5.1.6 Conclusions

In this work, a novel aptasensor based on gold-polyaniline graphite screen-printed electrodes has been designed and fabricated using alkaline phosphatase as enzyme label and signal amplification for the rapid acetamiprid detection. The promising platform based on the combination of gold-polyaniline modified screen-printed electrodes and aptamers could have great potential applications in environmental monitoring and food analysis.

5.2 References

- [1] M. Gross, *Curr. Biol.*, 18: R684, 2008.
- [2] N.M. Brito, S. Navickiene, L. Polese, E.F. Jardim, R.B. Abakerli, M.L. Ribeiro, *J. Chromatogr. A*, 957: 201-209, 2002.
- [3] S. Berijani, Y. Assadi, M. Anbia, M.R.M. Hosseini, E. Aghaee, *J. Chromatogr. A*, 1123: 1-9, 2006.
- [4] A.A. Boyd-Boland, S. Magdic, J.B. Pawliszyn, *Analyst*, 121: 929-937, 1996.
- [5] X. Wang, X. Lu, J. Chen, *Trends in Environmental Analytical Chemistry*, 2: 25-32, 2014.
- [6] G. Marrazza, *Biosensors (Basel)*, 4: 301-317, 2014.
- [7] C.S. Pundir, N. Chauhan, *Anal. Biochem.*, 429: 19-31, 2012.
- [8] S. Liu, Z. Zheng, X. Li, *Anal Bioanal Chem*, 405: 63-90, 2013.
- [9] L. Fan, G. Zhao, H. Shi, M. Liu, Z. Li, *Biosens Bioelectron*, 43: 12-18, 2013.
- [10] A. Ravalli, G.P. dos Santos, M. Ferroni, G. Faglia, H. Yamanaka, G. Marrazza, *Sensors Actuators B: Chem.*, 179: 194-200, 2013.
- [11] R.-S. Saberi, S. Shahrokhian, G. Marrazza, *Electroanal*, 25: 1373-1380, 2013.
- [12] Z. Taleat, A. Ravalli, M. Mazloun-Ardakani, G. Marrazza, *Electroanalysis*, 25: 269-277, 2013.

CHAPTER 6

6.1 Recent progress in biosensors for acetamiprid pesticide detection

Published in: *Rapini R, Marrazza G (2016) Recent progress in biosensors for acetamiprid detection. In: Vasić V (ed) 5th Workshop Specific methods for food safety and quality, Vinča Institute of Nuclear Sciences, Belgrade, Serbia, September 27th 2016 2016. Physical Chemistry 2016. Vinča Institute of Nuclear Sciences, Belgrade, Serbia, Belgrade, Serbia, pp 58-64*

6.1.1 Abstract

In this work, a simple and sensitive aptasensor based on sandwich approach for acetamiprid detection is presented. The aptamer, immobilised on poly-aniline and gold nanoparticles modified graphite screen-printed electrodes, is used to capture the analyte from the sample solution. The sandwich assay is then performed by adding secondary biotinylated aptamer. An enzyme-amplified detection scheme, based on the coupling of a streptavidin-alkaline phosphatase conjugate and biotinylated aptamer has been then applied. The enzyme catalysed the hydrolysis of the electro-inactive 1-naphthyl phosphate to 1-naphthol. The enzymatic product is electro-active and has been detected by differential pulse voltammetry. The experimental parameters have been investigated and have been optimised. The analytical performances of aptasensor in terms of sensitivity, reproducibility and selectivity have been studied.

6.1.2 Introduction

Neonicotinoids are a class of systemic pesticides worldwide used to protect several crops. They show a significant neurotoxic activity toward

insects, acting as nicotinic-acetylcholine receptor agonists in their central nervous system. Moreover, their systemic properties (associated to their solubility in water) allow neonicotinoids to move within the plant tissues protecting crops from both aerial and soil pests [1]. Recently, neonicotinoid pesticides have been included in the EU “watch list of substances for Union-wide monitoring in the field of water policy” [2]. For the analysis of these contaminants very low LOD are required (9 ng/L for neonicotinoids) in accordance with the substance-specific predicted no-effect concentration for each substance in the aqueous matrix. Currently, they can be achieved using chromatographic techniques, able to provide sensitive and selective, qualitative and quantitative detections [3]. In view of the development of an analytical platform for screening purposes, biosensors have been extensively investigated as potential analytical tools for pesticide analysis providing multiplexed analysis, simplicity, fast response, sensitivity and specificity in addition to lower cost [4]. Recently, the aptamers have been used as bioreceptors in the biosensors design for their chemical characteristics [5, 6]. A biosensors using aptamer as recognition element is called aptasensor. Pesticides are often present at ultra-low levels and require ultrasensitive methods for detection. To improve the analytical properties of aptasensors, the aptamer are often coupled to nanomaterials [7, 8]. In this study, a simple and sensitive aptasensor based on sandwich approach for acetamiprid analysis is presented. Acetamiprid is a very diffuse pesticide of the neonicotinoid class. Acetamiprid has shown a high toxicity, causing potential risk to humans who are exposed to the contaminated environment, so it is very important its detection [9, 10]. The aptamer, selected from the literature [11], has been immobilised on polyaniline and gold nanoparticles modified graphite screen-printed electrodes. The aptasensor is used to

capture the analyte from the sample solution. The sandwich assay is then performed by adding secondary biotinylated aptamer. An enzyme-amplified detection scheme, based on the coupling of a streptavidin-alkaline phosphatase conjugate and biotinylated aptamer has been then applied. The enzyme catalysed the hydrolysis of the electro-inactive 1-naphthyl phosphate to 1-naphthol. The enzymatic product is electro-active and has been detected by differential pulse voltammetry. The experimental parameters have been investigated and have been optimised. The analytical performances of aptasensor in terms of sensitivity, reproducibility and selectivity have been studied.

6.1.3 *Experimental*

Perchloric acid, sulfuric acid, aniline, potassium ferrocyanide, potassium ferricyanide, 1-naphthyl phosphate, streptavidin-alkaline phosphatase enzyme conjugate, di-sodium hydrogen phosphate and sodium di-hydrogen phosphate di-hydrate have been purchased from Merck (Milan, Italy). Tetrachloroauric acid, 6-mercapto-1-hexanol, KCl, NaCl, $MgCl_2$, sodium acetate, Bovine Serum Albumin (BSA), diethanolamine, Trizma® hydrochloride and DL-dithiothreitol (DTT), atrazine and acetamiprid have been purchased from Sigma-Aldrich (Milan, Italy). All reagents have been purchased at analytical grade. Milli-Q water has been used throughout the work.

The DNA sequences have been purchased from Eurofins MWG Operon, Ebersberg, Germany. The sequences are listed below:

thiol-tethered DNA aptamer 1 (Apt1):

CHAPTER 6

5'-(SH)-(CH₂)₆-

TGTAATTTGTCTGCAGCGGTTCTTGATCGCTGACACCATATTAT
GAAGA-3'

thiol-tethered DNA aptamer 2 (Apt2):

5'-(SH)-(CH₂)₆-

ATTGGACTAGCTGCAGCGATTCTTAATCGCTATGCTCCGCCCAA
TACTG-3'

biotinylated DNA aptamer 2 (Apt2biot):

5'(biot)TTTTTTTTTTTTTTTTATTGGACTAGCTGCAGCGATTCTTAA
TCGCTATGCTCCGCCCAATACTG-3'

Prior to use, the thiol-modified probes have been treated with dithiothreitol (DTT), purified by elution through the NAP-5 columns (GE Healthcare life Sciences illustra NAP-5) and then quantified by UV measuring absorption at 260 nm. All oligonucleotide stock solutions have been prepared in TRIS buffer and stored frozen.

In this work, the following buffer solutions have been used:

buffer A: 20 mM TRIS pH 7.4 with 0.1 M NaCl, 0.1 M KCl and 5 mM MgCl₂

buffer B: 10 mM TRIS pH 8.3

buffer C: 0.1 M acetate buffer pH 4.7

buffer D: 0.1 M phosphate buffer pH 7.0

buffer E: 0.1 M diethanolamine buffer (DEA) pH 9.6.

The transducers used for the aptasensor realisation are screen-printed cells, based on graphite working electrode (2.5 mm in diameter), counter graphite electrode and silver/silver chloride (Ag/AgCl) pseudo-reference electrode. Screen-printed cells were produced in house [12].

Electrochemical impedance spectroscopy (EIS) measurements have been performed in presence of 5.0 mM $[\text{Fe}(\text{CN})_6]^{3-/4-}$ redox probe (equimolar solution in 0.10 M KCl and phosphate buffer D). A voltage of 10 mV in amplitude (peak-to-peak), within the frequency range 100 kHz – 10 mHz, is superimposed to the applied bias potential. The dc potential is set up to +130 mV, the formal potential of $[\text{Fe}(\text{CN})_6]^{4-/3-}$ redox probe. Charge transfer resistance (R_{ct}) variations have been taken as signal.

Differential pulse (DPV) and cyclic voltammetry (CV) measurements have been performed with the portable potentiostat/galvanostat PalmSens electrochemical analyser (PalmSens, the Netherlands) controlled with the PSTrace 2.3 software. DPV measurements have been made using the following parameters: scan range potential from 0 mV to +600 mV, step potential 5 mV, modulation potential amplitude 70 mV, scan rate 40 mV/s, modulation time 0.05 s, interval time 0.15 s. All potentials are reported referring to the pseudo-reference Ag electrode contained in the screen-printed cells.

The aptasensor developed in this work is schematically represented in Figure 6.1.

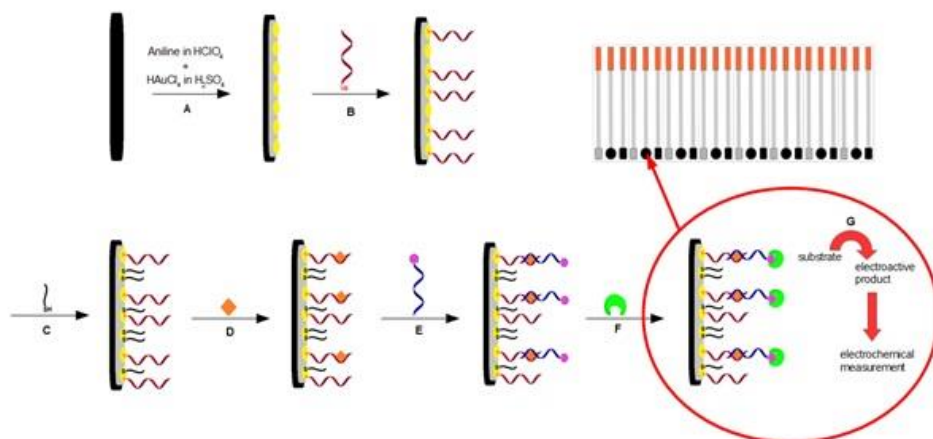


Figure 6.1: Scheme of aptamer-based sandwich assay for acetamiprid detection.

The modification of graphite screen-printed electrodes (GPSEs) with polyaniline (PANI) and gold nanoparticles (AuNPs) has been realised in accordance with the optimised procedure reported in our previous works [10, 12] (Figure 1, A). In order to immobilize the primary aptamer on the gold nanoparticles modified working electrode, 7 μL of thiolated aptamer solution (2 μM in TRIS buffer A) has been dropped onto the sensor surface and incubated overnight (≈ 16 h) at 4 $^{\circ}\text{C}$ in petri dishes to avoid the solution evaporation (Figure 1, B). This step has been followed by a mixed SAM formation by incubation with 6-mercapto-1-hexanol (MCH). A volume of 7 μL of 1 mM MCH solution has been dropped on the sensor surface and incubated for 1 hour (Figure 1, C). To obtain the calibration curve, several concentrations of the acetamiprid have been placed onto the aptasensor surfaces for 40 minutes (Figure 1, D). The control experiments have been also performed using atrazine, an herbicide of the triazine class, to investigate the aptasensor specificity. Then, the aptasensors have been exposed to 1 μM biotinylated aptamer solution for 5 minutes (Figure 1, E). After washing with DEA buffer, the aptasensors have been further incubated with 1 U/mL of the streptavidin alkaline-phosphatase enzyme

conjugate containing 8 mg/mL BSA in DEA buffer for 20 minutes (Figure 6.1, F). Finally, the electrochemical measurements have been performed by closing the circuit with 50 μ L of DEA buffer containing 1 mg/mL of enzymatic substrate, 1-naphthyl phosphate. After 20 min of incubation, the oxidation signal of the enzymatically-produced 1-naphthol has been measured by DPV and its current peak height at +0.2 V has taken as the analytical signal (Figure 1, G).

6.1.4 Results and discussion

In order to optimise all the steps involving the aptasensor development, the key experimental parameters have been studied.

The primary aptamer immobilised on the electrode surface with an appropriate orientation and flexibility for binding the target is of paramount importance for the performance of the aptasensor. For this purpose, the affinity reaction between the primary thiolated aptamer and the acetamiprid target molecule has been investigated using EIS measurements. The Apt1 and Apt2 have been used as capture probes immobilising them onto PANI and AuNPs electrochemically modified graphite-working electrodes (GSPEs). Both realised aptasensors have been incubated with 100 nM and 0 nM acetamiprid solutions for 40 minutes. EIS measurements have been then carried out. The charge transfer resistance difference values between the acetamiprid and the blank solutions ($R_{ctAcetamiprid} - R_{ctBlank} = \Delta R_{ct}$) are reported in Table 6.1. The measurements have been repeated at least five times using different screen-printed cells (SPCs). Results show that both the immobilised aptamers are able to interact with the acetamiprid. However, the charge transfer resistance difference is higher using Apt1 than Apt2 as capture

probe. Therefore, Apt1 has been chosen as the primary aptamer in the following experiments.

Table 6.1: Affinity reaction studies of Apt1 and Apt2 aptasensors performed by EIS measurements.

	Charge transfer resistance difference ΔR_{ct} (k Ω)	%RSD
Apt1 aptasensor	3.21	0.05
Apt2 aptasensor	1.27	0.60

The best conditions for binding the pesticide to the immobilised aptamer have been then investigated incubating the aptasensor arrays with a solution containing 100 nM acetamiprid and a blank solution at different times. In the Table 6.2, we report the difference of the current peak height ($I_{\text{Acetamiprid}} - I_{\text{Blank}} = \Delta I$) obtained by DPV measurements. The reproducibility of the aptasensor has been analysed by the relative standard deviation (%RSD) as measure of inter-assay reproducibility. The incubation time of 20 min is not sufficient, whereas higher signal have been obtained with 40, 60 and 120 minutes. The best results in terms of signal amplitude and reproducibility have been obtained for an incubation time of 40 min, which has been selected as optimal.

Table 6.2: Optimisation of the incubation time of the affinity reaction with acetamiprid.

Incubation time (min)	Current peak height difference ΔI (μA)	%RSD
20	0.94	0.20
40	1.28	0.17
60	1.79	0.28
120	1.25	0.32

To appraise the influence of the concentration and incubation time with secondary aptamer, the aptasensors have been incubated with different

concentrations of the secondary biotinylated aptamer (Apt2biot) at 5 and 10 minutes (Table 6.3). The best response of the aptasensor has been obtained with 1 μM secondary aptamer solution (Apt2biot) at 5 min incubation time in terms of current peak height difference and reproducibility.

Table 6.3: Concentration and incubation time optimisation of secondary aptamer

Apt2biot concentration (μM)	Apt2biot incubation time (min)	Current peak height difference ΔI (μA)	%RSD
1	5	0.38	0.05
	10	0.27	0.18
2	5	0.04	0.18
	10	0.26	0.17

Under optimised conditions, a response of the aptasensor has been obtained in the range between 25 nM and 1000 nM. The regression curve calibration between 25 nM and 100 nM shows a correlation coefficient (R^2) of 0.988 with a calculated detection limit (LOD) of 24 nM. The proposed system has also been tested in presence of the nonspecific target atrazine, a pesticide of the triazine class, showing an excellent selectivity. Results are reported in Figure 6.2.

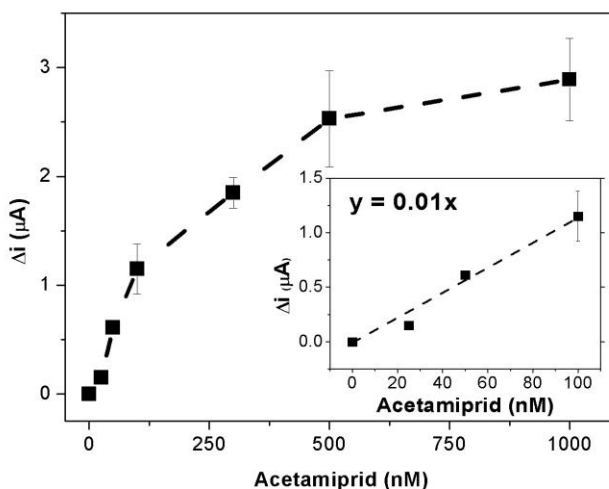


Figure 6.2: Curve calibration of the aptasensor.

The reproducibility of the aptasensor has been evaluated calculating the relative standard deviation on five repetition of every measurement with five different modified GSPEs. A value of 2.4 %RSD has been obtained for a concentration 50 nM of acetamidrid, confirming the proposed aptasensor as a promising assay for its detection.

6.1.5 Conclusion

In this work, a simple and rapid single use electrochemical aptasensor based has been developed for acetamidrid pesticide detection. The aptasensor is based on sandwich approach using poly-aniline and gold nanoparticles modified screen-printed arrays. The realised aptasensor shows a good sensitivity and a selectivity for the target demonstrating the potential practical applications in environmental samples.

6.1.6 Acknowledgement

This work was partially supported by the Italian Ministry of Foreign Affairs and International Cooperation, Executive programme for scientific

and technological cooperation between Italian Republic and Republic of Serbia 2016-2018; Project: "Nanobiosensor for organophosphate pesticides (OPs) determination in water".

6.2 References

- [1] P. Jeschke, R. Nauen, M. Schindler, A. Elbert, J. Agric. Food. Chem., 59: 2897-2908, 2011.
- [2] A. Aagaard, EFSA Journal, 11: 2013.
- [3] Amelin, V.G. Amelin, A.M. Andoralov, J. Anal. Chem., 71: 82-93, 2016.
- [4] N. Verma, A. Bhardwaj, Appl Biochem Biotechnol, 175: 3093-3119, 2015.
- [5] A. Vasilescu, J.L. Marty, Trac-Trend Anal Chem, 79: 60-70, 2016.
- [6] A. Ravalli, D. Voccia, I. Palchetti, G. Marrazza, Biosensors, 6: 39, 2016.
- [7] R. Sharma, K. Ragavan, M. Thakur, K. Raghavarao, Biosensors Bioelectron., 74: 612-627, 2015.
- [8] A. Ravalli, G. Marrazza, Journal of nanoscience and nanotechnology, 15: 3307-3319, 2015.
- [9] H. Shi, G. Zhao, M. Liu, L. Fan, T. Cao, J Hazard Mater, 260: 754-761, 2013.
- [10] R. Rapini, A. Cincinelli, G. Marrazza, Talanta, 161: 15-21, 2016.
- [11] J. He, Y. Liu, M. Fan, X. Liu, J Agric Food Chem, 59: 1582-1586, 2011.
- [12] R.-S. Saberi, S. Shahrokhian, G. Marrazza, Electroanal, 25: 1373-1380, 2013.

CHAPTER 7

7.1 Acetamiprid multidetection by disposable electrochemical DNA aptasensor

Published in: *Rapini R, Cincinelli A, Marrazza G (2016) Acetamiprid multidetection by disposable electrochemical DNA aptasensor. Talanta 161:15-21. doi: 10.1016/j.talanta.2016.08.026.*

7.1.1 Abstract

In this work, we propose an electrochemical DNA aptasensor for sensitive multidetections of acetamiprid based on a competitive format and disposable screen-printed arrays. To improve the sensitivity of the aptasensor, polyaniline film and gold nanoparticles were progressively electrodeposited on the graphite screen-printed electrode surface by cyclic voltammetry. Gold nanoparticles were then employed as platform for thiol-tethered DNA aptamer immobilisation. Different acetamiprid solutions containing a fixed amount of biotinylated complementary oligonucleotide sequence by DNA aptasensor arrays were analysed. Streptavidin-alkaline phosphatase conjugate was then added to trace the affinity reaction. The enzyme catalysed the hydrolysis of 1-naphthyl phosphate to 1-naphthol. The enzymatic product was detected by differential pulse voltammetry. A decrease of the signal was obtained when the pesticide concentration was increased, making the sensor work as signal off sensor. Under optimised conditions by testing key experimental parameters, a dose-response curve was constructed between 0.25-2.0 μM acetamiprid concentration range and a limit of detection of 0.086 μM was calculated. The selectivity of the aptasensor was also confirmed by the analysis of atrazine pesticide. Finally, preliminary

CHAPTER 7

experiments in fruit juice samples spiked with acetamiprid were also performed.

Keywords

electrochemical sensor, aptamer, screen-printed electrode, acetamiprid

7.1.2 Introduction

Acetamiprid is a neuro-active widespread pesticide of the neonicotinoid class, synthetic derivatives of nicotine. Neonicotinoids were introduced for agricultural control of sucking-type insects on leafy vegetables, fruits and tea trees in the early 90s and recently have become widely diffused representing around 24% of global market pesticide in 2008 [1]. Acetamiprid has shown a high toxicity, causing potential risk to humans who are exposed to the contaminated environment [2]. It has been classified as a probably non-carcinogenic substance but it is known also for its toxic effects, even chronic, for mammals [2-4]. It acts as nicotinic acetylcholine receptor agonist, causing to the contaminated organism paralysis and then death [5]. Due to the mentioned frequent and extensive usage, the development of an efficient and reliable analytical method for its detection in food samples remains an important target in order to prevent potential risk for human health. The maximum residue limits (MRLs) in the European Union admitted in fruits and vegetables are periodically updated by the European Food Safety Authority (EFSA) [4, 6]. Detection of neonicotinoid pesticides is usually carried out via conventional instrumental techniques based on chromatographic methods, like high-pressure liquid chromatography or gas chromatography, often coupled to mass spectrometry [7-9]. These techniques are time consuming and expensive; in addition, the instruments require highly skilled

technicians for their use and maintenance. In recent years, biosensor development for pesticide analysis has grown intensively, proposing itself as a cheaper and easy alternative, especially for screening analysis [10, 11]. To improve specificity and chemical stability of affinity biosensors, synthetic receptors such as molecularly imprinted polymers [12, 13] and aptamers were successfully used [14, 15]. Different electrochemical aptasensors for acetamiprid detection based on electrochemical impedance spectroscopy (EIS) were reported in literature [16, 17]. In this work, we realised an electrochemical DNA aptasensor for acetamiprid detection based on a competitive assay format. The method combines a special chip containing eight screen-printed electrochemical cells with a portable, computer-controlled instrument. The novelty of the proposed aptasensor compared to those reported in literature was the use of aptamer coupled with nanocomposite polymeric film modified electrochemical platforms as a first step for sensitive, disposable and cost-effective screening multianalysis on field.

The aptamers used in this work were selected from a library of aptamers, designed by SELEX [18-20] that showed to have the ability to recognise acetamiprid [21, 22]. The use of screen-printed cells is well known approach for the development of efficient biosensors, due to their relatively low cost, simplicity and rapidity of use coupled to small dimensions [23-27]. To improve sensitivity of the aptasensor, polyaniline film and gold nanoparticles were progressively electrodeposited on the graphite screen-printed electrode surface by cyclic voltammetry. Gold-polyaniline nanocomposite screen-printed electrodes were then modified with a mixed monolayer of a thiolated DNA aptamer and a spacer thiol, 6-mercapto-1-hexanol. Different acetamiprid solutions containing a fixed amount of biotinylated complementary oligonucleotide sequence with

CHAPTER 7

DNA aptasensor arrays were analysed. An enzyme-amplified detection scheme, based on the coupling of biotinylated oligonucleotide and streptavidin-alkaline phosphatase conjugate was then applied. The enzyme catalysed the hydrolysis of 1-naphthyl-phosphate to 1-naphthol. The enzymatic product is electroactive and was detected by Differential Pulse Voltammetry (DPV). This electrochemical technique was chosen because it offers a lower detection limit than linear sweep voltammetry, by increasing the ratio between faradic and non-faradic currents, sampling the current with a proper delay after the selected potential pulse [28]. A decrease of the signal was obtained when the pesticide concentration was increased, making the sensor work as signal off sensor.

Each step of the presented aptasensor was optimised and its analytical performances were studied. Finally, preliminary experiments in fruit juice samples spiked with acetamiprid were also performed.

7.1.3 Materials and methods

7.1.3.1 Chemicals

Perchloric acid (HClO_4), sulfuric acid (H_2SO_4), aniline, potassium ferrocyanide [$\text{K}_4\text{Fe}(\text{CN})_6$], potassium ferricyanide [$\text{K}_3\text{Fe}(\text{CN})_6$], streptavidin-alkaline phosphatase enzyme, di-sodium hydrogen phosphate (Na_2HPO_4), sodium di-hydrogen phosphate di-hydrate ($\text{NaH}_2\text{PO}_4 \cdot 2\text{H}_2\text{O}$) and formic acid have been purchased from Merck (Milan, Italy). Tetrachloroauric acid (HAuCl_4), 6-mercapto-1-hexanol (MCH), KCl, NaCl, MgCl_2 , Bovine Serum Albumin (BSA), diethanolamine, Trizma[®] hydrochloride, DL-dithiothreitol (DTT), acetamiprid, acetonitrile and HPLC ultrapure water have been purchased from Sigma-Aldrich (Milan,

Italy). All reagents were purchased at analytical grade. Milli-Q water was used throughout the work.

The DNA sequences, listed below, were purchased from Eurofins MWG Operon, Ebersberg, Germany:

thiol-tethered DNA aptamer (oligo1):

5'-(SH)-(CH₂)₆-

TGTAATTTGTCTGCAGCGGTTCTTGATCGCTGACACCATATTAT
GAAGA-3' biotinylated oligonucleotide complementary sequence
(oligo2):

5'-(biot)-TEG(triethylene glycol)-TCTTCATAATATGGTGTTCAG-3'

biotinylated oligonucleotide non-complementary sequence (oligo3):

5'-(biot)-TEG(triethylene glycol)- AGCTACATTGTCTGCTGGGTTTC-
3'

The buffer solutions used in this work are:

buffer A: 20 mM TRIS buffer pH 7.4, 0.1 M NaCl, 0.1 M KCl, 5 mM
MgCl₂

buffer B: 10 mM TRIS buffer pH 8.3

buffer C: 0.1 M diethanolamine buffer (DEA) pH 9.6

buffer D: 0.1 M phosphate buffer pH 7.0

Thiol-modified probe was treated with dithiothreitol (DTT), purified by elution through NAP-5 columns (GE Healthcare life Sciences illustra NAP-5) and then quantified by measuring UV absorption at 260 nm. All

CHAPTER 7

oligonucleotide stock solutions have been prepared in TRIS buffer B and stored frozen.

7.1.3.2 : Instrumentation

UV absorption measurements were carried out using a Varian Cary 100 Bio UV-spectrophotometer collecting the data with the related Cary WinUV thermal application 3.00(182) software.

Secondary structures of oligo1 and oligo2 sequences were predicted using the software Mfold [29-31].

Differential pulse and cyclic voltammetry measurements were carried out using the portable potentiostat/galvanostat PalmSens electrochemical analyser (PalmSens, the Netherlands), and the results analysed by PSTrace 2.3 software.

Electrochemical Impedance Spectroscopy (EIS) measurements were performed in a digital potentiostat/galvanostat AUTOLAB PGSTAT 30(2)/FRA2 controlled with General Purpose Electrochemical System (GPES) and Frequency Response Analyzer (FRA2) 4.9 software (Eco Chemie, Utrecht, the Netherlands).

The transducers used for the aptasensor development were screen-printed 8-sensor arrays, based on eight graphite working electrodes (diameter = 2.0 mm), each one with its own silver pseudo-reference electrode and graphite counter electrode. The arrays were screen-printed in-house using a DEK 248 screen-printing machine (DEK, Weymouth, UK). A polyester film was used as supporting material (Autostat CT5) from Autotype (Milan, Italy). Polymeric inks Electrodag PF-410 (silver) and Electrodag 423 SS (graphite) were purchased from Acheson (Milan, Italy). Vinylfast 36-100, obtained from Agron (Lodi, Italy) was used as insulating ink.

HPLC measurement were carried out using a Waters Alliance 2690 separations module (Waters corporation, Milford USA), equipped with a Supelco Supelcosil™ LC-PAH (25 cm x 4.6 mm, i.d. 5µm) column and coupled with a Waters DAD 996 detector (Waters corporation, Milford USA).

7.1.3.3 DNA melting curve studies

To evaluate the hybridization reaction between the DNA sequence (oligo1), used as capture aptamer, and the selected complementary sequence (oligo2), melting curves were recorded using the Varian Cary 100 Bio UV-spectrophotometer equipped with a 6+6 peltier thermostatable multicell holder and built-in temperature probes.

100 µL of 1.0 µM oligonucleotides solutions in TRIS buffer A were placed into quartz microcuvettes (10 mm path length). Measurements were carried out by increasing the temperature at a constant rate of 1.0 °C/min from 25 to 95 °C, monitoring the absorbance at 260 nm (spectral bandwidth: 1 nm). Temperature values were directly measured inside the cuvettes, using a probe immersed into the sample solutions. The instrumental accuracy of such measurements was within ± 0.05 °C. A TRIS buffer A solution was used as blank solution. T_m values were either acquired on independently prepared samples ($n \geq 4$) or by repetitive collection (through denaturation-reannealing cycles) on single samples ($n \geq 4$).

Melting temperatures were obtained as first-order derivate plot of Abs versus T using the Cary Thermal Analysis software.

CHAPTER 7

7.1.3.4 Electrochemical measurements

Electrochemical impedance spectroscopy (EIS) measurements were performed in presence of 5.0 mM $[\text{Fe}(\text{CN})_6]^{3-/4-}$ redox probe (equimolar solution in 0.10 M KCl and phosphate buffer D). A voltage of 10 mV in amplitude (peak-to-peak), within the frequency range 100 kHz – 10 mHz, was superimposed to the applied bias potential. The dc potential was set up to +130 mV, the formal potential of $[\text{Fe}(\text{CN})_6]^{4-/3-}$ redox probe. Charge transfer resistance (R_{ct}) variations were taken as signal.

Differential Pulse Voltammetry (DPV) measurements were performed using the following parameters: scan range potential from 0 mV to +600 mV, step potential 5 mV, modulation potential amplitude 70 mV, scan rate 40 mV/s, modulation time 0.05 s, interval time 0.15 s, in accordance with a previously reported protocol [32].

All reported potentials refer to the pseudo-reference silver electrode and the measurements were performed at room temperature.

To use the planar screen-printed array as single use drop-on sensor, a volume of 50.0 μL of sample solutions was placed on the disposable screen-printed cell.

7.1.3.5 Electrodeposition of polyaniline and gold nanoparticles onto SPEs and impedimetric characterization of modified SPEs

The polyaniline (PANI) and gold nanoparticles (AuNPs) modified graphite screen-printed electrodes (GPSEs) were realised in accordance with the optimised procedure reported in our previous works [26].

Briefly, electropolymerisation of polyaniline layer on the GPSEs was obtained performing 10 cyclic voltammetry scans in the range from -400

mV to +800 mV, using in the drop cell a solution 2.5 mM of aniline in 50 mM HClO₄ at 50 mV/s scan rate. After washing with 50 μ L of 0.5 M H₂SO₄, the gold nanoparticles were electrodeposited on the surface of polyaniline modified graphite screen-printed electrode (GSPE) using 15 cyclic voltammetry scans in the range from +200 mV to +1200 mV, from a solution 0.5 mM HAuCl₄ solution in 0.5 M H₂SO₄ at 100 mV/s scan rate. The modified GSPEs were then washed 3 times with Milli-Q water in order to remove the excess monomer and the free ions from the GSPEs surface. The modified GSPEs were characterised by EIS measurements, in order to characterise advantages provided by nanostructured surface.

7.1.3.5.1 Aptasensor development

The DNA aptasensor assay developed was based on a competitive approach as reported in Figure 7.1. Firstly, the electrodeposition of aniline and gold nanoparticles (AuNPs) on graphite screen-printed electrodes (GSPEs) was performed. Sensors were then modified by self-assembly of a mixed monolayer of thiolated DNA aptamer (oligo1) and 6-mercapto-1-hexanol (MCH). Then, a solution containing a proper concentration of the complementary oligo2 and the target pesticide was dropped on sensor surface and the competitive reaction between acetamiprid and complementary biotinylated oligonucleotide (oligo2) was carried out. The biotinylated hybrids formed onto the aptasensor surface were coupled with a streptavidin-alkaline phosphatase conjugate. The 1-naphthyl-phosphate was used as enzymatic substrate and the electroactive product was detected by Differential Pulse Voltammetry (DPV).

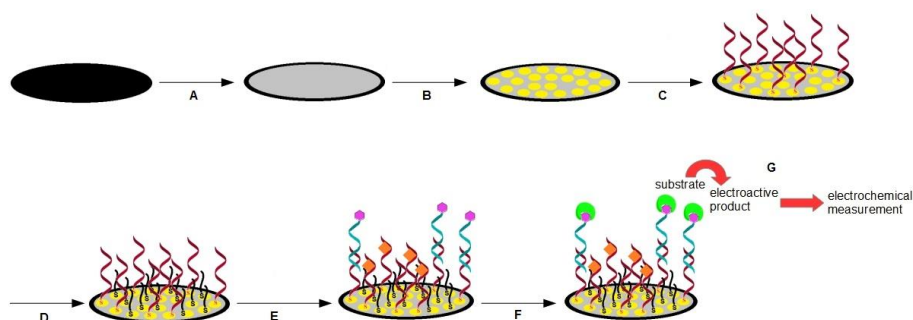


Figure 7.1: Scheme of the aptasensor assay for acetamiprid detection: A) electropolymerisation of aniline; B) electrodeposition of gold nanoparticles (AuNPs); C) oligo1 immobilization; D) mixed SAM formation with 6-mercapto-1-hexanol; E) competitive reaction between acetamiprid and complementary sequence (oligo2); F) coupling with streptavidin-alkaline phosphatase enzyme conjugate; G) incubation with 1-naphthylphosphate and electrochemical detection of enzymatic product by DPV.

7.1.3.5.2 Aptamer immobilisation

7 μL of 2.0 μM thiolated aptamer solution were deposited onto the working electrode surface. Chemisorption was allowed to proceed overnight (≈ 16 h). During this period, the sensors were stored in petri dishes to protect the solutions from evaporation.

To remove the unbound oligonucleotide sequences, the surface was washed three times with TRIS buffer A. The immobilisation step was followed by a mixed SAM (self-assembled monolayer) formation by incubation with 1.0 mM mercapto-1-hexanol (MCH) solution for 60 min. Finally, the aptasensors were washed three times with TRIS buffer A.

7.1.3.5.3 Acetamiprid detection

To perform the dose–response curve calibration, a competitive reaction between acetamiprid and complementary biotinylated oligonucleotide (oligo2) was performed. The aptasensor arrays were incubated with 7 μL acetamiprid solutions in the concentration range of 0–2.0 μM (prepared in

TRIS buffer A) containing 0.010 μM biotinylated complementary oligonucleotide (oligo2) for 40 minutes at room temperature. The aptasensors were then rinsed three times with DEA buffer C.

The control experiments were performed using atrazine solutions.

7.1.3.5.4 Labelling with alkaline-phosphatase and electrochemical measurements

The biotinylated hybrids formed on the aptasensor surface was further incubated with 7 μL solution containing 1.0 U/mL streptavidin–alkaline phosphatase conjugate and 8.0 mg/mL BSA in DEA buffer C. After 20 minutes, the aptasensors were washed 3 times with 0.1 M DEA buffer C.

To use the planar screen-printed modified cells as a drop-on sensor, 50 μL of a solution 1.0 mg/mL of the enzymatic substrate 1-naphtyl-phosphate in DEA buffer C were placed onto the disposable aptasensor and incubated for 20 minutes. The electroactive enzymatic product, 1-naphtol, has been the detected via DPV measurements. The current peak height was taken as the analytical signal.

The signal is expressed in percentage (relative) units as S_x/S_o (i.e. measured signal-to-blank signal ratio) and plotted versus acetamiprid concentration. The curve exhibited a typical sigmoidal shape of a competitive immunoassay.

The competitive curves were analysed with four-parameter logistic equation using proper software (Origin Pro 8.5.1, OriginLab) according to the formula equation [33]:

$$Y = A + (B - A) / (1 + 10^{[\log C - X] \wedge \text{Hillslope}})$$

CHAPTER 7

where A is the Y value at the top plateau of the curve, B the Y value at the bottom plateau of the curve, C is a parameter related to the target concentration necessary to halve the current signal and *HillSlope* is the slope of the linear part of the curve.

7.1.3.6 HPLC measurements

HPLC technique was performed as a reference method for comparing acetamiprid detections in spiked fruit juices, according to the protocol reported by Jovanov et al. [34]. The analysis was carried out using a mobile phase composed by two eluents in the ratio 80/20: HPLC ultrapure water containing 0.1% formic acid and acetonitrile. Isocratic elution was performed at 30°C T using a flow rate of 0.5 mL/min.

7.1.4 Results and discussion

7.1.4.1 Studies of DNA oligonucleotide sequences

Molecular interaction between aptamer and its target is based on conformational changes that bring to characteristic 3-dimensional structures. For this reason, secondary structures of DNA sequences play a fundamental role in binding selectively the analytes. In order to capture the target molecule, aptamer changes its conformation and forms many weak bonds via hydrogen bond interaction, van der Waals interaction and π -stacking interaction [20]. The MFold software was used to predict DNA secondary conformations of oligo1, used as DNA capture probe, and oligo2, used as complementary oligonucleotide in the competition reaction with acetamiprid (Figure 7.2 A and B). Oligonucleotide structures prediction was obtained setting up the temperature to 25°C, regulating ionic strength according to the used TRIS buffer A and selecting untangle

with loop fix as drawing mode. Other parameters were left as default settings.

From the theoretical conformations, oligo1 shows a prevalent single-stranded structure at 25°C in solution characterised by two different sized loops. Oligo2, shorter than oligo1, shows a structure characterised by a single loop in the same chemical conditions.

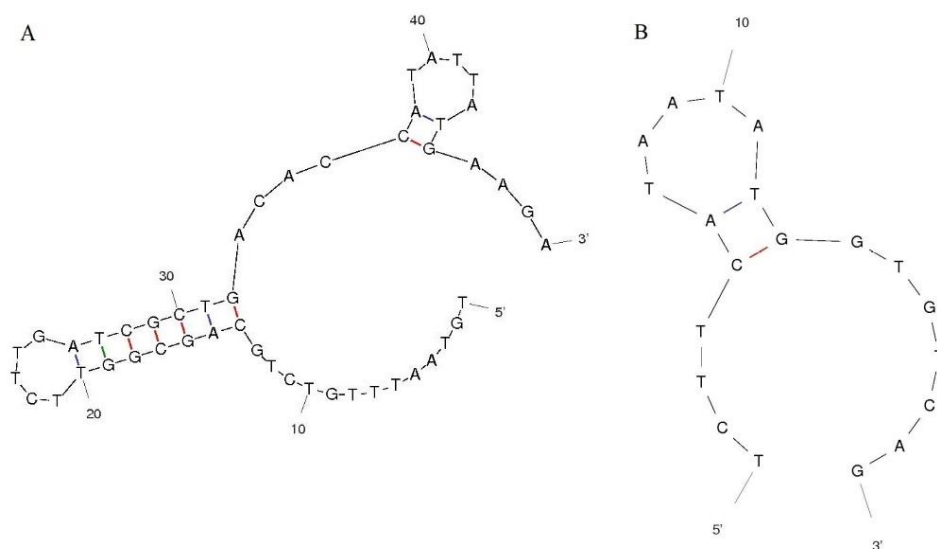


Figure 7.2: Predicted secondary structures of oligo1 (A) and oligo2 (B) sequences obtained by MFold software at 25°C in solution with NaCl 0.1M, MgCl₂ 5mM.

The calculated conformational models were compared with melting curves of the oligonucleotide sequences performed by UV measurements and were used to confirm experimental data. The melting curves, obtained by plotting the absorbance versus the temperature, are shown in Figure 7.3.

Melting curve of oligo1 sequence (1.0 μM) shows two different inflection points (T_{m1} 34.1 °C, T_{m2} 62.6 °C) associated with the successive opening of the two loops showed by its secondary structure. A higher value of T_m of the first inflection point (T_{m1} 35.6 °C) was obtained with oligo1

solution containing acetamiprid ($1.0\ \mu\text{M}$), proving that the interaction with analyte is localised in the smaller loop region. The obtained results were supported from data found in literature [35].

Melting curve of oligo2 sequence does not show any inflection point, because of the tiny dimension of the calculated structural loop. For this reason, the hybridisation reaction between oligo1 and oligo2 will be more efficient in comparison to an oligonucleotide sequence with a stable secondary structure.

The obtained T_m value of hybrid formed from $1.0\ \mu\text{M}$ oligo1 and $1.0\ \mu\text{M}$ oligo2 solutions is $61.3\ ^\circ\text{C}$. T_{m1} and T_{m2} previously obtained from oligo1 melting curves were no more detectable, confirming the formation of a DNA duplex by the hybridization reaction between oligo1 and oligo2.

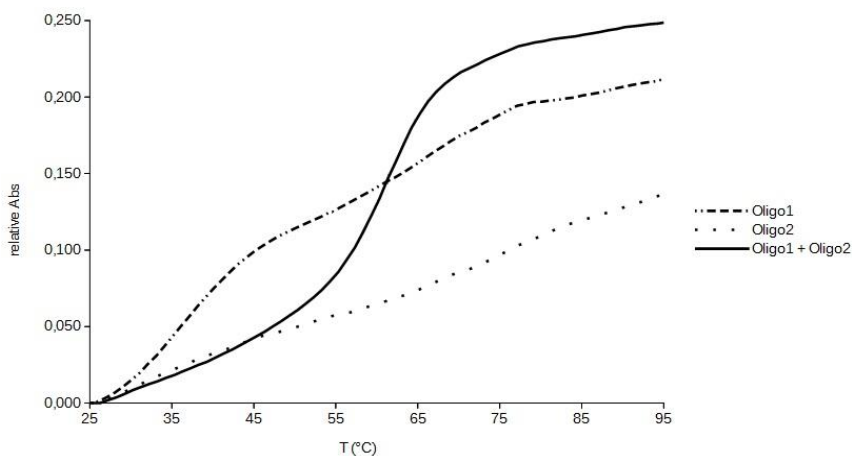


Figure 7.3: Recorded melting curves of oligo1, oligo2 and hybrid formed from $1.0\ \mu\text{M}$ oligo1 and $1.0\ \mu\text{M}$ oligo2 solution is $61.3\ ^\circ\text{C}$. The temperature was increased at a constant rate of $1.0\ ^\circ\text{C}/\text{min}$ from $25\ ^\circ\text{C}$ to $95\ ^\circ\text{C}$. Further details are described in the 7.1.3.3 paragraph.

7.1.4.2 Aptasensor development

7.1.4.2.1 Characterisation of PANI/AuNPs film on graphite screen-printed electrode

The primary surface modification of the graphite screen-printed working electrodes was obtained electrodepositing via cyclic voltammetry a polyaniline layer (PANI), followed by gold nanoparticles electrodeposition (AuNPs), carried out via cyclic voltammetry too, in accordance with previously reported studies [26]. The presence of AuNPs onto polyaniline film was confirmed by SEM analysis (data not shown).

The modified electrode surfaces were analysed via electrochemical impedance spectroscopy (EIS). The values of R_{ct} (charge transfer resistance) were used to make a comparison between the modified and bare graphite screen-printed electrode surfaces (GSPEs). The values of R_{ct} obtained are reported in Figure 7.4 A and B. The electrode conductivity increases after the electrodeposition of AuNPs onto the graphite electrode surface. The obtained reproducibility growth depends from the greater uniformity of the surface determined by the gold NPs electrodeposition. When a polyaniline layer and AuNPs were electrodeposited, the sensor showed a further conductivity increase. Immobilisation of the oligo1 aptamer was confirmed via EIS measurements observing an increase of R_{ct} to a mean value of $3.43 \pm 0.21 \text{ k}\Omega$, respect to the PANI/AuNPs modified electrodes.

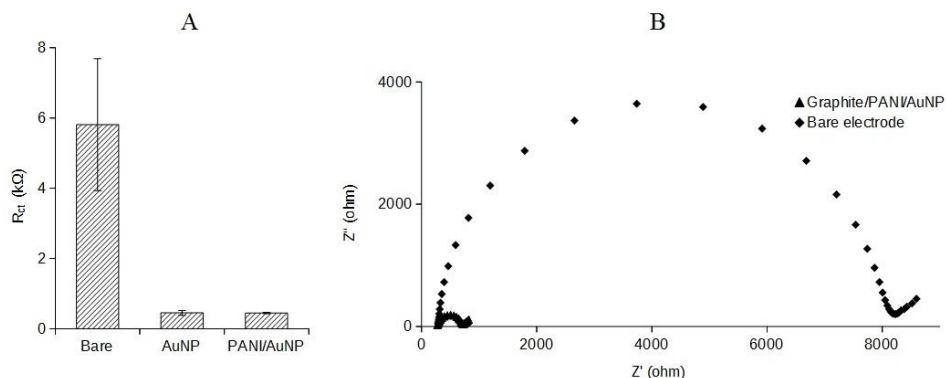


Figure 7.4: R_{ct} values obtained by EIS spectra for bare graphite screen-printed electrodes (GSPEs), AuNPs and PANI/AuNPs modified graphite screen-printed electrodes in 0.01 M $[\text{Fe}(\text{CN})_6]^{4-/3-}$ equimolecular mixture with 0.1 M KCl solution. PANI was electropolymerised with 10 cycles and AuNPs were electrodeposited with 15 cycles as described in section 2.5.1. Inset: Nyquist plots for GSPE/PANI/AuNPs and bare GSPE. The measurements were repeated at least 8 times using different GSPEs.

7.1.4.2.2 Competitive assay

In order to find the best conditions for the competitive assay, key experimental parameters such as hybridisation reaction, concentration of biotinylated complementary sequence (oligo2) and incubation time were studied.

As first point, the hybridisation reaction between immobilised DNA oligonucleotide sequence (oligo1) and biotinylated complementary sequence (oligo2) was performed.

The complementary oligonucleotide sequence, selected in this work, was able to overlap the acetamiprid binding region (as confirmed by T_m measurements reported in section 7.1.4.1). Only 20 bases of the aptamer are hybridised with the complementary oligonucleotide sequence to ensure the successes of the target induced displacement. The oligo2 is functionalised with biotin in 5' end, in order to interact with streptavidin-alkaline phosphatase enzyme conjugated as described in section 7.1.3.5.4.

The hybridisation curve was obtained using the optimised experimental parameters in our previous work [26], in 0.0025–0.020 μM concentration range of target sequence. The current peak increased linearly with the complementary sequence oligo2 concentration up to 0.01 μM , where a plateau was reached (Figure 7.5). This behaviour is due to a limited number of biorecognition sites were bound onto the sensor surfaces. In order to evaluate the selectivity of the biosensor, the effect of a non-complementary sequence (oligo3) (0.020 μM) was studied. The non-specific signal observed was negligible (data not shown). The results confirmed the selectivity of the hybridisation reaction.

The concentration of 0.010 μM complementary sequence was thus used for all experiments involving acetamiprid competitive assay.

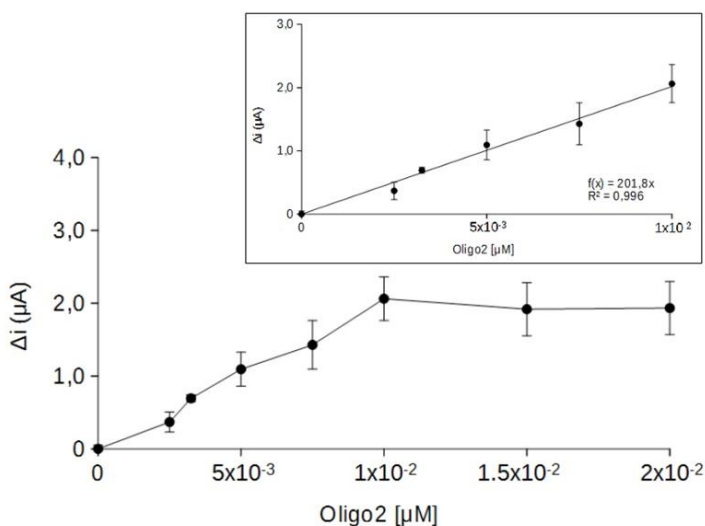


Figure 7.5: DNA aptasensor response for different target concentrations (oligo2) using 20 min hybridisation times. Further details are described in the 7.1.4.2.2 paragraph. Each point was repeated at least 8 times using different DNA aptamer biosensors.

Experiments for incubation time optimisation were performed incubating the aptasensor arrays with a solution containing 0.500 μM acetamiprid and 0.010 μM oligo2 at different times (S_x). These signals were compared with

CHAPTER 7

those obtained by a solution with 0 μM acetamiprid and 0.010 μM oligo2, called blank solution (S_0). In the Table 7.1, we reported the percentage ratio S_x/S_0 . The reproducibility of the aptasensor was analysed by the relative standard deviation (%RSD) as measure of inter-assay reproducibility.

The use of different incubation times allowed tuning the equilibrium interaction given from the competition between oligo2 sequence and acetamiprid for the binding site of aptamer. Increasing the incubation time of a solution containing 0.500 μM acetamiprid with 0.010 μM oligo2 a decrease of the percentage ratio S_x/S_0 was obtained. The higher competition time moves to the acetamiprid binding rather than the hybrid formation, increasing the incubation time over 40 minutes shows that $\%S_x/S_0$ value remains constant. An incubation time of 40 minutes was thus chosen for the following experiments.

Table 7.1: Optimisation of the incubation time. The signals are expressed in $\%S_x/S_0$. S_x is the signal of a solution containing 0.500 μM acetamiprid and 0.010 μM oligo2. S_0 is the signal obtained with 0 μM acetamiprid and 0.010 μM oligo2. The measurements were repeated at least 8 times using different aptasensors. The relative standard deviation (%RSD) is calculated as measure of inter-assay reproducibility.

Incubation time (min)	$\%S_x/S_0$	%RSD
10	88	25
20	80	16
30	69	12
40	65	6
100	63	12

7.1.4.3 Acetamiprid detection

The acetamiprid detection was performed by competitive assay. Various acetamiprid concentrations containing 0.010 μM oligo2 were evaluated. The concentration range was chosen according to the admitted maximum

residue limits (MRLs) for vegetable products commercially available in the European Union [36].

A dose–response curve of acetamiprid was obtained under optimised experimental conditions (Figure 7.6). The signal is reported as S_x/S_0 per cent units, that is the percentage of the signal decrease with respect to the blank value. A decrement of the current peak height was recorded increasing the concentration of the pesticide at fixed concentration of complementary sequence (oligo2).

The regression from the calibration curve shows a correlation coefficient R^2 of 0.995. The limit of detection (LOD) was calculated as reported by Taylor et al. [37] obtaining a value of 0.086 μM . Aptamer cross reactivity with other neonicotinoids was already tested in previous works [21, 22]; therefore, we focused our attention on atrazine, chosen as potential interfering molecule for its ubiquitously presence. Atrazine is a very diffused pesticide of the triazine class known for its clearly established high toxicity and strong environmental persistence [38-40]. Atrazine solutions at different concentrations were tested. As can be observed in Figure 7.6, very similar values compared to the blank solution were achieved. This result shows the appropriate aptasensor selectivity for acetamiprid detection.

In order to evaluate the reproducibility of the aptasensor, the relative standard deviation of eight repetitions of each standard solution was carried out. The average of 5% RSD was obtained for the tested concentrations of acetamiprid solutions, confirming the described aptasensor as a promising analytical tool for its detection.

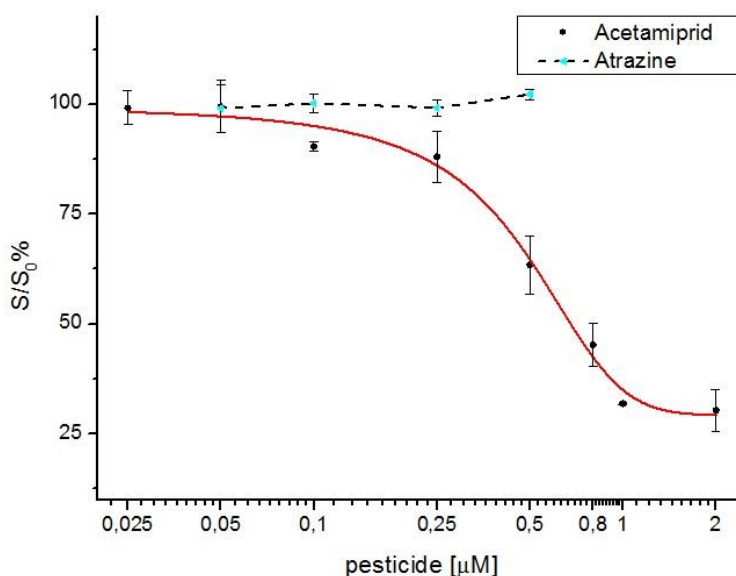


Figure 7.6: The dose-response curve of acetamiprid (●). The points correspond to $\%S_x/S_0 \pm R.S.D.$ The line that joins the points is referred to the theoretical curve calculated by sigmoidal data interpolation. Control experiments were carried out using several concentrations of an atrazine solution (◄). Each point was repeated at least 8 times using different aptasensors.

7.1.4.4 Fruit juice sample analysis

Once verified the suitability of the aptasensor to detect acetamiprid in standard solutions, preliminary experiments on spiked commercially available fruit juice samples were carried out. Acetamiprid was added to the samples after filtration (0.45 μm) and dilution in TRIS buffer A.

Different dilution ratios were tested. The aptasensor response was then determined by DPV measurements, in the same conditions used for acetamiprid calibration curve.

A decrease current signal was observed increasing the acetamiprid spiked concentration in analysed samples. The acetamiprid concentration in the fruit juice samples was determined by referring to a calibration curve realised daily. An acceptable bias of 10% was obtained with 10 times

diluted fruit juice samples confirming the possibility to use the aptasensor in real samples.

In order to confirm aptasensor results, HPLC analysis of the same spiked fruit juice samples was performed, demonstrating that the instrumental analysis provided similar results with a mean bias lower than 10% for all samples. A stronger matrix effect was only observed in case of the 1:2 diluted apricot juices due to an interfering substance. The results obtained with the spiked samples with standard addition of acetamiprid are shown in Table 7.2.

Control experiments with atrazine spiked in 1:10 diluted real samples were carried out to investigate the non-specific signal of the aptasensor. No decrease current signal was observed respect to the fruit juice sample proving the high selectivity of the developed aptasensor for the acetamiprid.

Table 7.2: Recoveries, biases of fruit juice samples spiked with acetamiprid using different dilution ratio. Each concentration was repeated at least 8 times using different aptasensors and 3 times with subsequently injections in HPLC analysis.

	dilution ratio	spiked (μM)	Aptasensor			HPLC		
			found (μM)	Recovery (%)	BIAS (%)	found (μM)	Recovery (%)	BIAS (%)
blackberry juice	1:2	0.30	0.33	108.5	+8.5	0.33	108.5	+8.5
		0.40	0.39	97.5	-2.5	0.39	97.5	-2.5
		0.80	0.64	80.0	-20.0	0.78	97.5	-2.5
peach juice	1:2	0.30	0.24	80.0	-20.0	0.51	170.0	+70.0
		0.40	0.36	90.0	-10.0	0.62	155.0	+55.0
		0.80	0.58	72.5	-27.5	1.04	130.0	+30.0
apricot juice	1:2	0.30	0.24	80.0	-20.0	0.29	96.7	-3.3
		0.40	0.32	80.0	-20.0	0.38	95.0	-5.0
		0.80	0.70	87.5	-12.5	0.79	98.8	-1.2
apricot juice	1:10	0.30	0.27	90.0	-10.0	0.27	90.0	-10.0
		0.40	0.43	107.5	+7.5	0.37	92.5	-7.5
		0.80	0.88	110.0	+10.0	0.76	95.0	-5.0

7.1.5 Conclusions

In this work, an innovative and simple aptasensor for acetamiprid detection, based on a competitive format and disposable screen-printed arrays, was developed. The analytical tool was simple and cost-effective, since it involved low amounts of reagents and low-cost mass-produced sensors. Compared to recently developed electrochemical aptasensors for acetamiprid multidetection, the proposed approach is based on a simpler, portable and easy-to-prepare (even for massive production) screen-printed cells; all these characteristics make this aptasensor particularly promising for the realisation of a commercial kit.

The performance of the assay in terms of sensitivity, reproducibility and selectivity was studied in acetamiprid buffered solutions. The dose–

response curve was constructed between 0.25-2.0 μM acetamiprid concentration range with a limit of detection of 0.086 μM . The average of 5% RSD was obtained for the tested acetamiprid concentrations. The selectivity of the aptasensor was also confirmed by the analysis of atrazine pesticide. Moreover, the aptasensor was applied for the detection of acetamiprid in spiked fruit juice samples showing high recovery percentage.

7.2 References

- [1] P. Jeschke, R. Nauen, M. Schindler, A. Elbert, J. Agric. Food. Chem., 59: 2897-2908, 2011.
- [2] A.M.J. Ragas, R. Oldenkamp, N.L. Preeker, J. Wernicke, U. Schlink, Environ. Int., 37: 872-881, 2011.
- [3] A.Y. Kocaman, M. Topaktas, Environ. Mol. Mutag., 48: 483-490, 2007.
- [4] A. Aagaard, EFSA Journal, 11: 2013.
- [5] K. Matsuda, S.D. Buckingham, D. Kleier, J.J. Rauh, M. Grauso, D.B. Sattelle, Trends Pharmacol. Sci., 22: 573-580, 2001.
- [6] EFSA, EFSA Journal, 12: 2014.
- [7] S. Chawla, H. Patel, K. Vaghela, F. Pathan, H. Gor, A. Patel, P. Shah, Anal Bioanal Chem, 408: 983-997, 2016.
- [8] Amelin, V.G. Amelin, A.M. Andoralov, J. Anal. Chem., 71: 82-93, 2016.
- [9] B. Zhang, X. Pan, L. Venne, S. Dunnum, S.T. McMurry, G.P. Cobb, T.A. Anderson, Talanta, 75: 1055-1060, 2008.
- [10] S. Liu, Z. Zheng, X. Li, Anal Bioanal Chem, 405: 63-90, 2013.
- [11] N. Verma, A. Bhardwaj, Appl Biochem Biotechnol, 175: 3093-3119, 2015.
- [12] Z. Altintas, A. Guerreiro, S.A. Piletsky, I.E. Tothill, Sensors Actuators B: Chem., 213: 305-313, 2015.
- [13] A. Martín-Esteban, Trends in Environmental Analytical Chemistry, 9: 8-14, 2016.
- [14] A. Vasilescu, J.L. Marty, Trac-Trend Anal Chem, 79: 60-70, 2016.
- [15] R. Sharma, K. Ragavan, M. Thakur, K. Raghavarao, Biosensors Bioelectron., 74: 612-627, 2015.

- [16] L. Fan, G. Zhao, H. Shi, M. Liu, Z. Li, *Biosens Bioelectron*, 43: 12-18, 2013.
- [17] A. Fei, Q. Liu, J. Huan, J. Qian, X. Dong, B. Qiu, H. Mao, K. Wang, *Biosens Bioelectron*, 70: 122-129, 2015.
- [18] C. Tuerk, L. Gold, *Science*, 249: 505-510, 1990.
- [19] A.D. Ellington, J.W. Szostak, *Nature*, 346: 818-822, 1990.
- [20] R. Stoltenburg, C. Reinemann, B. Strehlitz, *Biomol. Eng.*, 24: 381-403, 2007.
- [21] J. He, Y. Liu, M. Fan, X. Liu, *J Agric Food Chem*, 59: 1582-1586, 2011.
- [22] H. Shi, G. Zhao, M. Liu, L. Fan, T. Cao, *J Hazard Mater*, 260: 754-761, 2013.
- [23] A. Zani, S. Laschi, M. Mascini, G. Marrazza, *Electroanal*, 23: 91-99, 2011.
- [24] A. Ravalli, G.P. dos Santos, M. Ferroni, G. Faglia, H. Yamanaka, G. Marrazza, *Sensors Actuators B: Chem.*, 179: 194-200, 2013.
- [25] Z. Taleat, A. Khoshroo, M. Mazloun-Ardakani, *Microchimica Acta*, 181: 865-891, 2014.
- [26] R.-S. Saberi, S. Shahrokhian, G. Marrazza, *Electroanal*, 25: 1373-1380, 2013.
- [27] Z. Taleat, A. Ravalli, M. Mazloun-Ardakani, G. Marrazza, *Electroanal*, 25: 269-277, 2013.
- [28] *Analytical electrochemistry*, John Wiley & Sons 2006.
- [29] M. Zuker, *Nucleic Acids Res.*, 31: 3406-3415, 2003.
- [30] A. Waugh, P. Gendron, R. Altman, J. Brown, D. Case, D. Gautheret, S. Harvey, N. Leontis, J. Westbrook, E. Westhof, M. Zuker, F. Major, *RNA*, 8: 707-717, 2002.

CHAPTER 7

- [31] M. Zuker, A.B. Jacobson, *Rna-a Publication of the Rna Society*, 4: 669-679, 1998.
- [32] F. Lucarelli, G. Marrazza, M. Mascini, *Langmuir*, 22: 4305-4309, 2006.
- [33] S. Centi, E. Silva, S. Laschi, I. Palchetti, M. Mascini, *Anal Chim Acta*, 594: 9-16, 2007.
- [34] P. Jovanov, V. Guzsvany, M. Franko, S. Lazic, M. Sakac, B. Saric, V. Banjac, *Talanta*, 111: 125-133, 2013.
- [35] M. Jokar, M.H. Safaralizadeh, F. Hadizadeh, F. Rahmani, M.R. Kalani, *J. Biomol. Struct. Dyn.*, 1-13, 2015.
- [36] EFSA, *EFSA Journal*, 11(12): 2013.
- [37] J. Taylor, G. Picelli, D.J. Harrison, *Electrophoresis*, 22: 3699, 2001.
- [38] L. Jowa, R. Howd, *Journal of Environmental Science and Health, Part C*, 29: 91-144, 2011.
- [39] D.W. Kolpin, E.M. Thurman, S. Linhart, *Arch. Environ. Contam. Toxicol.*, 35: 385-390, 1998.
- [40] N.D. Jablonowski, A. Schäffer, P. Burauel, *Environmental Science and Pollution Research*, 18: 328-331, 2011.

CHAPTER 8

8.1 MIP-based electrochemical sensor with reduced interference signal

Rapini, R, Canfarotta, F, Marrazza G, Piletsky S A – paper in preparation.
Piletsky S A, Rapini, R, Canfarotta, F, Marrazza G, Guerreiro, A – patent in preparation.

8.1.1 Abstract

In this work, an electrochemical sensor with reduced interference signal based on molecularly imprinted polymeric nanoparticles (nanoMIPs) is described. Firstly, nanoMIPs were synthesised using a solid-phase approach, by means of functionalised glass beads, onto which ascorbic acid was bound, in order to be used as template for nanoMIPs synthesis. NanoMIPs were prepared in aqueous environment and their size and shape were characterised via dynamic light scattering (DLS) measurements and transmission electron microscopy (TEM). Obtained nanoMIPs were then applied in electrochemical measurements of ascorbic acid, testing their affinity and selectivity. A multi-pulsed amperometric detection for ascorbic acid was applied, using graphite screen printed electrodes (GSPEs) and measuring its oxidation current continuously performing several additions directly in sample solution. Measurements were carried out also in presence of synthesised nanoMIPs, evaluating their ability to subtract electroactive analyte from sample solution, suppressing its oxidation signal. Once obtained quantitative signal suppression, measurements of dopamine in presence of fixed concentration of ascorbic acid as interfering species were carried out. By means of synthesised nanoMIPs it was possible to measure dopamine in the range 100 – 500 nM

CHAPTER 8

in presence of 50 nM of ascorbic acid eliminating its interfering signal without any sample pretreatment. Lastly, experiments in real samples (spiked human serum) were also carried out.

8.1.2 *Introduction*

Being characterised by high selectivity and affinity towards many kinds of targets, molecularly imprinted polymers (MIPs) are generally recognised as a useful tool for molecular recognition processes, as well as probe macromolecules used in sensing systems development. Main advantages come from the use of the imprinting synthesis technique, especially because of the possibility to use low costs reagents to obtain surfaces or nanoparticles containing cavities able to bind several types of analytes, from biological or disease markers, to pharmaceutical compounds including almost every kind of synthetic chemicals [1-3]. Moreover, main advantages given by the use of MIPs, compared to classical natural receptors, include their high chemical stability at extreme pH values, their thermal stability and lower realisation costs [4].

Molecular imprinted polymers can be synthesised as nanoparticles (nanoMIPs), showing several advantages respect to bulk MIPs: nanoscale dimensions give the advantage of a higher surface-to-volume ratio, resulting in a greater total surface area per weight unit of polymer. Recognition capabilities are moreover increased by higher in number and more accessible binding sites increasing template removal after synthesis and binding kinetics [5, 6]. These characteristics have a key role in nanoMIPs application in sensors development. Several chemical and electrochemical strategies for nanoMIPs synthesis were reported [4, 7]: among these, the solid phase approach [8, 9] resulted particularly suitable,

being able to lead to the production of nanoparticles with high selectivity and affinity for the target as well as dimensionally uniform binding sites.

Ascorbic acid (AA) is an electroactive molecule commonly used as antioxidant in food, animal feed, pharmaceutical formulations and cosmetic applications [10]. It is also involved in many biological processes, e.g. free radical scavenging, cancer prevention and immunity improvement [11]. Dopamine (DA) is a neurotransmitter distributed in the mammalian central nervous system for message transfer, playing a central role in the functioning of central nervous, renal, hormonal and cardiovascular systems [12]. Ascorbic acid and dopamine coexist in biological fluids and selective determination of these molecules can be useful from a clinical point of view. Both were chosen as model analyte because it can be easily determined by electrochemical analysis oxidising them at electrode surface and measuring related anodic peak currents. Anyway, at bare, unmodified, electrodes, their selective determination is not possible because their oxidation potentials are very close [13, 14].

In a general way, in order to carry out an electrochemical detection, one of the challenges is to remove interfering substances that can generate signals of similar nature, resulting in analyte detection obscuration or masking. This problem is usually avoided by using sample pre-treatment procedure such as solid-phase extraction, chromatography or other kinds of separation methods. These procedures, as well as any other procedural step, increase analysis time and related costs.

In the present work, an innovative approach for suppressing signals of interfering species in the sample by providing specific nanoMIPs as binding agents capable of interacting with interfering species is described.

CHAPTER 8

Molecularly imprinted polymeric nanoparticles (nanoMIPs) were firstly synthesised in aqueous environment using a solid-phase approach. Ascorbic acid was used as template, linking it to chemically modified glass beads. Template functionalised glass beads were then used as solid support to carry out nanoparticles growth. Size and shape of obtained nanoMIPs were studied by means of dynamic light scattering (DLS) and transmission electron microscopy (TEM) measurements, while their interaction with the target was carried out by means of amperometric measurements. Effects of ascorbic acid oxidation signal variation in presence of nanoMIPs was studied until a quantitative signal suppression was achieved. Successively, measurements of dopamine in presence of a fixed concentration of ascorbic acid, acting as interfering species, were carried out in buffered solutions. Synthesised nanoMIPs were then also tested in spiked human serum samples. It is interesting to point out the novelty of the described nanoMIPs application in comparison with more classical nanoMIPs-based approaches for sensors development [4].

8.1.3 *Experimental*

8.1.3.1 *Materials and instruments*

Glass beads (Spherglass[®] 2429 CP00, 53-106 μm diameter) were purchased from Blagden Chemicals, UK. Acrylic acid (AA), *N*-isopropylacrylamide (NIPAm) *N,N'*-methylene-bis-acrylamide (BIS), *N*-tert-butylacrylamide (TBAm), ammonium persulfate (APS), tetramethylethylenediamine (TEMED), *N*-[3-(Trimethoxysilyl)propyl]ethylenediamine, *N*-ethyldiisopropylamine, sodium hydroxide (NaOH), ascorbic acid, toluene and acetone were purchased from Sigma-Aldrich, UK. Dopamine hydrochloride has been purchased from Sigma-Aldrich, Italy. Phosphate buffered saline (PBS),

pH 7.2 was prepared, as specified, from PBS buffer tablets (Sigma-Aldrich, UK) and consisted of phosphate buffer (0.01 M), potassium chloride (0.0027 M), and sodium chloride (0.137 M), pH 7.2. Double-distilled ultrapure water (Millipore, UK) was used for the experiments. Human serum H4522 (from human male AB plasma) was purchased from Sigma-Aldrich, Italy. The transducers used for the electrochemical measurements were screen-printed cells based on a graphite working electrode (diameter \approx 2.0 mm), with a silver pseudo-reference electrode and graphite counter electrode. The cells were screen-printed in-house using a DEK 248 screen-printing machine (DEK, Weymouth, UK). A polyester film was used as supporting material (Autostat CT5) from Autotype (Milan, Italy). Polymeric inks Electrodag PF-410 (silver) and Electrodag 423 SS (graphite) were purchased from Acheson (Milan, Italy). Vinylfast 36–100, obtained from Agron (Lodi, Italy) was used as insulating ink.

In all experiments double-distilled ultrapure (DI) water (Millipore, UK) was used. All chemicals and solvents were of analytical or HPLC grade and used without further purification.

The size of the nanoMIPs was determined by Dynamic Light Scattering (DLS) using a Zetasizer Nano (Malvern Instruments, UK). NanoMIPs were also characterised by Transmission Electron Microscope (TEM) analysis by means of a Philips CM12 (Koninklijke Philips Electronics N.V., The Netherlands).

UV absorption measurements have been carried out using a Cary 100 Bio UV-spectrophotometer (Agilent Technologies Inc., U.S.) collecting the data with the related Cary WinUV scanning application 3.00(182) software.

CHAPTER 8

Multi-pulsed Amperometry (MPA) and Cyclic Voltammetry (CV) measurements were carried out using the digital potentiostat/galvanostat AUTOLAB PGSTAT 10 equipped with the ECD module for low currents and controlled with General Purpose Electrochemical System (GPES) 4.9 software (Eco Chemie, Utrecht, the Netherlands). MPA measurements were carried out firstly using the standard connection setup and, in a second time, continued connecting the working electrode to the ECD module, capable of decreasing the current detection limit down to 100 pA.

8.1.3.2 *Methods*

8.1.3.2.1 *Preparation of ascorbic acid-modified solid-phase*

The protocol for the preparation of ascorbic acid modified solid-phase was adapted from Canfarotta et al. [9]. Briefly, glass beads were activated by boiling them in NaOH for 10 min and washed with DI water and acetone. After drying in the oven at 80 °C overnight, the beads were incubated in a 2% v/v solution of GOPTS (3-glycidyloxypropyl trimethoxysilane) in anhydrous toluene, containing also *N*-ethyldiisopropylamine 2 mg/mL, at 55 °C for 5 h. Afterwards, the glass beads were poured into a Buchner funnel, rinsed with toluene twice, then with acetone (800 mL) and eventually dried under vacuum. These epoxy-functionalised beads were then incubated in a solution of ascorbic acid 2 mg/mL in PBS 0.01 M pH 7.2 overnight. Finally, the glass beads were filtered and rinsed with water (800 mL water for 150 g beads), dried under vacuum and stored under inert atmosphere (N₂) at 4 °C until use.

8.1.3.2.2 *Synthesis of ascorbic acid imprinted nanoMIPs*

To synthesise nanoMIPs imprinted against ascorbic acid, a polymerisation in PBS was performed, adapting the protocol described by Hoshino et al.

[15, 16]. In particular, N-isopropylacrylamide (Sigma-Aldrich) (39 mg), N-tert-butylacrylamide (Sigma-Aldrich) (33 mg), N-(3-aminopropyl)methacrylamide hydrochloride (Polysciences, Inc.) (5.8 mg), acrylic acid (Sigma-Aldrich) (2.2 μ L), and N,N'-methylenebisacrylamide (Sigma-Aldrich) (2 mg) were dissolved in 100 ml PBS. Prior to initiate the polymerisation process, the mixture was purged with N₂ and sonicated for 30 min. At the same time, functionalised beads were purged with N₂ for 20 min. The beads were then added to the polymerisation solution and purged with N₂ for 5 min. The mixture of beads and polymerisation solution was swirled gently and then the polymerisation was started by adding ammonium persulfate (APS) (60 mg/ml) and N,N,N',N'-tetramethylethylenediamine (TEMED) (22 μ L) as catalysts. The polymerisation was performed overnight at room temperature, after flushing the headspace of the bottle used for the reaction with N₂ for 30 seconds. The following day, the beads were washed with deionised water, following the steps described by Canfarotta et al. [9], by using a 60 mL solid-phase extraction (SPE) cartridge fitted with a frit of 20 μ m porosity. Afterwards, the high-affinity nanoMIPs were eluted at 65°C with deionised water, until a total volume of 100 mL of solution was reached. All the process is schematised in Figure 8.1.

8.1.3.2.3 *Size and concentration analysis*

Prior to DLS and TEM measurements, the solution of nanoMIPs was ultra-sonicated for 3 min to disrupt possible aggregates. To perform DLS, 1 mL of the nanoMIP dispersion was analysed by DLS at 25 °C in a 3 cm³ disposable polystyrene cuvette. Attenuator position, measurement duration and number of runs were automatically chosen by the instrument. For TEM analysis, a drop of the nanoMIPs solution was placed on a carbon-

coated copper grid and dried in a fume hood before measurement, setting up the instrument with an 80 kV voltage. To estimate nanoMIPs solution concentration (obtaining information relative to polymer amount as weight/volume) a small volume of nanoMIPs solution was boiled until complete evaporation of DI water. Dry residue was then weighted.

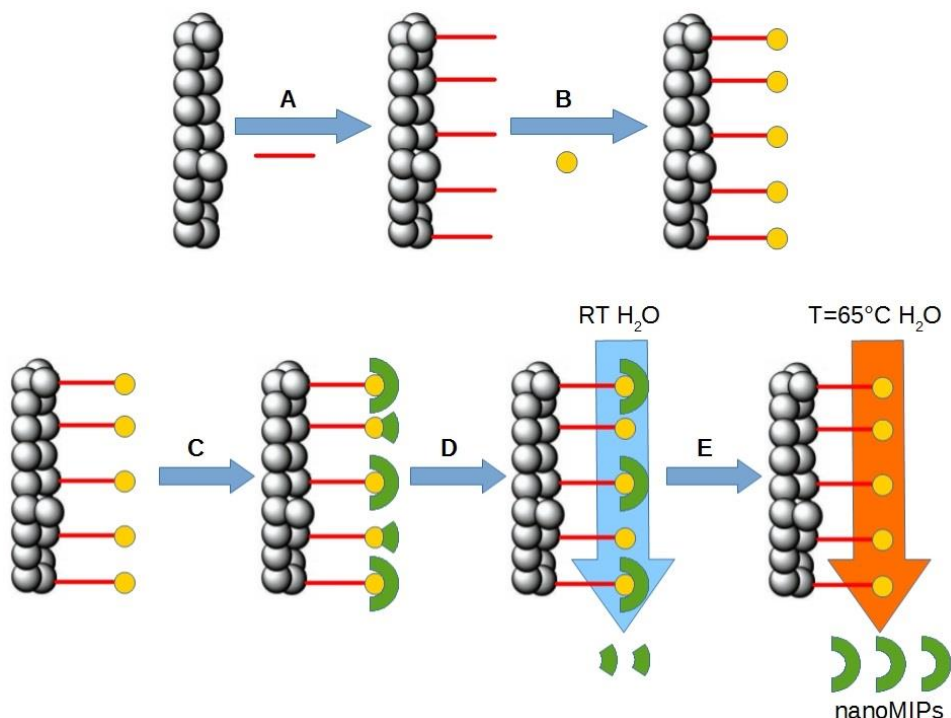


Figure 8.1: Scheme of the solid-phase synthesis process. A: OH activated glass beads are grafted with GOPTS (3-glycidyloxypropyl trimethoxysilane); B: silanised glass beads are incubated with ascorbic acid (AA), which is then bound for their functionalisation; C: functionalised glass beads are immersed in a solution containing the polymerisation mixture and purged with N_2 flow: initiators are then added in order to carry out the synthesis; D: a first elution step using RT (room temperature) DI water is used to remove unreacted monomers, free template and low affinity nanoMIPs; E: a second elution step using $T = 65^\circ\text{C}$ DI water is used to remove and collect synthesised nanoMIPs.

8.1.3.2.4 UV analysis

Absorbance values were recorded in the range from $\lambda=350$ to $\lambda=190$ nm to evaluate absence of monomers or intermediate reactants in the synthesised

particles batches, also collecting absorbance at $\lambda=197$ nm to evaluate the relative nanoMIPs concentrations.

8.1.3.2.5 *Electrochemical procedures*

Cyclic Voltammetry (CV) was performed to obtain the value of oxidation potentials of the chosen electroactive molecules, setting the following parameters: scan range from -0.6 V to +0.5 V, step potential of 0.025 V, scan rate 0.1 V/s. Measurements were performed using the screen printed cells as a drop on cell, placing 50 μ L of solution onto the electrodes surfaces and performing the scans.

Multi-pulsed Amperometry (MPA) was performed adapting the procedure described by Takátsy et al. [17] by setting the following parameters: number of pulses 2, E_{pulse1} 0.250 V, E_{pulse2} 0 V, t_{pulse1} 0.2 sec, t_{pulse2} 1.5 sec. Current was recorded during the application of E_{pulse1} . Measurements were performed immersing the screen printed cell into a 5 mL sample solution under stirring.

All reported potentials refer to the pseudo-reference silver electrode and the measurements were performed at room temperature.

8.1.3.2.6 *Ascorbic acid and dopamine measurements*

Amperometric measurements based on the oxidation of electroactive targets at the electrode surface were carried out continuously. Volumes of ascorbic acid and dopamine solutions were directly added from buffered 100 μ M stock solutions to the 5 mL volume sample solution kept under stirring. Total volume variation was neglected. Tested concentrations were within 50-550 nM and 12-35 μ M for ascorbic acid (AA) and 50-500 nM for dopamine (DA). Current increases after each addition were taken as analytical signal, reporting $\Delta(i-i_0)$ versus analyte concentration. All

CHAPTER 8

measurements were carried out in PBS pH=7.2 buffered solutions or PBS pH=7.2 diluted matrices.

8.1.3.2.7 Electrochemical nanoMIPs characterisation

Electrochemical measurements carried out for ascorbic acid and dopamine were repeated in PBS pH=7.2 buffered solutions containing the synthesised nanoMIPs, in order to investigate their ability to selectively suppress ascorbic acid oxidation signal. Current increases after each addition were considered as analytical signal, reporting $\Delta(i_{\text{MIP}}-i_{\text{OMIP}})$ versus analyte concentration and comparing them to those previously obtained in PBS pH=7.2 buffered solutions without nanoMIPs. Per cent decrease of current increases after every analyte addition was also used to evaluate signal suppression. Thermal stability of synthesised nanoMIPs was also investigated by heating a sample volume of nanoMIPs solution at 45°C for 3h (solvent evaporation was avoided). Electrochemical measurements in the presence of ascorbic acid were carried out after cooling the solution at T_{amb} and repeated after leaving the solution to rest overnight at T_{amb} , to evaluate potential changes in their interaction with the target.

8.1.4 Results and discussion

8.1.4.1 Size characterisation of nanoMIPs

DLS measurements showed a mean size of 374 nm for the synthesised batches of nanoMIPs, with a polydispersity index within the range 0.39 – 0.5. In order to confirm this data and gain more precise information about particles size and shape, electronic microscopy measurements were performed. Results are reported in Figure 8.2.

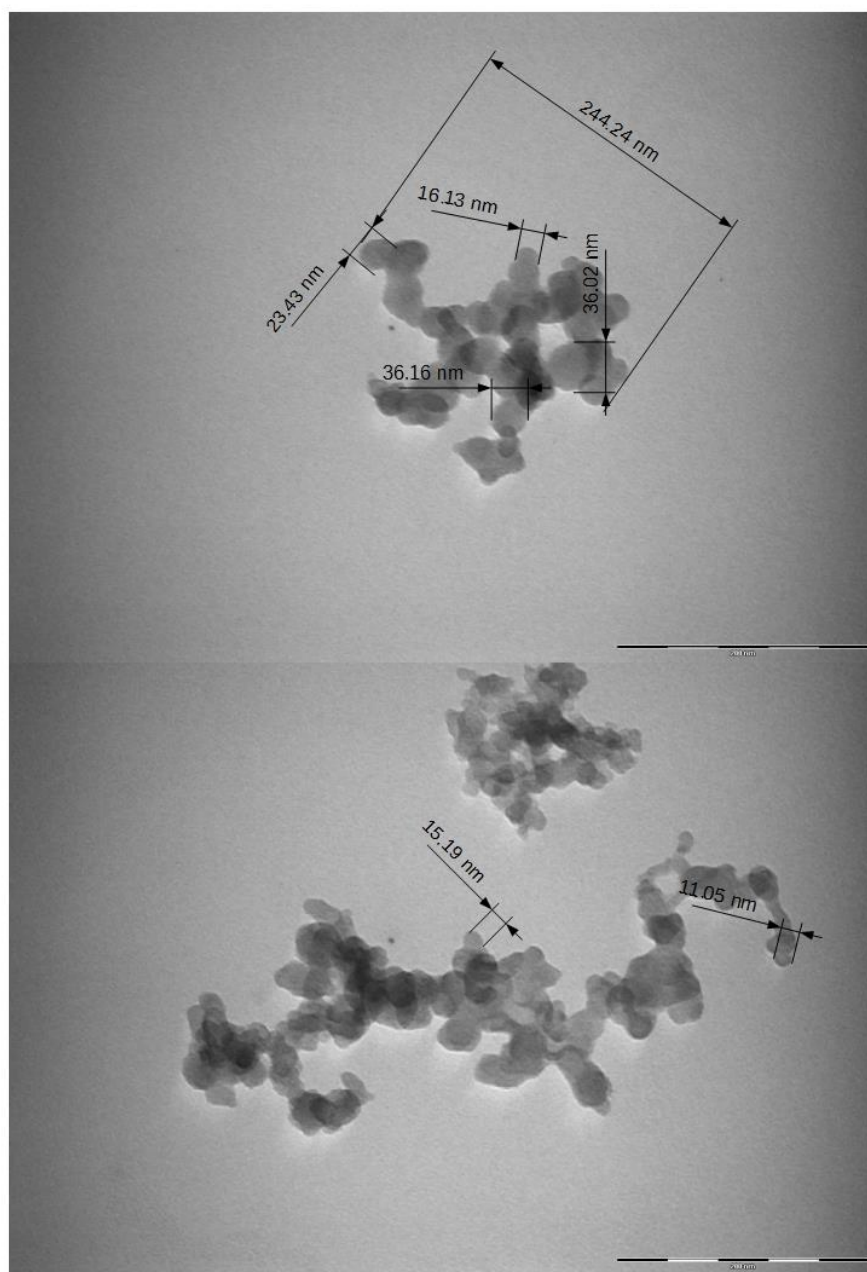


Figure 8.2: Collected TEM images for synthesised nanoMIPs. Particles size and shape appear homogeneous, with diameter dimensions within the range 11 – 36 nm.

CHAPTER 8

Observing TEM images, it is possible to notice the presence of tiny particles with diameter much smaller respect to those estimated by DLS measurements. NanoMIPs show a spherical shape and sizes included in the range from 11 to 36 nm. An explanation about differences in results between the two applied techniques can be given observing in TEM images the presence of aggregate multi-particles structures with dimensions in the order of hundreds of nm. DLS measurements were unable to distinguish nanoparticles from aggregates.

8.1.4.2 UV characterisation of nanoMIPs

UV absorption spectra were used to characterise the purity of the synthesised batches and their relative concentrations. Figure 8.3 shows recorded spectra of solutions containing the polymerisation mixture and the polymerisation mixture including ascorbic acid (AA), compared with the spectrum obtained from a solution of nanoMIPs. The spectrum related to the polymerisation mixture including ascorbic acid (AA) shows an intense peak at 256 nm, due to AA, together with a shoulder peak at ≈ 215 nm, depending on the presence of the polymerization mixture, including polymerisation initiator. Both signals are absent in the spectrum related to the nanoMIPs solution, confirming total removal of unreacted polymerisation molecules and unbound template during room temperature washing steps. Furthermore, collecting absorbance value at 197 nm it was possible to estimate relative concentrations of synthesised nanoMIPs (data not shown), obtaining an RSD value of 10% on the mean polymeric concentration calculated from all synthesised batches.

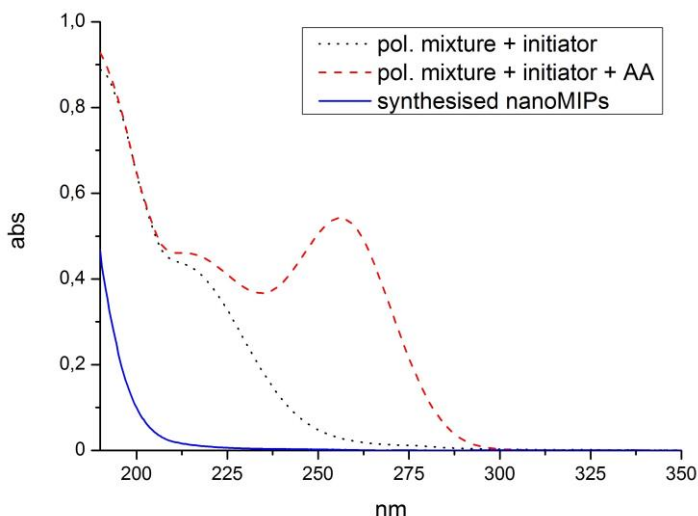


Figure 8.3: Recorded UV spectrum of synthesised nanoMIPs solution compared to those obtained from monomers mixture with and without the template.

8.1.4.3 *Electrochemical and thermal characterisation of nanoMIPs for ascorbic acid*

Firstly, oxidation potential of ascorbic acid (AA) and dopamine (DA) (model analyte chosen) were studied. Cyclic voltammetry experiments were set up as described in section 2.2.4 in order to determine the oxidation potential for following multi-pulsed amperometry measurements. Results are showed in Figure 8.4, which reports experimental voltammograms obtained for PBS pH=7.2 buffered solutions containing 1 mM ascorbic acid and 1 mM dopamine. It can be clearly seen that used graphite screen-printed electrodes (GSPEs) were not able to discriminate between the oxidation potential of the two molecules, making them a perfect interfering/analyte to test the signal suppression efficiency of nanoMIPs. According to experimental data, an oxidation potential of +0.250 V was selected for successive amperometric measurements.

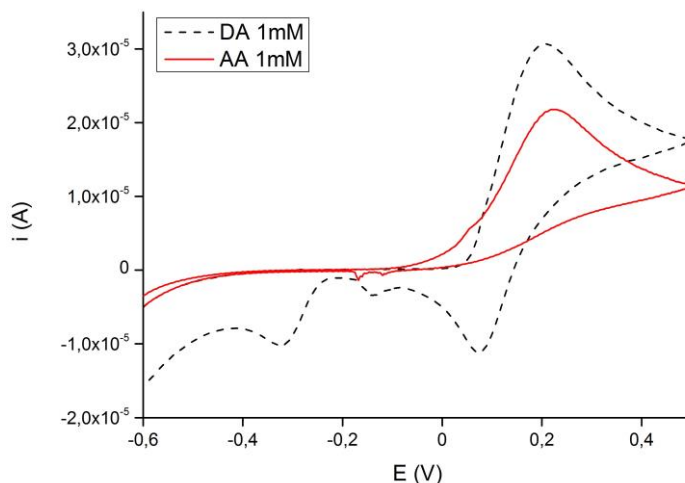


Figure 8.4: Obtained voltammograms for solutions containing ascorbic acid (AA) 1mM and dopamine (DA) 1mM. Reported potentials are related to the Ag/AgCl pseudo-reference electrode of the GSP cell.

In order to evaluate the nanoMIPs electrochemical behaviour, multi-pulsed amperometry was firstly applied to measure current response of ascorbic acid in the micromolar concentration range to obtain preliminary information. Under stirring conditions, a standard addition of ascorbic acid solution was made to the 5 mL solution every 50 sec, measuring current values continuously. After that the steady state was reached, the mean current value of every addition was recorded. Examples of the recorded chrono-amperograms are reported in Figure 8.5. Measurements were carried out first in PBS buffered solution and then repeated using the same procedure in a PBS buffered solution of synthesised nanoMIPs, comparing results. Recorded currents for tested ascorbic acid concentrations are showed in Figure 8.6: the obtained values showed a significant decrease of current response given from ascorbic acid oxidation after addition of same amounts of electroactive molecule, in the presence of nanoMIPs.

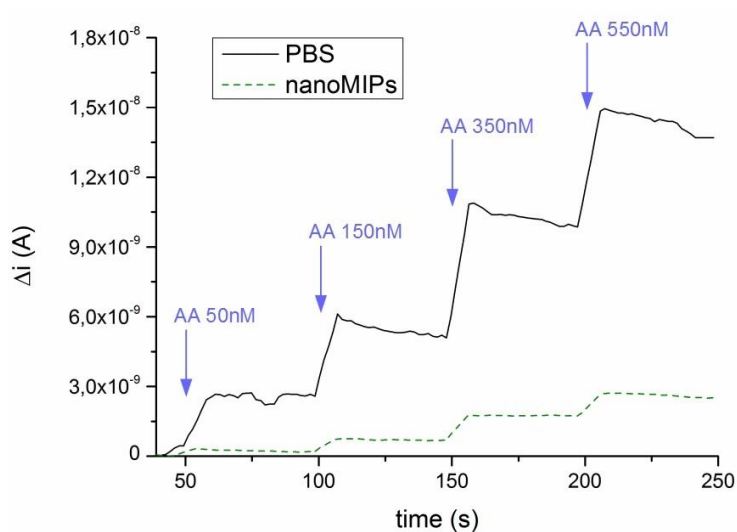


Figure 8.5: Examples of recorded chrono-amperograms. Current values are collected continuously and plotted vs. time. Highlighted in blue are AA concentrations in sample solution after every addition.

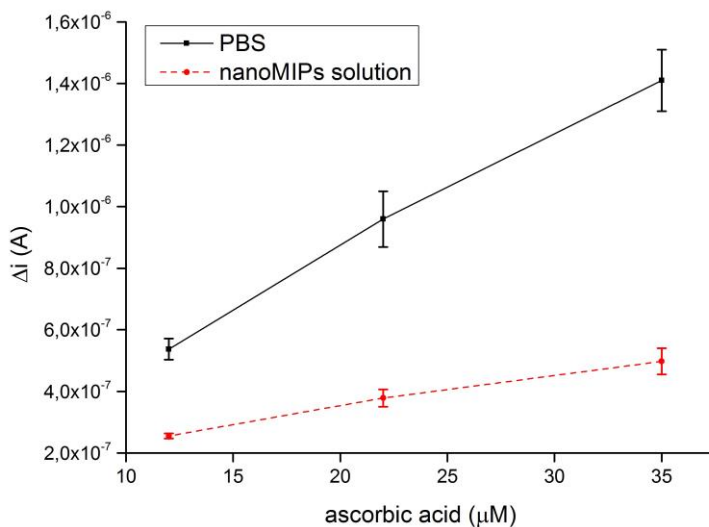


Figure 8.6: Recorded current values after successive additions of ascorbic acid (AA) in different sample solutions. Δi values refer to the difference $i_x - i_{\text{blank}}$ where x is the concentration of AA in sample solution after each addition and i_{blank} refers to the current value recorded before the first addition.

CHAPTER 8

Calculations of the per cent values of suppressed current, reporting $[\Delta(i_{\text{MIP}} - i_{0\text{MIP}}) / \Delta(i - i_0)]\%$, confirm a constant per cent ratios around 60% for tested concentrations Table 8.1.

Table 8.1: Obtained per cent ratios of recorded currents between buffered water solution measurements and nanoMIPs solution measurements for the tested AA concentrations.

conc. AA (μM)	% signal suppression
12	56
22	64
35	69

Possible effects given from non-specific interactions were also tested, measuring current changes after addition of AA in a non-specific nanoMIPs solution and an unreacted polymerization mixture (including initiator), always comparing them with signals obtained from AA oxidation in PBS buffered solution. Results are reported in Figure 8.7.

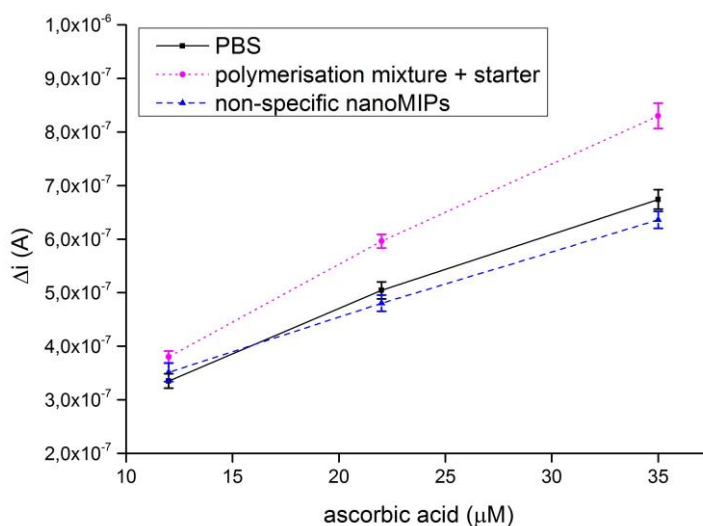


Figure 8.7: Recorded current values after successive additions of ascorbic acid (AA) in different sample solutions. Δi values refer to the difference $i_x - i_{\text{blank}}$ where x is the concentration of AA in sample solution after each addition and i_{blank} refers to the current value recorded before the first addition.

Chosen non-specific nanoMIPs were able to bind vancomycin and were formerly synthesised according to the procedure reported by Mazzotta et al. [18]. No significant differences in recorded oxidation currents were observed in both cases, confirming the specific current suppression effect given by AA nanoMIPs previously described. Thermal stability of the synthesised nanoMIPs was also investigated by heating a sample volume of nanoMIPs solution at 45°C for 3h. Electrochemical measurements in presence of ascorbic acid were carried out after cooling the solution at T_{amb} and compared with measurements carried out in PBS buffered solution. Comparing it to measurements in absence of nanoMIPs, a not significant signal difference ($\approx 10\%$ for AA 12 μ M) between oxidation currents was obtained, showing that the applied thermal treatment affected binding capability of the synthesised nanoMIPs. This result can be explained considering that heating treatment can produce some structural changes to the nanoMIPs, due to shrinking or swelling effects. A deeper analysis, despite its potential interest, is not a subject of this paper and, moreover, experimental evidences show that after leaving the solution to rest overnight, and after repeating measurements, a recovery of $\approx 70\%$ of the suppression efficiency by nanoMIPs was regained. The observed result confirms that a structural conformation re-arrangement is able to partially bring back particles to their original shape after the longer resting period at room temperature.

8.1.4.4 Quantitative electrochemical suppression of ascorbic acid oxidation current

In order to obtain a proof of concept about the possibility to apply the proposed method for suppressing interfering currents in sensing devices, multi-pulsed amperometric measurements were carried out lowering the

CHAPTER 8

tested concentration range of AA in order to obtain a quantitative suppression. Analysis of ascorbic acid was performed in the nanomolar range, from 50 nM to 550 nM (Figure 8.5). Current response of tested AA concentrations in PBS buffered solution was compared to measurements carried out in nanoMIPs solution, obtaining a quantitative current suppression for AA concentrations close to the limit of 50 nM. Figure 8.8 shows recorded signals for subsequent AA additions in sample solution.

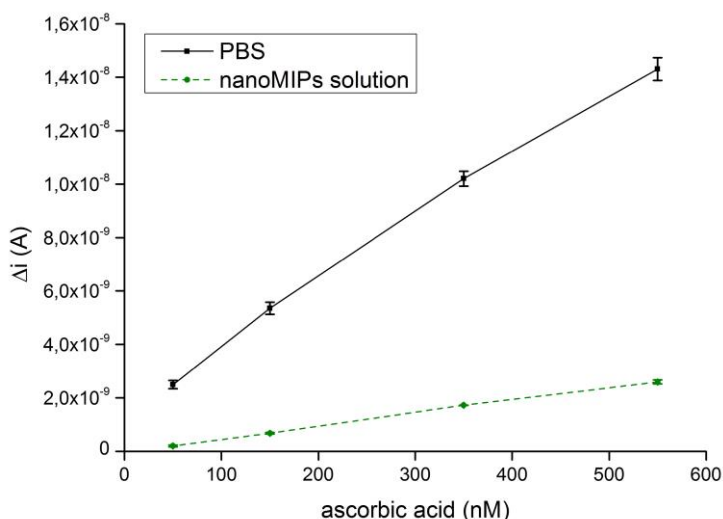


Figure 8.8: Recorded current values after successive additions of ascorbic acid (AA) in different sample solutions. Δi values refer to the difference $i_x - i_{\text{blank}}$ where x is the concentration of AA in sample solution after each addition and i_{blank} refers to the current value recorded before the first addition.

Calculations of the per cent values of suppressed current, reporting $[\Delta(i_{\text{MIP}} - i_{0\text{MIP}}) / \Delta(i - i_0)]\%$ shows values $\geq 90\%$ for AA concentrations lower than 100 nM (Table 8.2).

Table 8.2: Obtained per cent ratios of recorded currents between buffered water solution measurements and nanoMIPs solution measurements for the tested AA concentrations.

conc. AA (nM)	% signal suppression
50	92
150	87
350	83
550	82

8.1.4.5 Dopamine detection

Measurements of dopamine (DA) were carried out, in order to complete the proof of concept for the proposed model, i.e. the possibility to detect it in presence of an interfering concentration of ascorbic acid avoiding any sample pretreatment to eliminate interfering signal. Firstly, current response to subsequent DA additions in PBS buffered solution was analysed in the range 50-500 nM. After that, measurements were repeated in the presence of 50 nM and 100 nM AA, in order to evaluate current response. The experiment was then repeated in a nanoMIP solution in order to verify if their selective interaction with ascorbic acid was able to suppress its signal even in presence of another electroactive molecule, the analyte dopamine. The results (Figure 8.9) clearly show that the synthesised nanoMIPs were able to selectively suppress AA interfering current in an electrochemical detection of DA in PBS. The maximum AA concentration that could be quantitatively sequestered with the described setup was 50 nM, allowing to correctly determining DA using a multi-pulsed amperometric measurement method, avoiding any other sample pretreatment.

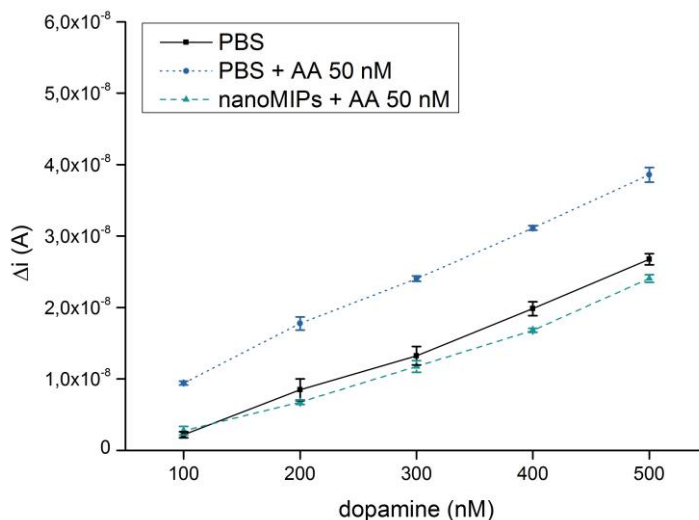


Figure 8.9: Recorded current values after successive additions of ascorbic acid (AA) in different sample solutions. Δi values refer to the difference $i_x - i_{\text{blank}}$ where x is the concentration of AA in sample solution after each addition and i_{blank} refers to the current value recorded before the first addition.

8.1.4.6 Real samples

Considering that our novel approach demonstrated to allow the measurement of DA in the presence of AA as interfering molecule in standard solutions, we applied the proposed method to analyse DA in real samples. Measurements were carried out in diluted human serum samples, applying the same experimental setup as described in section 8.1.4.5. Results are showed in Figure 8.10. Nevertheless, interfering current generated by the presence of a fixed concentration of AA is still capable to affect measurements, generating errors in DA detection. Concluding, nanoMIPs were able to suppress interfering current even in real samples, maintaining their stability and selectivity characteristics, thus representing a novel analytical tool for the electrochemical suppression of potential interfering species.

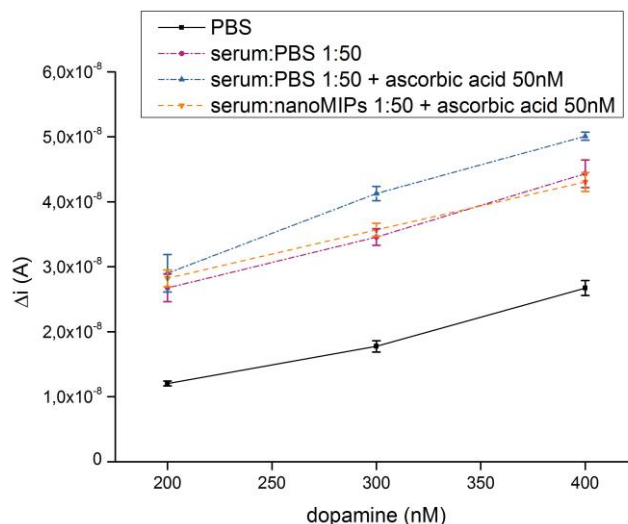


Figure 8.10: Recorded current values after successive additions of ascorbic acid (AA) in different sample solutions. Δi values refer to the difference $i_x - i_{\text{blank}}$ where x is the concentration of AA in sample solution after each addition and i_{blank} refers to the current value recorded before the first addition.

8.1.5 Conclusions

A novel application of molecularly imprinted polymeric nanoparticles for the realisation of an electrochemical sensor with reduced interference was described. Synthesised nanoMIPs were obtained by means of a solid-phase synthetic approach, using ascorbic acid as immobilised template. Obtained nanoMIPs size and shape was investigated by means of DLS and TEM measurements, as well as their ability to bind the target molecule, that was tested via electrochemical amperometric measurements, evaluating AA oxidation current suppression in presence of nanoMIPs. A quantitative signal suppression for AA was achieved, furthermore measurements of dopamine in presence of fixed concentrations of AA were carried out, being able to correctly evaluate its concentration because of the suppression of AA interfering signal in presence of nanoMIPs. Nanoparticles were able to suppress AA interfering current even in real

CHAPTER 8

samples, maintaining their stability and selectivity characteristics, thus representing a novel analytical tool for the electrochemical suppression of interfering molecules. It is worth mentioning that, thanks to the fact that the imprinting approach herein used to generate nanoMIPs can be virtually applied to any target molecule, the proposed method is generic in nature, allowing targeting a wide range of interfering molecules.

8.2 References

- [1] E.V. Dmitrienko, I.A. Pyshnaya, O.N. Martyanov, D.V. Pyshnyi, *Russian Chemical Reviews*, 85: 513, 2016.
- [2] P. Wang, X. Sun, X. Su, T. Wang, *Analyst*, 141: 3540-3553, 2016.
- [3] G. Díaz-Díaz, D. Antuña-Jiménez, M.C. Blanco-López, M.J. Lobo-Castañón, A.J. Miranda-Ordieres, P. Tuñón-Blanco, *TrAC Trends in Analytical Chemistry*, 33: 68-80, 2012.
- [4] A. Poma, A.P. Turner, S.A. Piletsky, *Trends Biotechnol.*, 28: 629-637, 2010.
- [5] D. Gao, Z. Zhang, M. Wu, C. Xie, G. Guan, D. Wang, *J. Am. Chem. Soc.*, 129: 7859-7866, 2007.
- [6] S. Tokonami, H. Shiigi, T. Nagaoka, *Anal. Chim. Acta*, 641: 7-13, 2009.
- [7] J. Wackerlig, P.A. Lieberzeit, *Sensors Actuators B: Chem.*, 207, Part A: 144-157, 2015.
- [8] A. Poma, A. Guerreiro, M.J. Whitcombe, E.V. Piletska, A.P. Turner, S.A. Piletsky, *Adv. Funct. Mater.*, 23: 2821-2827, 2013.
- [9] F. Canfarotta, A. Poma, A. Guerreiro, S. Piletsky, *Nat. Protocols*, 11: 443-455, 2016.
- [10] C. André, I. Castanheira, J.M. Cruz, P. Paseiro, A. Sanches-Silva, *Trends Food Sci. Technol.*, 21: 229-246, 2010.
- [11] G.F. Combs Jr, *Am. J. Clin. Nutr.*, 53: 755-763, 1991.
- [12] H.E.C. Damier P., Agid Y. , Graybiel A. M., *Brain*, 122: 1437-1448, 1999.
- [13] J. Chen, C.-s. Cha, *J. Electroanal. Chem.*, 463: 93-99, 1999.
- [14] P. Kalimuthu, S.A. John, *Bioelectrochemistry*, 77: 13-18, 2009.
- [15] Y. Hoshino, H. Koide, T. Urakami, H. Kanazawa, T. Kodama, N. Oku, K.J. Shea, *J. Am. Chem. Soc.*, 132: 6644-6645, 2010.

CHAPTER 8

- [16] K. Yoshimatsu, H. Koide, Y. Hoshino, K.J. Shea, *Nature protocols*, 10: 595-604, 2015.
- [17] A. Takátsy, B. Csóka, L. Nagy, G. Nagy, *Talanta*, 69: 281-285, 2006.
- [18] E. Mazzotta, A. Turco, I. Chianella, A. Guerreiro, S.A. Piletsky, C. Malitesta, *Sensors Actuators B: Chem.*, 229: 174-180, 2016.

CHAPTER 9

9.1 General conclusions

In this work a general introduction about the state of art of food safety analysis using biosensors was provided, including a description of classes of pesticides that can be used in food production. In recent years there was an intense growth of system based on bio- or bio-mimetic molecules for pesticides detection, using assays based on biological macromolecules like enzymes or antibodies, synthetic biomolecules like aptamers and artificial macromolecules like MIPs. Their potential for environmental analytical purposes has not been much explored and this makes their development one of the most fascinating targets in analytical chemistry.

A deep analysis of recent described aptasensors for food contaminants coupled to electrochemical techniques is then included. In the last years many works were proposed, describing advances in aptamer sequences realisation, as well as combination of probe sequences with nanomaterials in order to improve detection procedures. Works presented show that aptamer based devices still represent one of the most promising approach for biosensor development and their application in environmental analysis, and small molecules analysis in general is still one of the less explored field.

In this way two different approaches for aptasensors development are presented, using gold nanoparticles as sensing platform. Nanostructured gold surfaces were obtained by means of cyclic voltammetry (CV) and used to increase electrochemical performances of the working electrode as well as active surface in order to immobilise probe aptamers. Every electrode surface modification step was characterised by electrochemical

CHAPTER 9

impedance spectroscopy (EIS). Proposed aptasensors were applied for acetamiprid, a pesticide of the neonicotinoid class, electrochemical detection.

In the first two reported aptasensors, a sandwich approach was used, starting from a gold-polyaniline modified graphite screen-printed electrode on which the primary thiolated aptamer was immobilised, via Au-S interaction. The primary aptamer was able to bind the analyte, then a secondary aptamer was used in order to interact with the primary aptamer-target adduct. The used secondary aptamer was labelled with biotin: a streptavidin marked alkaline phosphatase enzymatic label for signal amplification was then applied for rapid and sensitive acetamiprid detection, using enzymatic reaction to convert 1-naphtyl phosphate to 1-naphtol and measuring it using differential pulse voltammetry (DPV). After several optimisation steps, a calibration curve in buffered solution was realised, detecting the analyte in the concentration range between 25 nM and 1000 nM, with a linear response within the range 25 – 100 nM.

The second described aptasensor is realised using the same primary probe aptamer immobilised on the polyaniline/gold modified graphite screen printed electrodes. A short DNA sequence, properly selected to be complementary to the binding site of the primary aptamer was then used in a competitive approach, realising a signal-off enzyme amplified detection method (enzyme-produced 1-naphtol was measured using DPV). After several optimisation steps, the developed aptasensor was able to detect acetamiprid in buffered solution within the range 0.025 μM – 2 μM . A further application to spiked real samples is reported, including a comparison of obtained results with a reference HPLC method, obtaining recoveries within 90.0 and 100.0 % on analysed samples.

The realised platform based on the combination of gold-polyaniline modified screen-printed electrodes and aptamers showed great potential applications in environmental monitoring and food analysis, realising, coupled with the competitive approach, analytical performances comparable to those obtained on the same samples with a reference HPLC method.

The last part of this thesis work is focused on an application of molecularly imprinted polymeric nanoparticles for the realisation of an electrochemical sensor with reduced interference. The developed approach started from amperometric detection of a model analyte, ascorbic acid, that was carried out by means of bare graphite screen printed electrodes. Molecularly imprinted polymeric nanoparticles (nanoMIPs) able to selectively bind ascorbic acid were synthesised using a solid phase approach: activated glass beads were grafted with 3-glycidyloxypropyl trimethoxysilane (GOPTS), able to bind ascorbic acid. Functionalised glass beads were then used to complete the templated synthesis of molecularly imprinted polymeric nanoparticles. The obtained nanoMIPs were characterised using dynamic light scattering (DLS) and transmission electronic microscopy (TEM). After that they were tested via amperometric measurements in order to suppress electrochemical signal given by ascorbic acid oxidation. Measurement setup was optimised in order to reach quantitative signal suppression within the concentration range 50 – 550 nM. After that, measurements of dopamine in presence of fixed concentrations of ascorbic acid were carried out. The proposed procedure allowed measuring dopamine in the concentration range 100 – 500 nM in presence of 50 nM of ascorbic acid, preventing any quantification error given by ascorbic acid interfering current and avoiding any pretreatment procedure. Moreover, synthesised nanoMIPs were tested

CHAPTER 9

in real sample measuring spiked dopamine in human serum solutions in presence of a concentration 50 nM of ascorbic acid, obtaining same suppression effect.

The proposed proof of concept about the possibility to carry out electrochemical measurement reducing signals given from interfering species represent, as far as it concerns to the authors, the first application of nanoMIPs as scavenger for interfering species signals suppression. Potential application of this methodology can bring to the development of fast pretreatment-free electrochemical sensors with reduced interferences.